DEVELOPMENT AND ANALYSIS OF LOW CALCIUM FLYASH BASED GEOPOLYMER FOR STRUCTURAL APPLICATIONS

By

GAURAV NAGALIA

Presented to the Faculty of the Graduate School of

The University of Texas at Arlington in Partial Fulfillment

of the Requirements

for the Degree of

MASTER OF SCIENCE IN MATERIALS SCIENCE & ENGINEERING

THE UNIVERSITY OF TEXAS AT ARLINGTON

AUGUST 2014

Acknowledgements

Foremost, I would like to express my sincere gratitude to my thesis advisor Dr. Pranesh Aswath, Professor and Associate Dean for Graduate Affairs; for the continuous support of my study and research, for his patience, motivation, enthusiasm and immense knowledge. His guidance helped me in all the time of research and writing of this thesis.

Besides my advisor, I would like to thank my supervisor Dr. Ali Abolmaali for funding my research and allowing me to use all the resources at his disposal and for his reviews and insightful advice with this research project.

I would also like to thank Dr. Kinash Oleh and Dr. Yeonho Park from the civil engineering laboratory building and Dr. Jiechao C. Jiang from the characterization center for materials and biology for volunteering their time and providing the necessary materials to make this research possible. I also thank Preeti Shreshtha, Akshay Hande, Anna Zaman, Soundarya Pondichery Sathyanar and my research group members Vibhu Sharma, Megen Velten, Ami Shah and Kush Shah for their advice and help in carrying out the experiments.

I am grateful to my family for their unceasing encouragement and support. Last but not the least; I would like to thank all who, directly or indirectly, have lent their helping hand in this venture.

August 11, 2014

Abstract

DEVELOPMENT AND ANALYSIS OF LOW CALCIUM FLYASH BASED GEOPOLYMER FOR STRUCTURAL APPLICATIONS

Gaurav Nagalia, M.S

The University of Texas at Arlington, 2014

Supervising Professor: Pranesh Aswath

Geopolymers are an innovative ceramic material composed of long chains and networks of inorganic molecules are being used as an alternative to conventional Geopolymer cement for infrastructure construction, replacement of intersection and localized repairs. Some of the advantages of this material is due to its ultra-fast setting time, rapid strength development and the phenomenal reduction in carbon foot print as compared to Geopolymer cement. However, this material is yet to be commercialized due to the variability in its mechanical strength when using flyash from different sources.

In this study aluminosilicate geopolymers with different alkali oxides (feldspars) have been prepared by mixing class F-flyash and alkaline solution. The samples were cured under different experimental conditions and then tested for compressive strength. X-ray diffraction (XRD) and scanning electron microscopy (SEM/EDS) have been used to identify the new phases formed in geopolymeric matrix. In addition, these techniques were used to follow the curing process and the formation of these phases and to map the

underlying relationship between the flyash properties and mechanical properties of the geopolymer.

Table of Contents

List of Illustrations

List of Tables

Chapter 1

Introduction

1.1. General Introduction

In recent years, there has been a substantial development in a new type of inorganic binder that is being used to replace the conventional Portland cement (PC). The economic significance for flyashst track construction has created a need for early-age estimates of concrete strength. Accelerated construction schedules that put a new, repaired or overlaid pavement into service require adequate concrete strength to withstand traffic loads. Typical applications include localized repairs, replacement of busy intersections and major slip-form paving. This class of binders, termed “geopolymers” which was first coined by French scientist Joseph Davidovits (1978) to represent a broad range of materials characterized by networks of inorganic molecules. It is an alkali-activated binder produced by a polymeric reaction of alkaline liquids with the silicon and the aluminum oxides in source materials of geological origin like metakaolinite (calcined kaolinite) or by-product materials such as fly ash (FA) and rice husk ash (Davidovits, 1999).

1.1.1.Research Framework

A number of researchers have dedicated efforts to study the chemistry behind geopolymer binders to provide an insight to geopolymerization kinetics. These studies are typically performed using a highly pure source of silica and alumina, such as metakaolin (Provis and van Deventer, 2007; De Silva et al., 2007; Provis et al., 2005). However, flyash exhibits a significantly different particle morphology and chemistry which impacts the mechanical properties of the resulting geopolymer (Provis et al, 2010) and typically contains other impurities that vary from one flyash source to another, thus it is difficult to predict the properties of a flyash based geopolymer. Research efforts have also been made to identify the characteristics inherent to the flyash that impact its potential as source material for geopolymerization (Fernandez-Jimenez and Palomo, 2003; van Jaarsveld et al., 2003; Diaz et al. 2010). Although a good approach, it flyashlls short in its effort to correlate the relationship between the chemistry of fly ash and the mechanical properties of the geopolymer. While the premise "Flyash with relatively high fineness will produce geopolymer with higher compressive strength" is true, it does not provide specific optimum

values or ranges of mixes nor takes into account the interaction of the flyash chemistry with others process variables that may affect the mechanical strength of geopolymer.

Other studies have focused on investigations that promote the use of geopolymer, highlighting the environmental benefits of recycling flyash into geopolymer concrete (van Deventer et al., 2010; Weil et al., 2007). However, these studies fail to solve some of the fundamental issues such as variability in the flyash and its effect on geopolymer mechanical properties, the study of kinetics of the geopolymerization process and long term properties of geopolymers. This is the reason that prevents geopolymer concrete from being commercially available in the market. In addition, some studies have focused on developing an understanding on the effects of mix proportion, activator solution concentrations, curing conditions, etc. on the mechanical properties of geopolymer concrete (Sofi et al, 2007; Fernandez-Jimenez et al., 2006; Hardjito et al., 2004). To date limited attention was given to evaluating correlations between the mechanical properties of geopolymer with the flyash chemical properties. A key contribution of the proposed research work is the capturing of the variability posed by using a flyash stockpile and producing geopolymer cement by using different mix formulations and developing a fundamental understanding between chemistry of constituents and properties of the geopolymer cement.

1.1.2.Objective

The main objective of this research project is to determine the underlying relationship between the chemical make-up of the flyash and the mechanical properties of the geopolymer that is formed by its reaction with alkaline solutions. Two different sources of flyash are examined in terms of chemical composition, one with low calcium content and the other with high calcium content. The fabricated geopolymer cylinders were evaluated in terms of chemical composition, microstructure properties, mechanical strength as a function of setting time, curing time and various mix factors. A model is created with the aim of predicting the properties of fresh and hardened geopolymer cement using this relationship.

1.1.3.Limitations

The present research does not attempt to classify geopolymer with respect to their molecular structures nor attempts to study the kinetics of geopolymerization. Instead, it attempts to provide practical forecasting tools that use flyash characteristics as input to predict the potential mechanical properties of geopolymer cement. Moreover, it attempts to provide empirical equations that explain key relationships that exist within its mechanical attributes.

1.1.4.Engineering Significance

This study will help to gain better understanding of flyash as raw material for geopolymer concrete by analyzing flyash stockpiles with distinct characteristics and correlating those characteristics with the mechanical properties of geopolymer concrete. Discerning the relationship between the physical, chemical and crystallographic characteristics of flyash and the mechanical properties of geopolymer concrete is an important step towards producing large quantities of geopolymer concrete with reasonably consistent and predictive engineering properties. Another important challenge for the widespread use of geopolymer concrete is the lack of design equations that represent the correlations and tendencies among its mechanical properties. This study will also attempt to get a better understanding of the mechanical behavior of geopolymer concrete, based on the effects posed by using different combinations of raw materials, i.e. the flyash and the alkaline solutions.

Chapter 2

Literature Review

2.1. Introduction

According to the most recent survey released by the American Coal Ash Association (EPA, 2011), the U.S. produced approximately 135 million tons (MT) of coal combustion products (CCPs) in 2009, making it the second largest by-product stream in the US. The main types of CCPs are fly ash, bottom ash, boiler slag and flue gas desulfurization material (FGD). Flyash occupies over 45% of the total CCP production with approximately 63 MT per year. Flyash is composed of fine spherical particles that rise with the flue gases during the combustion of coal which are captured by pollution control devices. Although 25 of the 63 MT of flyash were used beneficially in 2009, 38 MT were disposed in landfills and storage lagoons at a significant cost and posing a potential risk to local aquifers due to possible leaching of heavy metals (EPA, 2011). However, an imminent change to the current amount of flyash used in beneficial applications is expected to happen in the near future. The US Environmental Protection Agency (EPA) is currently developing new regulations with which many of the current beneficial applications of flyash, such as soil stabilization and mine reclamation that are considered "un-encapsulated" may be banned allowing only the recycling of flyash in encapsulated applications, namely, concrete In addition, the cost of landfilling operations is expected to increase due to new stricter requirements (liners, groundwater monitoring, etc.) derived from the new regulations (EPA, 2011).

Flyash has been used in ordinary concrete as a "supplementary cementitious material" for many years to improve the rheology of the fresh mix and durability of the hardened product and typically occupies up to 20% of the total mix. However, flyash alone is capable of producing a strong cementitious binder when activated under highly alkaline conditions.

Most researchers agree that the outcome of the polymerization reaction that leads to the formation of geopolymer is an amorphous 3D network of silicon and aluminum atoms linked by oxygen atoms in a four-fold coordination similar to the one exhibited by zeolites (Fernandez-Jimenez and Palomo, 2004; Davidovits, 1991). The positive ion (Na^+ or K^+) provided by the activator solution serves to

balance the negative charge generated by having aluminum atoms in a four-fold coordination. This, gives geopolymer a set of mechanical and chemical properties that are equivalent, or even superior to those of geopolymer cement concrete (Provis and van Deventer, 2007; De Silva et al., 2007). This is in direct contrast to the conventional Portland cement hydration reaction which results in hydrated calcium silicate known as gypsum that acts as the binder.

The main challenge faced while producing flyash-based geopolymer concrete commercially is the significant variability of flyash. The chemical properties of flyash depend on the type, size and composition of its precursor coal. The main components of the geopolymer network are silica and alumina molecules and thus the amount and ratio of these materials influence the resulting mechanical properties of geopolymer. Apart from silica and alumina components, there are various other factors that also play a significant role in the mechanical properties of geopolymers. Impurities, such as CaO, have a positive impact in geopolymer but cause shorter setting times as they create nucleation sites (Temuujin et al., 2009). Another important factor is the fly ash's crystallographic properties (i.e., the way the molecules are arranged within the flyash). Since amorphous compounds are easier to dissolve than crystalline compounds during the first step of geopolymerization (dissolution of species), they yield higher amounts of reactive SiO_2 and Al_2O_3 to combine during the transportation/coagulation phase of the geopolymeric reaction, resulting in a higher degree of geopolymerization and consequently higher mechanical strength. The physical properties are mainly a result of the degree of pulverization of the precursor coal, since a significant part of the reaction occurs at the particle-liquid interface, the finer the particles the greater is the surface area and the more reactive is the flyash. A second physical factor is the burning efficiency, since a poor burning process yields unburned coal in the flyash (quantified as Loss on Ignition, LOI). High content of unburned carbon with high surface area could adversely impact the behavior of the fresh mixture, thereby creating a demand for the addition of activator solution well beyond what is needed to activate the source material, to obtain a workable mixture (Diaz et al., 2010).

2.2. Cement Footprint

In the present context, global warming is one of the greatest environmental issues. Global warming is caused by the emission of greenhouse gases like CO_2 to the atmosphere. It has been reported that the worldwide cement industry contributes around 1.65 billion tons of the greenhouse gas emissions annually (Malhotra, 2002; McCaffrey, 2002; Hardjito et al., 2004). The production of one ton of Portland cement emits approximately one ton of CO_2 into the atmosphere (Davidovits, 1994c; McCaffrey, 2002). Due to the production of Portland cement, it is estimated that by the year 2020, emissions will rise by about 50% from the current levels (Naik, 2005; Salloum, 2007).

The emissions associated with the production of Portland cement can be divided into two categories: combustion and calcination. Combustion is associated with the fact that the production of cement requires temperatures of approximately 1440°C inside a rotator kiln, consuming significant amounts of energy. Fossil fuels are commonly used to reach such temperatures. The burning of fossil fuels accounts for 40% of the total CO_2 emitted in a cement production process and the remaining 60% is attributed to the calcination process. The calcination of cement's main raw materials to produce clinker releases CO_2, mainly due to the decomposition of $CaCO_3$ into CaO and CO_2. However, it has been suggested that as concrete ages it absorbs back a portion of the CO_2 released during the manufacturing process through its carbonation. It is estimated that, with good recycling practices, 57% of the CO_2 can be reabsorbed through concrete carbonation after 100 years (WBCSD, 2009; Pade and Guimaraes, 2007).

The pollutant nature of cement's production creates an imperative need to develop new construction materials that reduce the human footprint. Furthermore, it presents the opportunity to search for materials that can be recycled to create a strong binder like cement. In order to reduce the environmental impact due to cement production, it is necessary to develop a new type of binder. In this respect, the geopolymer technology is one of the revolutionary developments resulting in a low-cost and greener substitute for Portland cement. It is demonstrated that geopolymeric cement generates 5-6 times less CO_2 than Portland cement, thus helping to reduce global warming (Davidovits, 2005).

2.3. Geopolymer

2.3.1. Geopolymer Chemistry

The process through which geopolymers harden is typically referred to as geopolymerization and is carried out by reacting flyash with alkaline activator solution, which results in the formation of polymeric chains due to the polycondensation. Poly(sialate) is the term used for the chemical designation of geopolymer based on silico-aluminate (Davidovits, 1988a, 1988b, 1991; Van Jaarsveld et al., 2002a); Sialate is an abbreviation for silicon-oxo aluminate. Poly(sialates) are chain and ring polymers with Si^{4+} and Al^{3+} in IV-fold coordination with oxygen and range from amorphous to semi-crystalline with the empirical formula:

$$\mathbf{M_n(-(-SiO_2)_z\text{-}AlO_2)_n.H_2O}$$

Figure 2-0: Empirical Formula of Poly(sialate)

Where “z” is 1,2 or 3 or higher up to 32; M is a monovalent cation such as potassium or sodium, and “n” is a degree of polycondensation (Davidovits, 1988b, 1991, 1994b, 1999). The structures of these polysialates can be schematized as in Figure 2-2.

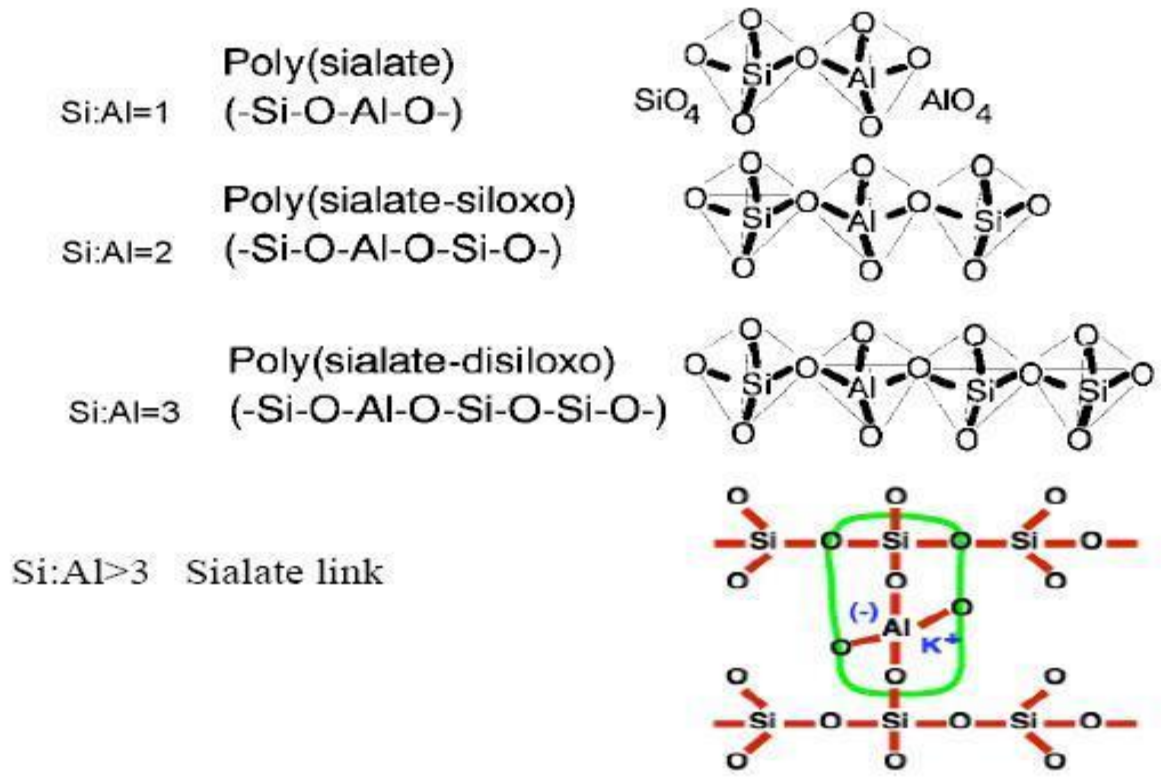

Figure 2-1 Chemical Structures of Polysialates (Davidovits, 1988b; 1991; 1994b; 1999)

Xu and van Denter (2000) proposed that the geopolymerization reaction can be divided into three steps:

1. Dissolution of silicon and aluminum species from the source material through the action of the highly alkaline solution.
2. Transportation of species and formation of monomers (coagulation/gelation).
3. Polycondensation and growth of polymeric structures resulting in the hardening of the material.

However, these steps typically overlap each other under thermal curing and are hard to isolate (Palomo et al., 1999). In addition, some impurities in flyash can cause hydration reactions that many times impact the kinetics of geopolymerization. Therefore, since pure geopolymers rarely occur,

especially when using flyash as source material, many authors refer to geopolymer as inorganic polymer concrete, alkaline cements or Alkaline Activated flyash (Fernandez-Jimenez and Palomo, 2004; Sofi et al., 2007). Although some details are still debated, many researchers agree that paralleled to the formation of geopolymer gel, calcium in the mixture reacts with silicate and aluminate monomers dissolved from the source material, forming calcium silicate hydrates (CSH) and calcium aluminosilicate hydrates (CASH). The hydration of these compounds leads to water deficiency and thus raise the alkalinity of the mixture. The increase in alkalinity promotes higher and faster dissolution of silicate and aluminate species from the source material, increasing the rate of poly-condensation/geopolymerization. Thus, the presence of calcium contributes to mechanical strength of the resulting hardened matrix not only by forming CSH and CASH, but also by enhancing the geopolymerization process (Diaz et al., 2010; Temuujin et al., 2009).

The schematic formation of geopolymer material by polycondensation is shown in the equation given below:

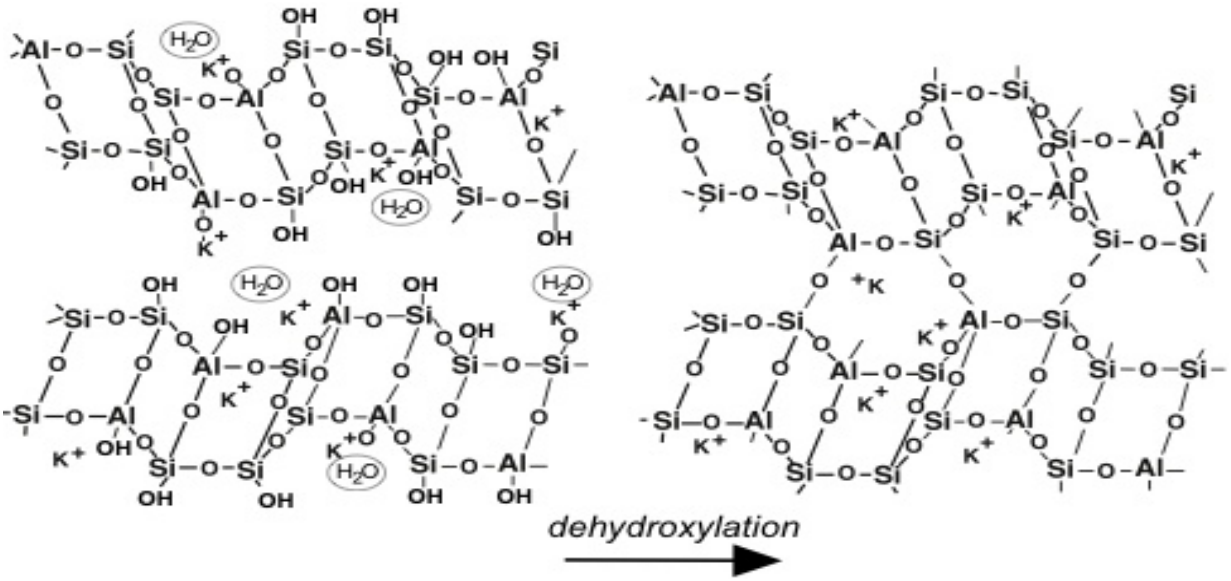

Figure 2-2 Schematic Formation of Geopolymer Material

Since this is dehydroxylation reaction, water is expelled from the geopolymer matrix during the reaction that occurs while curing. Due to this, there is a formation of discontinuous nanopores which result in a strengthened structure formation.

2.3.1.1. CONSTITUENTS OF GEOPOLYMER

The main constituents of geopolymers are the source materials and the alkaline liquids.

1. Aggregates
2. Sand — Source Materials
3. Flyash

4. Sodium Hydroxide Solution — Alkaline Liquids
5. Sodium Silicate

6. Super Plasticizer — Adding agents to improve workability of mix
7. Water

Source Materials: The source materials should be rich in silica and alumina. Natural materials like kaolinite, clays, micas, sand, etc and by products like flyash, slag, bottom ash, silica fume, etc. can be used as source material. Selection of source material for preparing geopolymers depends on various factors such as availability of raw material, cost and type of application. In this study, low calcium flyash will be the main source of silica and alumina.

Flyash: The combustion of finely ground coal to produce electricity typically leaves behind two main waste streams: (1) bottom ash, composed of particles of sizes ranging from 63 to 1000 um many times fused together that drop to the bottom of the boiler, hence the term bottom ash; and (2) flyash, which is transported along with the flue gases and then captured by pollution control devices namely, electrostatic precipitators or baghouses and occasionally by scrubber systems. Physically, flyash is a very fine and powdery material composed mainly of spherically shaped particles that range in size from a few microns to over 100 um. The chemical composition of flyash is very similar to that of volcanic ash having as main components: silica, alumina, iron oxide and calcium oxide in some cases. Typically, a small portion of the chemical components is arranged in a crystalline form (mainly quartz and mullite, but lime, magnetite and traces of others are present in some cases) with the rest being amorphous with no particular arrangement due to its rapid cooling after leaving the boiler (Diaz et al., 2010).

Flyash is also considered a pozzolan, i.e., a material that will react with calcium hydroxide in the presence of water and create cementitious compounds. Therefore, more than half of the concrete produced in the US uses flyash as a partial substitute for Portland cement in concrete mixes (Kosmatka et al. 2009). Flyash is classified, according to ASTM standard C 618, into three different groups:

1. Low-calcium fly ash (Class F): CaO content less than 10%. Usually produced from anthracite and bituminous coals. Corresponds to ASTM 618 class F.
2. High-calcium fly ash (Class C): CaO content greater than 10%. Usually produced from sub-bituminous and lignite coals. Corresponds to ASTM 618 class C.
3. Other types of fly ash (Class N): This type of flyash groups raw or calcined natural pozzolans such as opaline cherts, shales, volcanic ashes, pumicites and various materials with minimum sum of 70% of silicon, aluminum and iron oxide. It must also have a maximum of 10% LOI among other chemical and physical requirements.

Table 2-1 Range of Chemical Composition for low and high-calcium fly ashes. (Jarrige, 1971)

Composition	**Class F (%)**	**Class C (%)**
SiO_2	47.2 – 54	18 – 24.8
Al_2O_3	27.7 – 34.9	12.1 – 14.9
Fe_2O_3	3.6 – 11.5	6.3 – 7.8
CaO	1.3 – 4.1	13.9 – 49
Free Lime Content	0.1	18 – 25
MgO	1.4 – 2.5	1.9 – 2.8
SO_3	0.1 – 0.9	5.5 – 9.1
Na_2O	0.2 – 1.6	0.5 – 2
K_2O	0.7 – 5.7	1 – 3

Van Jaarsveld et. al. (2003) reported that the particle size, calcium content, alkali metal content, amorphous content, and morphology and origin of the fly ash affected the properties of geopolymers. It was revealed that the calcium content in fly ash played an important role in strength development and final compressive strength as the higher calcium content resulted in faster strength development and

higher compressive strength. However, Fernandez-Jimenez & Palmo, (2003) claimed that in order to obtain the optimal binding properties of the material, fly ash as a source material should have low calcium content and other characteristics such as unburned material lower than 5%, Fe_2O_3 content not higher than 10%, 40-50% of reactive silica content, 80-90% particles with size lower than 45 μm and high content of vitreous phase. Gourley (2003) also stated that the presence of calcium in fly ash in significant quantities could interfere with the polymerization setting rate and alters the microstructure. Therefore, it seems that the use of Low-calcium (ASTM Class F) fly ash is preferred as a source material than High-calcium (ASTM Class C) fly ash to make geopolymer (Wallah and Rangan, 2006).

Alkaline liquids*:* The alkaline liquids are from soluble alkali metals usually based on sodium (Na) or potassium (K). Sodium silicate (Na_2SiO_3) or potassium silicate (K_2SiO_3) mixed with sodium hydroxide (NaOH) or potassium hydroxide (KOH) is the most common type of alkaline liquid used in the geopolymerization (Davidovits, 1999; Palomo et al., 1999; Barbosa et al., 2000; Xu and van Deventer, 2000; Swanepoel and Strydom, 2002; Xu and van Deventer, 2002).

Palomo et al (1999) concluded that the type of alkaline liquid played an important role in the polymerization process. Reactions occurred at a high rate when the alkaline liquid contained soluble silicate, either sodium or potassium silicate, compared to the use of only alkaline hydroxides. They used the combination of sodium hydroxide with sodium silicate or potassium hydroxide with potassium silicate as alkaline liquids. Xu and van Deventer (2000) confirmed that the addition of sodium silicate solution to the sodium hydroxide solution as the alkaline liquid enhanced the reaction between the source material and the solution. Furthermore, after a study of the geopolymerization of sixteen natural Al-Si minerals, they found that generally the NaOH solution caused a higher extent of dissolution of minerals than the KOH solution.

2.4. Research Summary

The purpose of this research is to determine the underlying relationship between the chemical make-up of the flyash and the mechanical properties of the geopolymer. For this purpose, two different sources of flyash are utilized to fabricate geopolymer concrete and studied and evaluated in terms of

chemical composition, microstructure properties, mechanical strength, setting time, curing time and various mix factors.

For the mechanical properties, the concrete is tested for their setting time and cast into cylinders. These cylinders are tested for their compressive strength. Further analysis of the concrete is carried out using x-ray diffraction and scanning electron microscope in order to evaluate the chemical and crystallographic properties. These properties are compared with the mechanical properties, thus laying a map for the correlation between the flyash chemical properties and the geopolymer mechanical properties.

Chapter 3

Material Development and Testing Procedure

3.1. Introduction

This chapter describes the experimental work performed in the laboratory. It presents the different types of mix designs produced and the material behavior results of testing the geopolymer concrete cylinders under compression according to ASTM C39 'Standard Test Method for Compressive Strength of Cylindrical Concrete Specimens'.

The materials used for making geopolymer concrete specimens in this research are low-calcium dry fly ash as the source material, aggregates of different sizes, alkaline liquid, water and super plasticizer. The fly ashes used in this study were supplied from Boral Material Technology. This distributor supplied the fly ash from Stillesboro, GA and Rockdale, TX. The fly ash from Stillesboro, GA contained 1.29% CaO and that from Rockdale, TX 9.42% CaO. The ASTM C618 'Standard Specification for Coal Fly Ash and Raw or Calcined Natural Pozzolan for Use in Concrete' Test Reports of the fly ash are presented in Appendix A.

A combination of sodium hydroxide solution and sodium silicate solution was used as the alkaline liquid. Sodium hydroxide in the form of flakes was purchased from a local supplier. Sodium silicate solution (Na_2O=10.6%, SiO_2=26.5% and density=1.39g/ml at 250^oC) was also purchased from a local supplier. More than 1000 cylinders were produced during the research using different mix designs and were tested in accordance with ASTM C39.

3.1.1. Mixture Proportions

Based on the limited past research on geopolymer pastes available in the literature and the experience gained during the preliminary experimental work, the following ranges were selected for the constituents of the mixtures:

1. Ratio of Sodium Silicate to Sodium Hydroxide = 2.5
2. Ratio of Activator Solution to Flyash = 0.3 – 0.4

3. Molarity of NaOH = 8M – 14M
4. Aggregates constituted 75 – 80% of entire mix
5. Super Plasticizer constituted 0 – 2% of entire mix.

3.1.2. Geopolymer Mix Procedure

The basic procedure for preparing the mix has been kept consistent.

1. The required amount of Sodium Hydroxide flakes is weighed and dissolved in measured quantity of water to prepare either an 8M or 14M solution.
2. The reaction being exothermic; the solution is allowed to cool for an hour and then measured quantity of sodium silicate solution is added to it. This mixture of sodium hydroxide and sodium silicate solutions is prepared 24 hours in advance prior to use.
3. Measured quantities of aggregates, sand and flyash is added to the concrete mixer and mixed for roughly 3 minutes till a uniform mixture is obtained.
4. Measured quantities of the alkaline solution, water and super plasticizer is added to this and is mixed in with the source materials for another 2 – 3 minutes. (Note: This mix was designed by trial and error method.)

Figure 3-1 Concrete Mixer

Figure 3-2 Compaction of geopolymer into cylindrical molds

3.1.3. Curing Conditions

Curing is a term in polymer chemistry and process engineering that refers to the toughening or hardening of a polymer material by cross-linking of polymer chains, brought about by electron beams, heat or chemical additives. In the case of geopolymer concrete, curing is an ongoing process and can be aggravated by different heating conditions. The different curing methods include:

1. Oven – Curing : Dry conditions, 158^{o}F
2. Steam – Curing : 100% Humidity, 115^{o}F
3. Curing at Room Temperature

These curing methods are utilized in order to observe the effect of different temperatures and curing environment on the mechanical properties of the geopolymer. For this method, the Geopolymer cement cylinders are wrapped in plastic and kept in a chamber with the necessary conditions. Lastly, curing at room temperature is carried out so that there is a reference for comparison.

3.2. Compressive Cylinder Test

Cylinders were produced from different mix designs and tested according to ASTM C39 “Standard Test Method for Compressive Strength of Cylindrical Concrete Specimens.” In this test, the compressive load was applied axially to the cylinder at a rate within a prescribed range until failure occurred. The compressive strength of the cylinder was then determined by dividing the maximum load obtained during the test by the cross-sectional area of the cylinder. Cylinders of 4 inch x 8 inch (100 mm x 203 mm) diameter were produced and tested at 1, 3, 7, and in some cases, 28 days after production. Since the cylinders were prepared by using dry cast method, the compressive strength obtained on 7 days was sufficient for comparison purpose.

The cylinders were produced and tested in the Civil Engineering Laboratory Building (CELB) at the University of Texas at Arlington. The cylinder specimens were produced using plastic molds to assure the correct dimensions. Mold release agent was applied to the interior of the molds to ease the removal of the casted specimen. The molds were securely placed onto a vibrating table near the batching location. Concrete mix was placed in multiple lifts, compacted and tamped while under vibration. At least eight cylinders were prepared from each mix design. After curing, the cylinders were stripped from their molds and capped at each end so as to create a smooth and leveled testing surface (ASTM C617). Sulfur flake was used as a capping material.

3.2.1. Test Set Up

The testing equipment had compressive capabilities up to 500 kilo-inch-Pascals. The machine was power operated and applied load continuously at the prescribed loading rate as described below. It consisted of two steel bearing blocks with hardened faces, one of which remained on the upper surface of the cylinder and the other on which the cylinder rested. The bearing faces of the blocks should be at least 3% greater in diameter than the testing specimen. The cylinder was placed in the machine and centered relative to the upper bearing block. Before starting the test, the machine was adjusted until the cylinder and the upper block came in contact. The typical test set up is given in Figure 3-3.

3.2.2. Loading History

The rate at which the cylinder was tested was 35 ± 7 psi/s (0.25 ± 0.05 MPa/s). This was applied continuously and slowly without shock, throughout the test. ASTM C39 states that higher loading rates can be applied during the first half of the loading phase but should be in a controlled manner so that the cylinder is not subjected to shock loading. As it reached the ultimate load, there was no need to adjust the rate of movement and the stress rate decreased due to cracking in the cylinder. The compressive load was applied until the load indicator showed that the load decreased steadily. The loading rate was applied manually and was displayed in the digital reader. Figure 3-4 shows the part of the testing apparatus which controlled the rate.

Figure 3-3 Compressive Cylinder Testing Machine

Figure 3-4 Control unit for mechanical tester

Chapter 4

Mechanical Test Results

4.1. Introduction

This preliminary study was aimed at gaining better understanding of the relationship between the chemical composition of the flyash, its reaction with alkaline materials and the mechanical properties of the geopolymer. In order to better understand this relationship, different formulations of geopolymer mix were created and the geopolymer cement was tested under different conditions for its compressive strength

4.2. Experimental Data

In this Chapter, the experimental results are presented and discussed. Each of the compressive strength test data plotted in Figures 4-1 to 4-15 or given in Tables 4-2 to 4-12 corresponds to the mean value of the compressive strengths of five test concrete cylinders in a series. Two sources of flyash have been used for the mixes; (a) 9.42% CaO flyash and (b) 1.29% CaO flyash.

4.2.1. Effect of Variable Parameters

Quite a few factors have been identified as important parameters affecting the properties of geopolymers. Some of the factors which have been known to affect the strength of the mix are:-

1. Type of flyash: varies with the percentage of CaO (9.42%, 1.29%)
2. Source of flyash
3. Type of alkaline solution used (NaOH, KOH, LiOH, $Al(OH)_3$, $Ba(OH)_2$, $Mg(OH)_2$)
4. Molarity of alkaline solution (8M or 14M)
5. Source material aggregate size
6. Curing time (24 hrs or 48hrs)
7. Curing temperature (75^oC, 115^oC, 131^oC, 158^oC)
8. Added Additives (Steel Fibers or Crumb Rubber)

While studying the added effect of all variable parameters, only one parameter was varied and all the rest of the parameters were held constant. For example, in order to study the effect of size and amount of aggregates in the compressive strength, the variable parameter was the size and amount of aggregates (3/8 or 5/8 or both) and all the rest of the constituents and curing conditions like concentration of sodium hydroxide, types of fly ash, amount of chemicals, curing time, curing temperature and method were considered constant. The compressive strength at 7 days was considered for comparison purposes.

4.2.1.1. Alkaline Solutions

For this study, all other parameters were kept constant and only the type of alkaline solution is varied. The 9.42% CaO fly ash is considered. All the mixes are cured at 131 F for 24 hours and then tested for compressive strength after 7 days. The mix is as it is seen in Table 4-2. Tables 4-3 through 4-5 were made to study the effect of using different combination of alkaline hydroxide solutions on the compressive strength of geopolymer cement. All the mixes from these tables are based on the 9.42% CaO Flyash with 14 M alkaline solution. The cylinders cast from these mixes are cured at 131 F for 24 hours and then tested for compressive strength after 1 day and 3 days. The only parameter that has been varied is the type of alkaline hydroxide solution. Table 4-3 represents the data for replacing 100% NaOH by various other alkaline solutions. Figure shows that the compressive strength reduces significantly by using any alkaline solutions other than sodium hydroxide solution. The mix for magnesium hydroxide (II) and aluminum hydroxide (III) do not cast and is not reported here. Table 4-4 represents the data for replacing 10% NaOH. The only alkaline complex mix which comes close to the 100% sodium hydroxide mix is the 10% NaOH + 90% KOH solution. Most of the magnesium hydroxide (II) mixes do not cast. Table 4-5 represents the data for replacing 50% NaOH. All the mixes in this case have a much lower strength result on comparing it with a 100% NaOH. Most of the magnesium hydroxide (II) mixes do not cast. On comparing Tables 4-3 through 4-5, it can be observed that as we reduce the concentration of sodium hydroxide, the strength reduces drastically. Although, there is some amount of curing reaction taking place as can be seen from comparing the 1 day compressive strength results to the 3 day compressive strength results, they are too low from an industrial stand point.

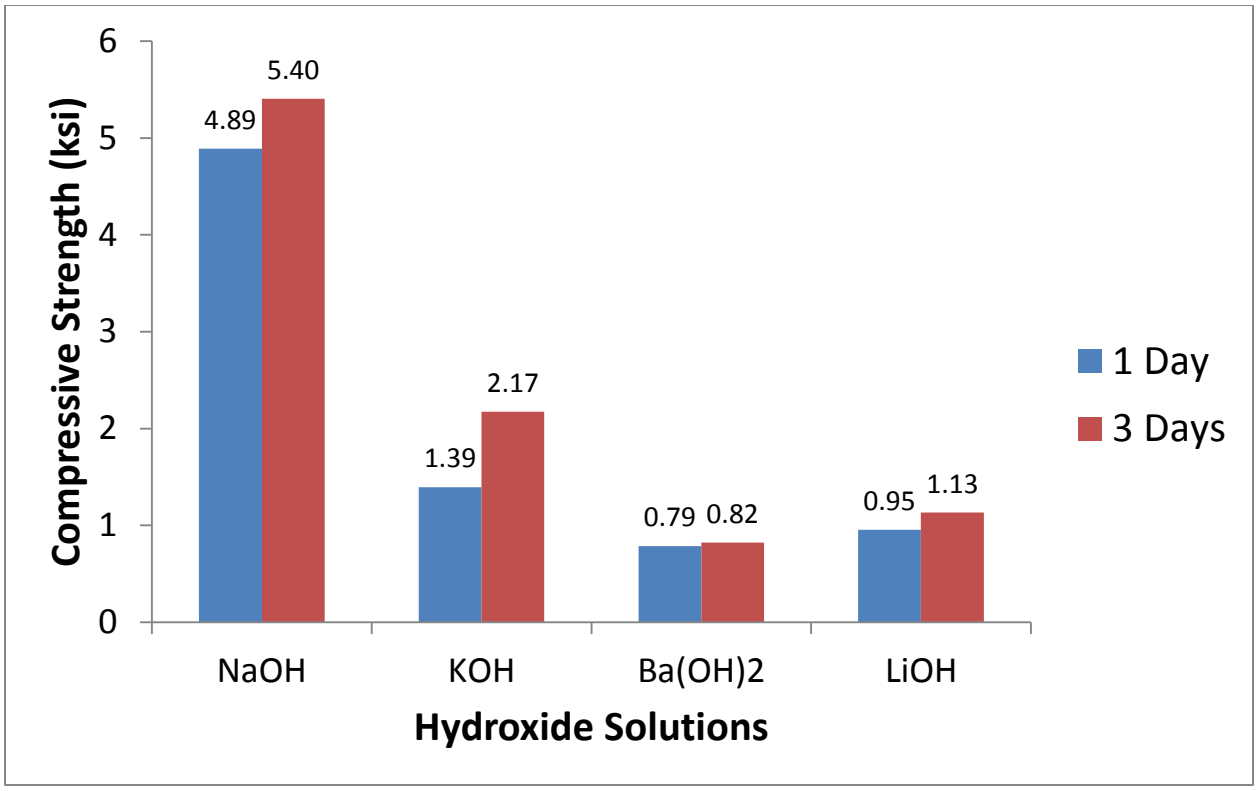

Figure 4-1 Compressive Strength Vs 100% Alkaline Solutions

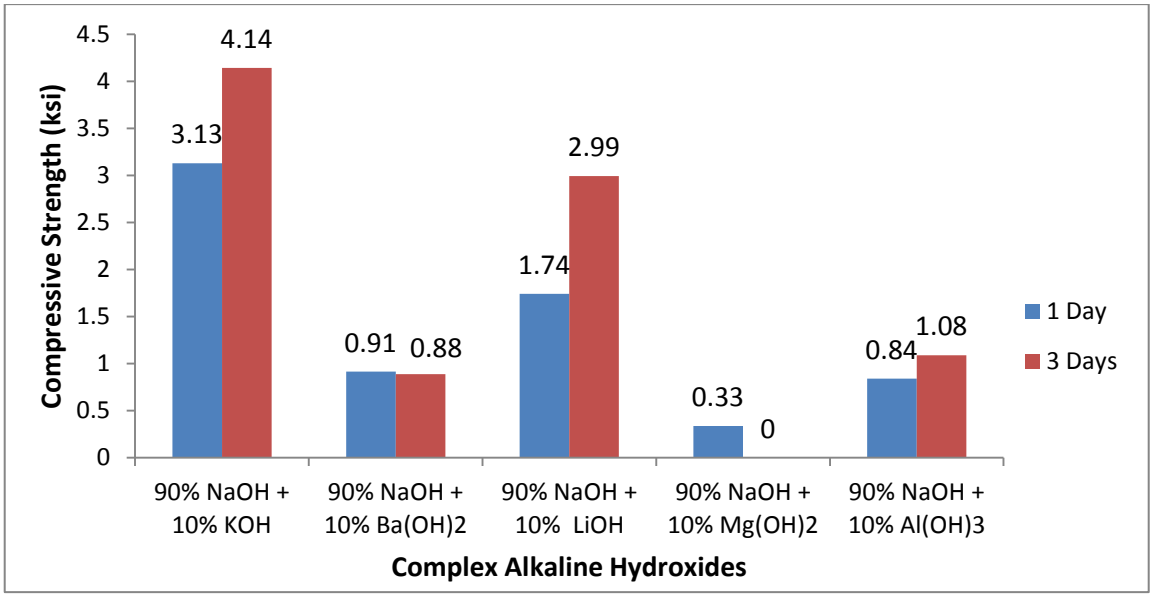

Figure 4-2 Compressive Strength Vs Complex Alkaline Hydroxides

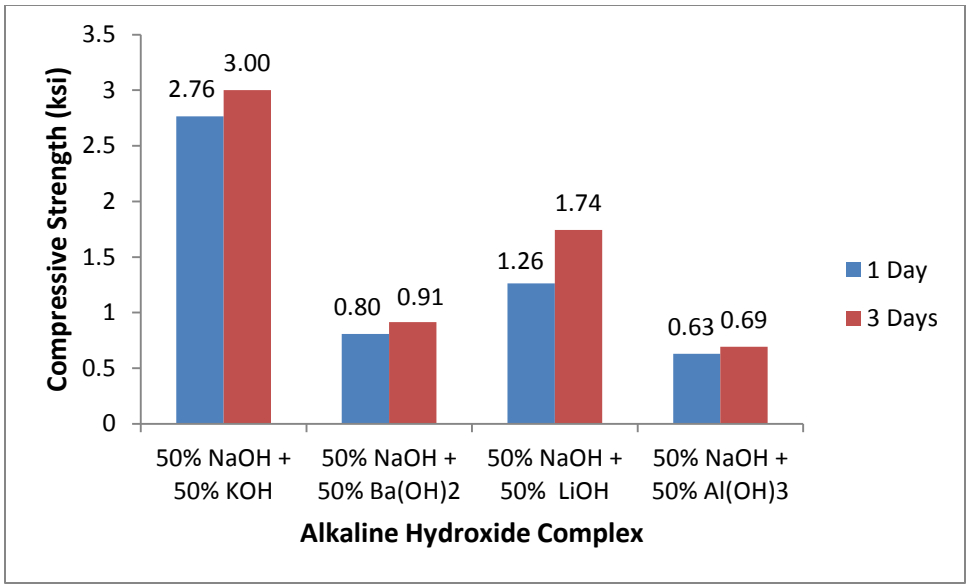

Figure 4-3 Compressive Strength Vs. Complex Alkaline Hydroxide Solutions

4.2.1.2. Molarity of Solution

Mixes 1 through 4 (Table 4-6) were made to study the effect of concentration of sodium hydroxide (NaOH) solution in terms of molarity on the compressive strength of the concrete. Keeping all other parameters constant, only the molarity of the alkaline solution is varied. Two types of fly ash, 9.42% CaO fly ash and 1.29% CaO fly ash were considered. All the mixes are cured at 158 F for 24 hours and then tested for compressive strength after 7 days.

According to Figure 4-4, with an increase in molarity of Sodium Hydroxide solution, there is an increase in the compressive strength for the 9.42% CaO flyash based geopolymer, whereas there is a decrease in the compressive strength of the 1.29% CaO flyash based geopolymer. This indicates that the compressive strength of the geopolymer concrete is dependent upon an optimum level of CaO to alkaline solution reaction.

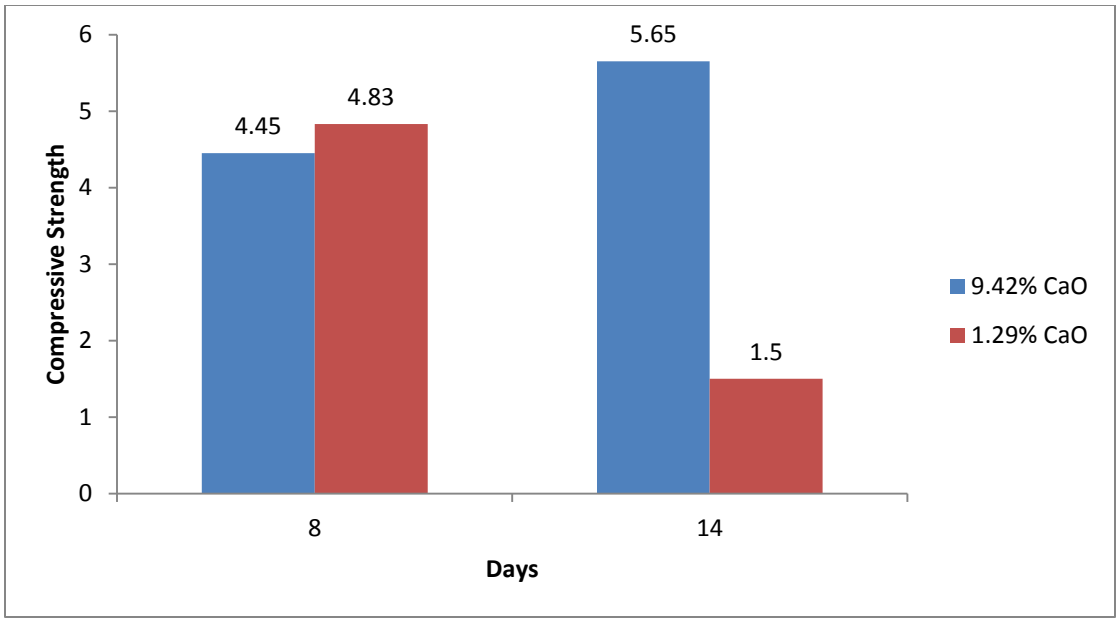

Figure 4-4 Effect of Molarity on Compressive Strength of Geopolymer Concrete

4.2.1.3. Size and Amount of Aggregates (3/8 or 5/8 or both)

Mixes I through 5 (Table 4-7) were prepared to study the effect of size and amount of aggregates on the compressive strength of the concrete. Three types of mixes, A, B and C with different sizes and amounts of aggregates were prepared (Table 4-1). Mixes 1 to 3 are based on the 9.42% CaO Flyash and mixes 4 to 5 are based on the 1.29% CaO. 14 M alkaline solutions are used in all 5 mixes. The cylinders cast from these mixes are cured at 131 F in the oven for 24 hours and then tested for compressive strength after 7 days.

Table 4-1 Types of Mix

Type of Mix	Aggregates (lb)		
	3/8	5/8	Sand
A	50	15	50
B	80	-	35
C	60	-	55

From the mixes, it can be observed that there is a substantial change in the surface area of the aggregates where the chemical reaction between the flyash and the alkaline solution takes place.

For, the 9.42% CaO flyash based geopolymer, when comparing Mix A to B, the surface area more or less remains the same as we replace the large aggregates and a portion of the sand with small aggregates whereas the compressive strength increases. On comparing Mix B to C, the compressive strength decreases with an increase in the surface area of the reaction site as a part of the smaller aggregates is replaced with sand. Thus, we can conclude that the presence of larger aggregates results in higher compressive strength in the geopolymer.

For the 1.29% CaO flyash based geopolymer, when comparing Mix A to B, there is a decrease in the compressive strength. We can conclude that the presence of larger aggregates results in higher compressive strength.

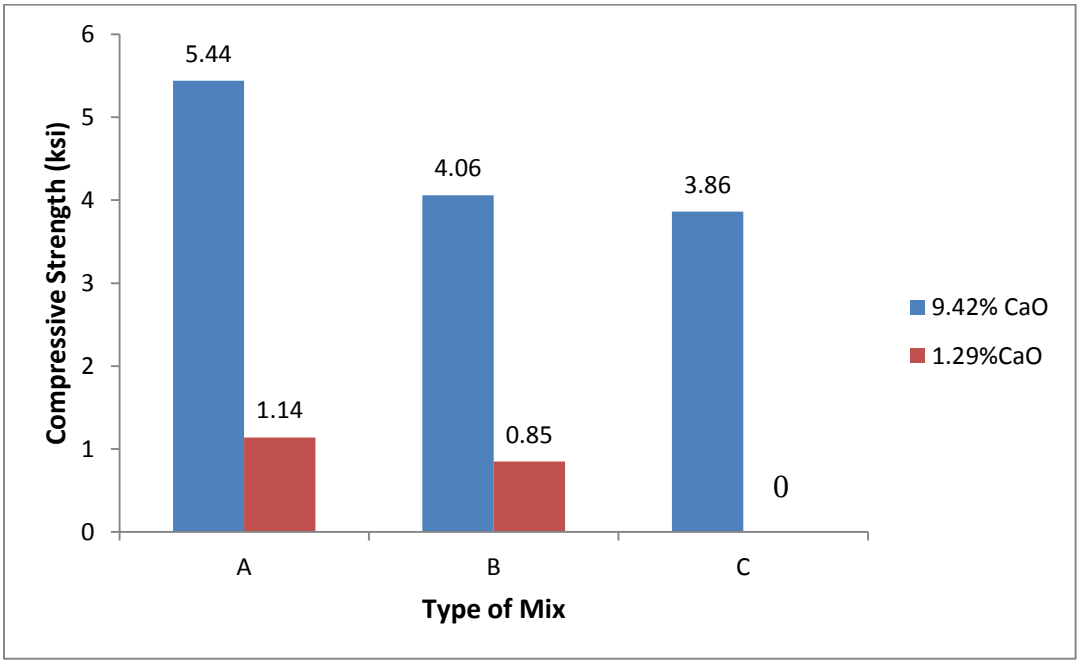

Figure 4-5 Compressive Strength Vs Type of Mix

4.2.1.4. Curing Temperature and Curing Method

Mixes 1 through 5 (Table 4-8) were made to study the effect of different curing temperatures and curing methods on the compressive strength of the concrete. The curing methods include oven – curing & steam – curing. The tests were carried out for 9.42% CaO fly ash based geopolymer for both 8M and 14M alkaline solutions. The cylinders cast are cured at 115F, 131F and 158F for 24 hours and then tested for compressive strength after 7 days. According to the research carried out, it is seen that oven curing gives the geopolymer with the most ideal mechanical properties. Although, the method itself is not ideal from a commercial point of view. Steam curing is carried out at 100% humidity in order to avoid evaporation of water from the geopolymer concrete

From the figure 4-6, it can be observed that the compressive strength increases with an increase in temperature. The highest strength is obtained by curing at 158°F in an oven. It can be concluded that the polymerization reaction taking place is a temperature driven process.

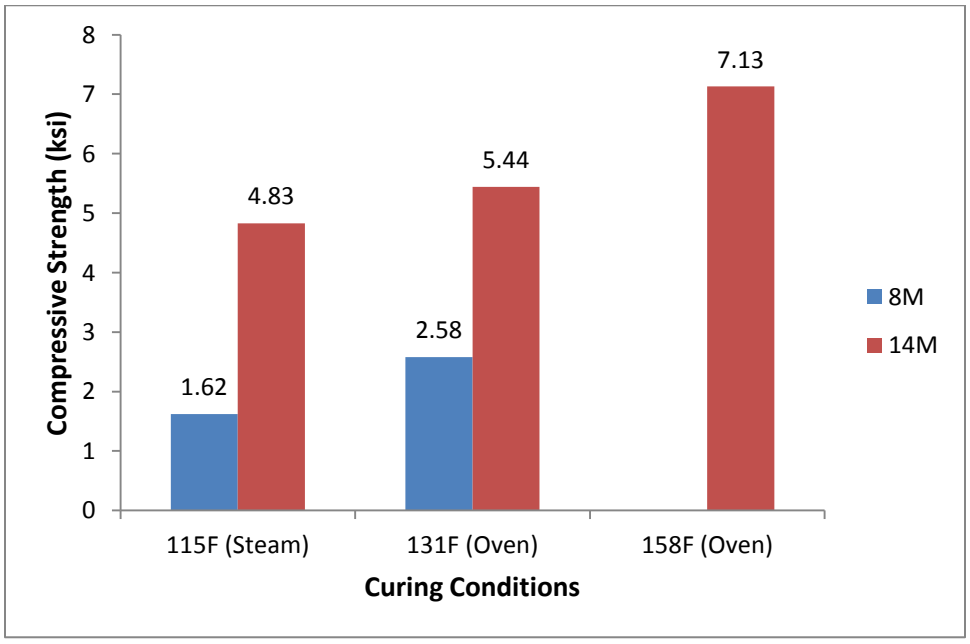

Figure 4-6 Compressive Strength Vs Curing Conditions (For 9.42% CaO Fly Ash based Geopolymer)

4.2.1.5. Curing Time

Mixes 1 through 4 (Table 4-9) were prepared to study the effect of curing time on the compressive strength of the concrete. The mixes are based on the 9.42% CaO flyash based geopolymer for both 8M and 14M alkaline solutions. The mixes were cured for 24 and 48 hours in the oven at 131F and then tested for compressive strength after 7 days. Figure 4-7 shows that the mix cured for 48 hours yields higher compressive strength than the mix cured for 24 hours. Thus, it can be concluded that the polymerization reaction taking place is a time dependent reaction. The higher molarity of NaOH enhances the kinetics of the reaction resulting in peak strength being achieved after 1 day where as in the lower molarity NaOH geopolymer there is a significant increase in strength between 1 and 2 days.

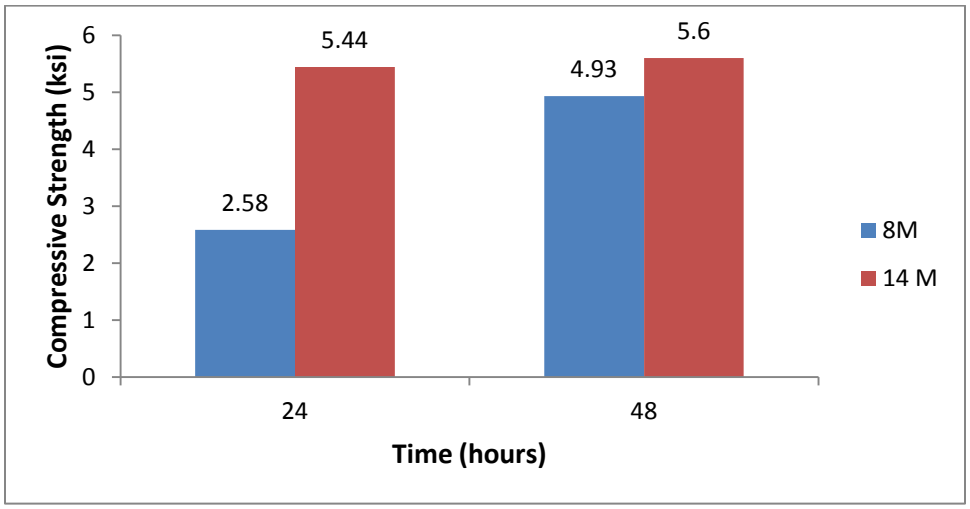

Figure 4-7 Compressive Strength Vs Time (For 9.42% CaO FlyAsh based Geopolymer)

4.2.1.6. Types of Fly Ash

Mixes 1 through 2 (Table 4-10) were made to study the effect of the fly ash on the compressive strength of the concrete. The chemical composition of fly ash varies with its place of origin (Appendix A). For this data, two different sources of flyash have been utilized. One contains 9.42% CaO and the other contains 1.29% CaO. All the parameters in both mixes remain constant. A 14M NaOH solution is used for

the chemical reaction. The cylinders cast are cured at 158 F in the oven for 24 hours and then tested for compressive strength after 7 days.

Figure 4-8 shows that mix containing fly ash of 9.42% CaO has the highest 7 days compressive strength of 5.65 ksi. It can be concluded that the percentage of CaO present in the fly ash plays a significant role in the compressive strength of the geopolymer concrete.

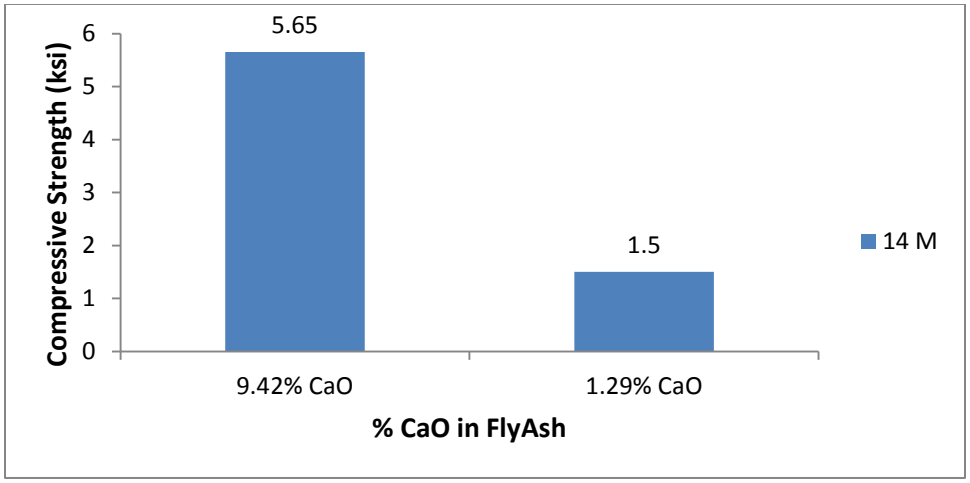

Figure 4-8 Compressive Strength Vs %CaO in Flyash

4.2.2. Mix Design

This study is focused around the design of experiment given in Tables 4-11 and 4-12. A detailed study was performed using a single class fly ash stockpile as potential source material for Geopolymer cement and chemical, X-ray diffraction (XRD), scanning electron microscopy (SEM), and energy dispersive spectroscopy analyses were performed on the Geopolymer cement and flyash samples. In addition, setting time and compressive strength tests were performed on Geopolymer cement monoliths.

A narrowed and detailed study of the 9.42% CaO flyash based geopolymer was carried out. For this mix design three different concentrations of sodium hydroxide solutions, i.e., 8M, 12M and 14M and two curing temperatures of 115F and 158 F were used. The cast cylinders were then tested for compressive strength after 1 day, 7 days and 28 days. A total of 6 batches with 36 cylinders were made

in order to understand and evaluate the underlying relationship between the chemical composition of flyash and the mechanical strength of the geopolymer formed.

4.2.3. Design of Experiments

The test specimens in this study were mainly 4” x 8” and these cylinders were used to study the compressive strength. Figure 4-9 depicts the cast cylinders. Apart from the molarity sodium hydroxide solution, curing temperature and ageing time, everything else remains constant in all 6 mixes. The following observations have been drawn:

- From Fig: 4-11, it is observed that the geopolymer formed by reacting with 8M NaOH and cured at 115 F, there is a significant increase in the compressive strength when ageing the material from 1 day to 28 days.
- From Fig: 4-11, it is observed that the geopolymer formed by reacting with 8M NaOH and cured at 158 F, there is an increase in the compressive strength when ageing the material from 1 day to 28 days.
- The setting time for all 8M NaOH mixes was observed to be about 20 minutes
- From Fig: 4-13, it is observed that For the geopolymer formed by reacting with 12M NaOH and cured at 115 F, there is a slight increase in the compressive strength when ageing the material from 1 day to 7 days and then it stabilizes, remaining the same for the 28 day test.
- From Fig: 4-13, it is observed that the geopolymer formed by reacting with 12M NaOH and cured at 158 F, there is a definite increase in the compressive strength when ageing the material from 1 day to 28 days
- The setting time for all 12M NaOH mixes was observed to be about 16 minutes.
- From Fig: 4-15, it is observed that the geopolymer formed by reacting with 14M NaOH and cured at 115 F, there is an increase in the compressive strength when ageing the material from 1 day to 28 days showing a linear increase.
- From Fig: 4-15, it is observed that the geopolymer formed by reacting with 14M NaOH and cured at 115 F, there is an increase in the compressive strength when ageing the material from 1 day to 28 days showing a linear increase with time.
- The setting time for all 14M NaOH mixes was observed to be about 8 minutes.

Figure 4-9 Cast Geopolymer Cylinders (a) 8 M (b)12 M and (c) 14 M NaOH geopolymers all with 9.42% CaO

Figure 4-10 Failure Pattern of 8M NaOH Geopolymer with 9.42% CaO flyash.

Figure 4-10 shows the failure pattern of 9.42% CaO flyash based geopolymer by reacting with 8M NaOH solution. It can be clearly observed that, there has been a columnar break which is a typical fracture behavior as observed for capped concrete cylinders under compressive loads.

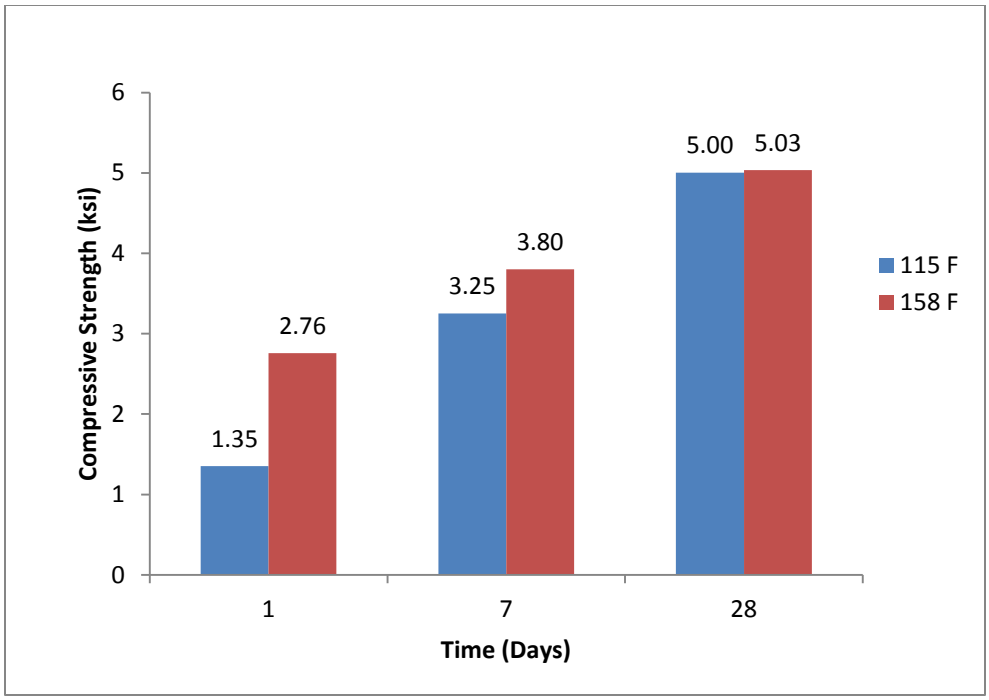

Figure 4-11 Compressive Strength Vs. Time (For 8M NaOH Geopolymer with 9.42% flyash)

Figure 4-12 Failure Pattern of 12M NaOH Geopolymer with 9.42% flyash.

Figure 4-12 shows the failure pattern of 9.42% CaO flyash based geopolymer by reacting with 12M NaOH solution. The failure pattern is a mix between a columnar break and a shear failure which is slightly different from an outright columnar break. In shear failure, the crack propagates at an angle as it moves from one end of the cylinder to the other end. This type of fracture generally indicates the cylinder failed prematurely, yielding results lower than the actual strength of the concrete.

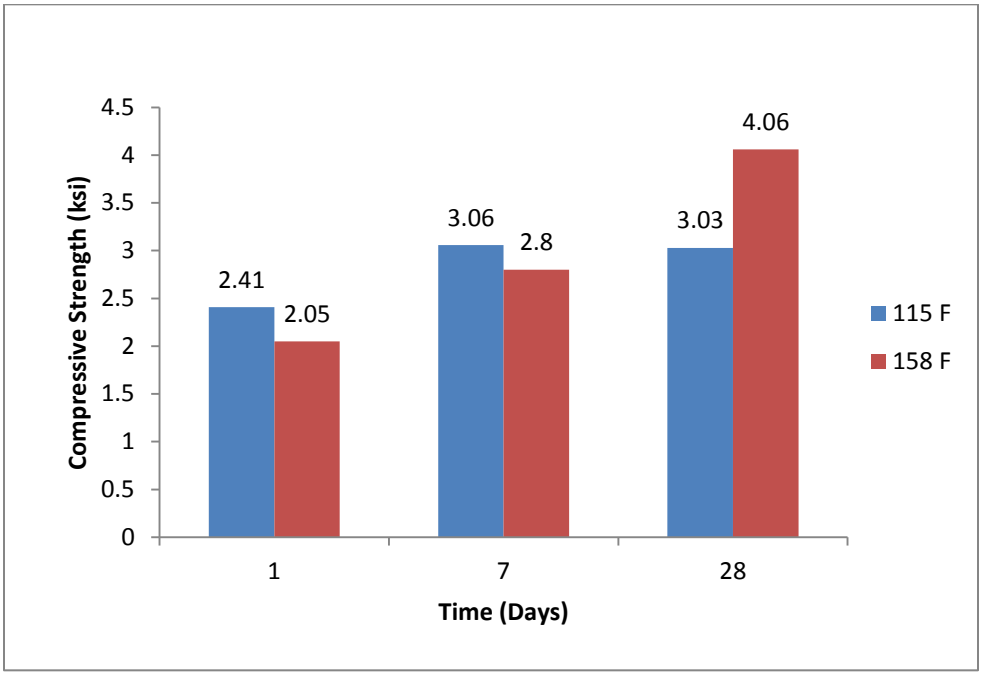

Figure 4-13 Compressive Strength Vs. Time (For 12M NaOH Geopolymer with 9.42% flyash)

Figure 4-14 Failure Pattern of 14M NaOH Geopolymer with 9.42% flyash

Figure 4-14 shows the failure pattern of 9.42% CaO flyash based geopolymer by reacting with 14M NaOH solution. The failure pattern is a mix between a columnar break and a shear failure which is slightly different from an outright columnar break. In shear failure, the crack propagates at an angle as it

moves from one end of the cylinder to the other end. This type of fracture generally indicates the cylinder failed prematurely, yielding results lower than the actual strength of the concrete.

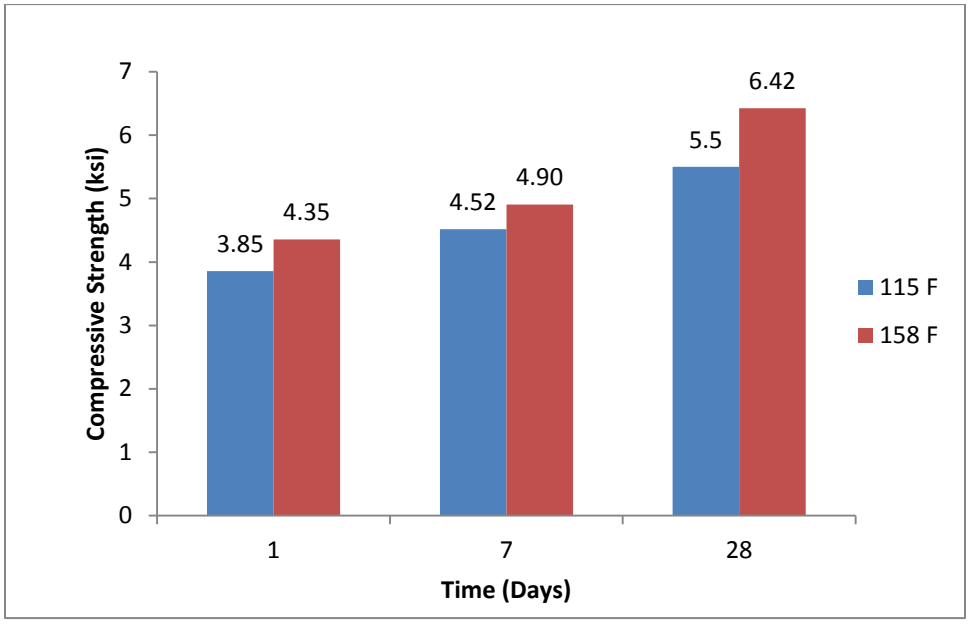

Figure 4-15 Compressive Strength Vs. Time (For 14M NaOH Geopolymer)

Table 4-2 Mix Design for different types of alkaline complexes/ solutions

Mix #	FlyAsh (lb)	Aggregates (lb)			Sodium Hydroxide Solution (lb)	Sodium Silicate Solution (lb)	Concentration of Sodium Hydroxide solution (M)	SP (lb)	Added Water	Curing Conditions		
		3/8	5/8	Sand						Time (hrs)	Temp (^{o}F)	Method
1	25.5[(a)]	50	15	50	2.6	6.5	14	0.4	1	24	131	Oven

Table 4-3 Compressive Strength of mixes with different alkaline solutions

Mix #	Hydroxide Formula	Compressive Strength (ksi) at 100% Humidity			
		1 Day		3 Days	
1.	100% NaOH	4.83	4.95	5.16	5.65
2.	100% KOH	1.56	1.23	2.13	2.22
3.	100% $Ba(OH)_2$	0.802	0.772	0.838	0.811
4.	100% LiOH	0.951	0.958	1.204	1.062
5.	100% $Mg(OH)_2$	D.N.C	D.N.C	D.N.C	D.N.C
6.	100% $Al(OH)_3$	D.N.C	D.N.C	D.N.C	D.N.C

(Note: D.N.C = Did Not Cast)

Table 4-4 Compressive Strength of mixes with complex Hydroxide solutions

Mix #	Hydroxide Formula	Compressive Strength (ksi) at 100% Humidity			
		1 Day		3 Days	
1.	90% NaOH + 10% KOH	3.254	3.006	4.133	4.154
2.	90% NaOH + 10% $Ba(OH)_2$	0.948	0.880	1.002	0.771
3.	90% NaOH + 10% LiOH	1.630	1.855	2.620	3.365
4.	90% NaOH + 10% $Mg(OH)_2$	0.336	D.N.C	D.N.C	D.N.C
5.	90% NaOH + 10% $Al(OH)_3$	0.797	0.885	1.089	D.N.C

Table 4-5 Compressive Strength of mixes with complex Hydroxide solutions

Mix #	Hydroxide Formula	Compressive Strength (ksi) at 100% Humidity			
		1 Day		3 Days	
1.	50% NaOH + 50% KOH	D.N.C	2.765	D.N.C	3.002
2.	50% NaOH + 50% $Ba(OH)_2$	0.797	0.818	0.919	0.912
3.	50% NaOH + 50% LiOH	1.238	1.285	1.630	1.855
4.	50% NaOH + 50% $Mg(OH)_2$	D.N.C	D.N.C	D.N.C	D.N.C
5.	50% NaOH + 50% $Al(OH)_3$	0.602	0.659	0.704	0.681

Table 4-6 Mix Design with Compressive Strength (Molarity of the NaOH solution)

Mix #	FlyAsh (lb)	Aggregates (lb)			Sodium Hydroxide Solution (lb)	Sodium Silicate Solution (lb)	Concentration of Sodium Hydroxide solution (M)	SP (lb)	Added Water	Curing Conditions			Compressive Strength(ksi) at 7 days
		3/8	5/8	Sand						Time (hrs)	Temp (^{o}F)	Method	
1	25.5[(a)]	80	-	35	2.6	6.5	8	0.4	1	24	158	Oven	4.54
2	25.5[(a)]	80	-	35	2.6	6.5	14	0.4	1	24	158	Oven	5.65
3	25.5[(b)]	80	-	35	2.6	6.5	8	0.4	1	24	158	Oven	4.83
4	25.5[(b)]	80	-	35	2.6	6.5	14	0.4	1	24	158	Oven	1.5

Table 4-7 Mix Design with Compressive Strength (Sizes and amounts of aggregates)

Mix #	FlyAsh (lb)	Aggregates (lb)			Sodium Hydroxide Solution (lb)	Sodium Silicate Solution (lb)	Concentration of Sodium Hydroxide solution (M)	SP (lb)	Added Water	Curing Conditions			Compressive Strength(ksi) at 7 days
		3/8	5/8	Sand						Time (hrs)	Temp (^{o}F)	Method	
1	25.5[(a)]	50	15	50	2.6	6.5	14	0.4	1	24	131	Oven	5.44

Table 4-7: *Continued*

2	25.5[(a)]	80	-	35	2.6	6.5	14	0.4	1	24	131	Oven	4.06
3	25.5[(a)]	60	-	55	2.6	6.5	14	0.4	1	24	131	Oven	3.86
4	25.5[(b)]	50	15	50	2.6	6.5	14	0.4	1	24	131	Oven	1.14
5	25.5[(b)]	80	-	35	2.6	6.5	14	0.4	1	24	131	Oven	0.85

Table 4-8 Mix Design with Compressive Strength (Curing Temperature & Method)

Mix #	FlyAsh (lb)	Aggregates (lb)			Sodium Hydroxide Solution (lb)	Sodium Silicate Solution (lb)	Concentration of Sodium Hydroxide solution (M)	SP (lb)	Added Water	Curing Conditions			Compressive Strength(ksi) at 7 days
		3/8	5/8	Sand						Time (hrs)	Temp (^{o}F)	Method	
1	25.5[(a)]	50	15	50	2.6	6.5	8	0.4	1	24	115	Steam	1.62
2	25.5[(a)]	50	15	50	2.6	6.5	8	0.4	1	24	131	Oven	2.58
3	25.5[(a)]	50	15	50	2.6	6.5	14	0.4	1	24	115	Steam	4.83
4	25.5[(a)]	50	15	50	2.6	6.5	14	0.4	1	24	131	Oven	5.44
5	25.5[(a)]	50	15	50	2.6	6.5	14	0.4	1	24	158	Oven	7.13

Table 4-9 Mix Design with Compressive Strength (Curing Time)

Mix#	FlyAsh (lb)	Aggregates (lb)			Sodium Hydroxide Solution (lb)	Sodium Silicate Solution (lb)	Concentration of Sodium Hydroxide solution (M)	SP (lb)	Added Water	Curing Conditions			Compressive Strength(ksi) at 7 days
		3/8	5/8	Sand						Time (hrs)	Temp (^{o}F)	Method	
1	25.5[(a)]	50	15	50	2.6	6.5	8	0.4	1	24	131	Oven	2.58
2	25.5[(a)]	50	15	50	2.6	6.5	14	0.4	1	24	131	Oven	5.44
3	25.5[(a)]	50	15	50	2.6	6.5	8	0.4	1	48	131	Oven	4.93
4	25.5[(a)]	50	15	50	2.6	6.5	14	0.4	1	48	131	Oven	5.60

Table 4-10 Mix Design with Compressive Strength (% CaO in FlyAsh)

Mix #	FlyAsh (lb)	Aggregates (lb)			Sodium Hydroxide Solution (lb)	Sodium Silicate Solution (lb)	Concentration of Sodium Hydroxide solution (M)	SP (lb)	Added Water	Curing Conditions			Compressive Strength(ksi) at 7 days
		3/8	5/8	Sand						Time (hrs)	Temp (^{o}F)	Method	
1	25.5[(a)]	60	-	55	2.6	6.5	14	0.4	1	24	158	Oven	5.65
2	25.5[(b)]	60	-	55	2.6	6.5	14	0.4	1	24	158	Oven	1.5

Table 4-11 Mix Design with Compressive Strength (For detailed study and anlysis)

Mix #	FlyAsh (lb)	Aggregates (lb)			Sodium Hydroxide Solution (lb)	Sodium Silicate Solution (lb)	Concentration of Sodium Hydroxide solution (M)	SP (lb)	Added Water	Curing Conditions		
		3/8	5/8	Sand						Time (hrs)	Temp (^{o}F)	Method
1	25.5[(a)]	60	-	55	2.6	6.5	8, 12, 14	0.4	1	24	115, 158	Oven

Table 4-12 Design of Experiments (For detailed analysis)

Molarity (M)	Curing Temperature (F)	Time (Days)	Compressive Strength (ksi)		Average Compressive Strength (ksi)
8	115	1	1.3	1.41	1.355
		7	3.32	3.18	3.25
		28	4.78	5.23	5.005
	158	1	2.72	2.8	2.76
		7	3.68	3.92	3.8
		28	5.18	4.89	5.035

Table 4-12 - *Continued*

12	115	1	2.68	2.14	2.41
		7	2.96	3.16	3.06
		28	2.94	3.12	3.03
	158	1	2.14	1.96	2.05
		7	2.68	2.92	2.8
		28	4	4.12	4.06
14	115	1	3.57	4.14	3.855
		7	4.48	4.56	4.52
		28	5.32	5.68	5.5
	158	1	4.23	4.48	4.355
		7	4.89	4.92	4.905
		28	6.13	6.72	6.425

Chapter 5

Microstructural and Chemical Analysis

5.1. Introduction

This preliminary study was aimed at getting a better understanding the mechanical properties of the geopolymer formed. This is achieved by analyzing six different batches of 9.42% CaO flyash based geopolymer with distinct characteristics and co-relating them to their mechanical properties. The main aspect of this study is to pinpoint the variables that affect the mechanical strength of the geopolymer by identifying the physical, chemical and crystallographic factors of the flyash and the geopolymer formed. The attributes of the geopolymer mix that are considerably influenced by flyash characteristics are the setting time and the overall mechanical properties. The setting time is influenced mainly by the CaO content in flyash as proposed in the preliminary study. In the case of the mechanical properties, in order to reduce the number of dependent variables, only the compressive strength values were used as response to perform the evaluation. The flexural strength and elastic modulus can also be obtained using the compressive strength. The compressive strength of Geopolymer cement is dependent on a fusion of physical, chemical and crystallographic factors of the FLYASH and its reaction with the alkaline solution.

5.2. XRD Analysis

XRD data was obtained using a Bragg-Brentano geometry powder diffractometer with the following testing parameter: 40KV, 30mA, and CuKα radiation. The XRD patterns were obtained by a scanning rate of 1 degree per minute from 10 to 80 degrees (2θ) and steps of 0.05 degrees (2θ). The wavelength selected was 6.065 X 10^{-7} in (15.40562 nm) (Cu). An extended review of the chemical, mineralogical and physical properties of American flyash relevant to its use in concrete has been presented by Mc. Carthy et al. (6). Table 5-1 and Table 5-2 shows the list of the crystalline phases found in the sample of the 9.42% CaO flyash and the 36 geopolymer samples. A single letter or set of letters is assigned to each phase to facilitate easier representation.

Table 5-1 List of Peaks found in the 9.42% CaO Flyash

Peaks	Compounds	Formula
Q	Quartz	SiO_2
C	Calcite	$CaCO_3$
M	Mullite	$Al_6Si_2O_{13}$
A	Alumina	Al_2O_3
X	Ca-Al-Si Complex	Albite, Microcline
L	Larnite	Ca_2SiO_4
B	Brownmillerite	$Ca_2(Al,Fe+3)_2O_5$
P	Periclase	MgO

Table 5-2 List of Peaks found in the 9.42% CaO Flyash based Geopolymer

Peaks	Compounds	Formula
Q	Quartz	SiO_2
C	Calcite	$CaCO_3$
A	Alumina	AL_20_3
X	Complex Silicate	

5.2.1. Specimen Preparation

Approximately 5g of the geopolymer is collected after carrying out the compressive test for the cast cylinder. The collected pieces of geopolymer are grounded to a fine powder by using a hammer to it. This powder consists of particles with sizes of 100µm or less. This is insured by passing the ground powder through a sieve shaker with a 100µm sieve. The fine powder is then collected and fit into a sample holder of 0.5 in radius and 0.1 in height.

The flyash, is already present as a fine powder, and is used as it is for the X-ray study.

5.2.2. Qualitative Analysis

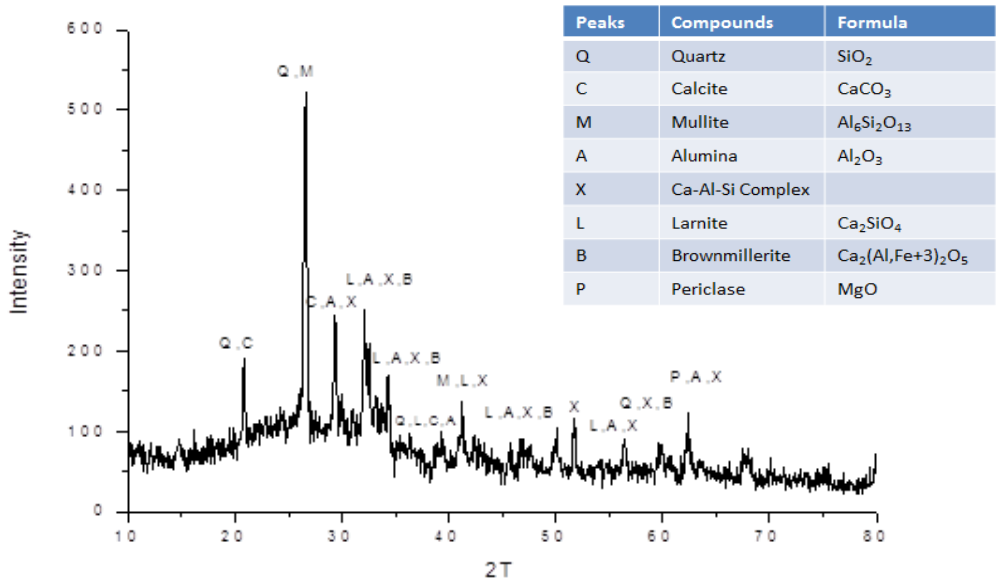

Peaks	Compounds	Formula
Q	Quartz	SiO_2
C	Calcite	$CaCO_3$
M	Mullite	$Al_6Si_2O_{13}$
A	Alumina	Al_2O_3
X	Ca-Al-Si Complex	
L	Larnite	Ca_2SiO_4
B	Brownmillerite	$Ca_2(Al,Fe{+}3)_2O_5$
P	Periclase	MgO

Figure 5-1 9.42% CaO FlyAsh

Figure 5-1 illustrates the XRD pattern for 9.42% CaO flyash. The major components of this raw ash are quartz (SiO_2) and sodium-aluminum-silica complex such as albite and microcline. The other trace materials present in this curve are alumina, larnite, brownmillerite, periclase and calcite. The presence of a broad elevation, i.e., hump from 20^o to 38^o indicates the presence of amorphous silicates which is difficult to characterize. Amorphous compounds are easier to dissolve than crystalline compounds during the first step of geopolymerization (dissolution of species), yielding higher amounts of reactive $SiO_{2\ 1}$and Al_2O_3 to combine during the transportation/coagulation phase of the geopolymeric reaction, therefore resulting in a higher degree of geopolymerization and consequently higher mechanical strength (Fernandez-Jimenez and Palomo, 2003; van Jaarsveld et al., 2003).

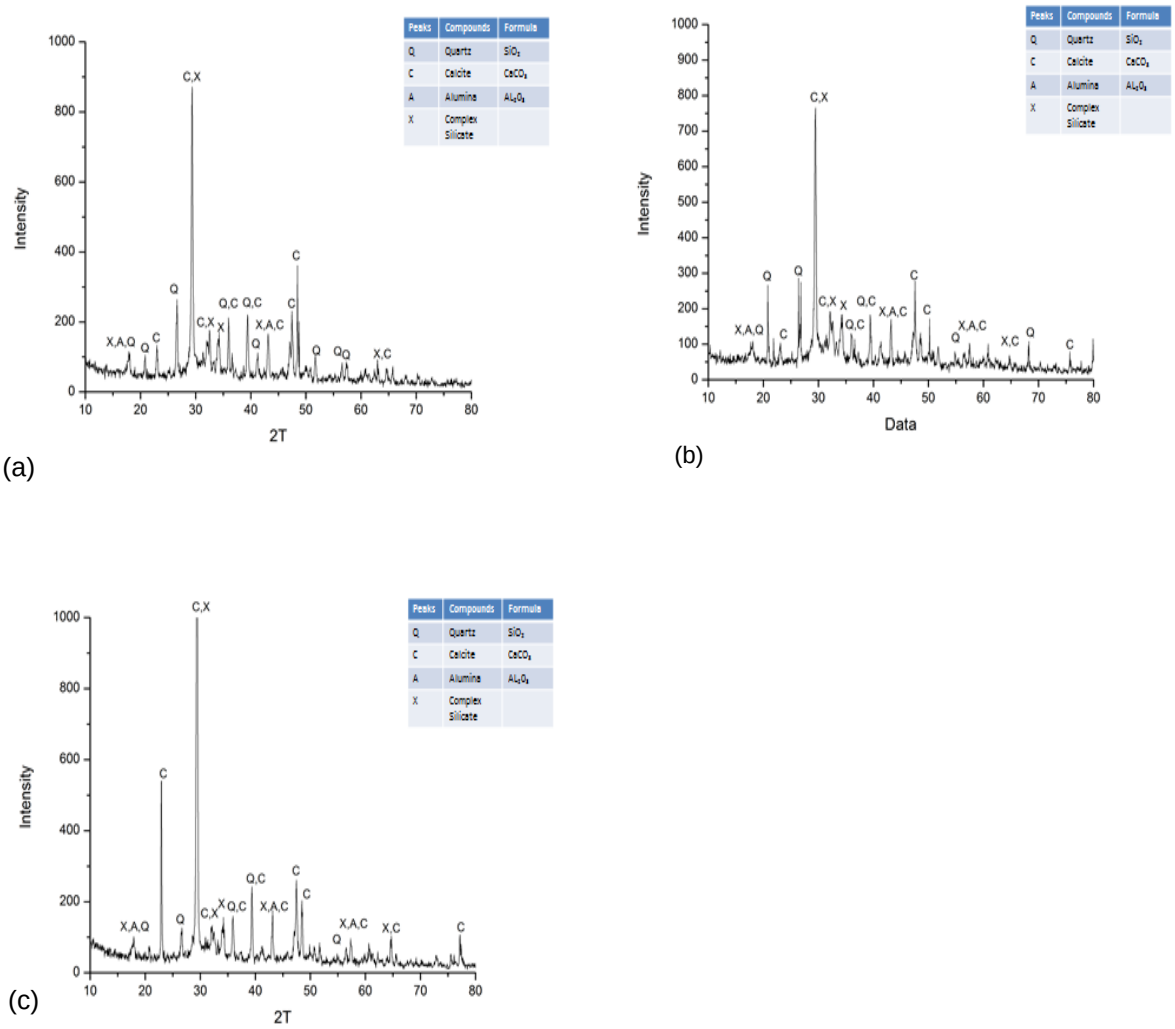

Figure 5-2 9.42% CaO, 8M NaOH, 115F (a) 1-Day (b) 7-Day (c) 28-Day

Figure 5-2 illustrates the XRD pattern for 9.42% CaO flyash based geopolymer fabricated by reaction with 8M sodium hydroxide solution, cured at 115 F and tested after 1 day, 7 days and 28 days. The main peaks correspond to Calcite ($CaCO_3$) which is formed due to the interaction between the CaO present in flyash and the alkaline solution. The quartz peaks can be attributed to the aggregate fraction in the geopolymer mix.

The unidentified complex peaks can be attributed to the formation of calcium aluminum silicate hydrate glass structures in addition to the geopolymerization products augmenting the strength of the hardened matrix.

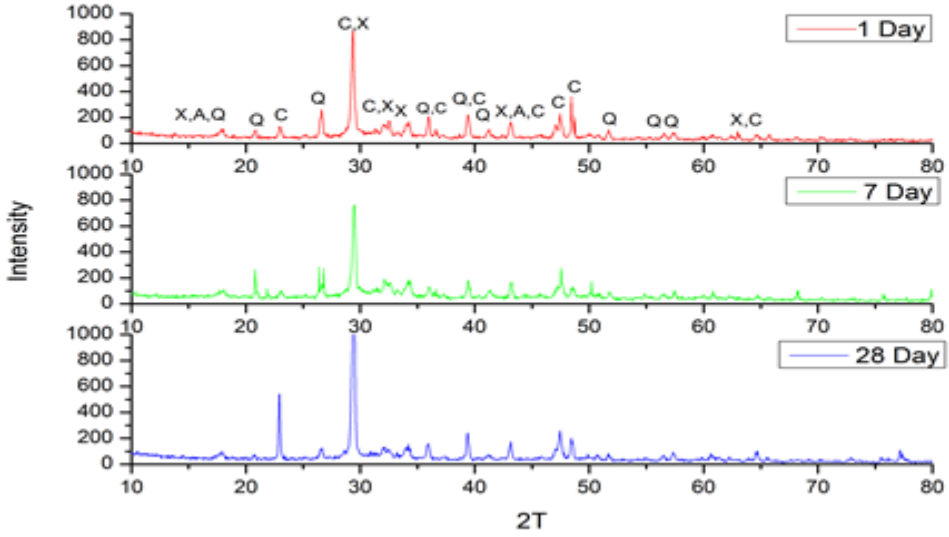

Figure 5-3 (9.42% CaO + 8M NaOH) Geopolymer at 115F

On comparing the three samples tested at 1 day, 7 days and 28 days, there is a sharpening in the calcite peaks, which indicates a continuous ongoing reaction in the mix. The increase in mechanical strength is the result of the reacted amorphous phase that cannot be identified by X ray diffraction.

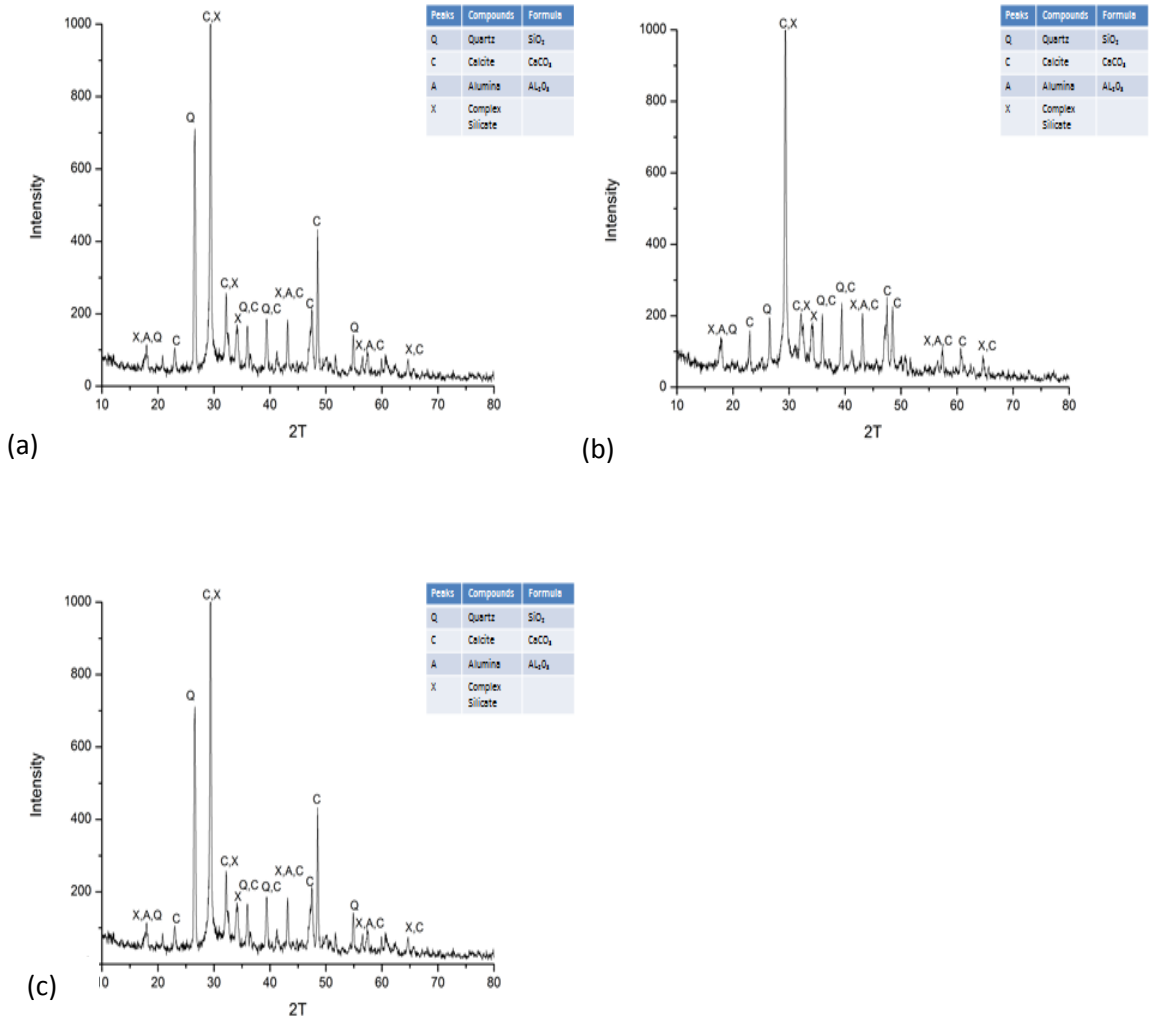

Figure 5-4 9.42% CaO, 8M NaOH, 158 F (a) 1-Day (b) 7-Day (c) 28-Day

Figure 5-4 illustrates the XRD pattern for 9.42% CaO flyash based geopolymer fabricated by reaction with 8M sodium hydroxide solution, cured at 158 F and tested after 1 day, 7 days and 28 days. The main peaks correspond to Calcite ($CaCO_3$) which is formed due to the interaction between the CaO present in flyash and the alkaline solution. The quartz peaks can be attributed to the aggregate fraction in the geopolymer mix. The unidentified complex peaks can be attributed to the formation of calcium

aluminum silicate hydrate glass structures in addition to the geopolymerization products augmenting the strength of the hardened matrix.

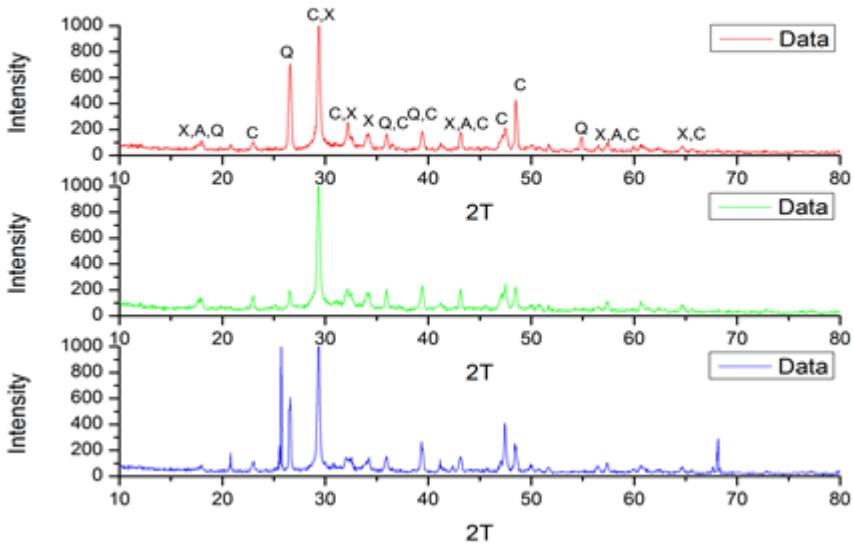

Figure 5-5 (9.42% CaO + 8M NaOH) Geopolymer at 158F

On comparing the three samples tested at 1 day, 7 days and 28 days, there is a sharpening in the calcite peaks, which indicates a continuous ongoing reaction in the mix. The increase in mechanical strength is the result of the reacted amorphous phase that cannot be identified by X ray diffraction.

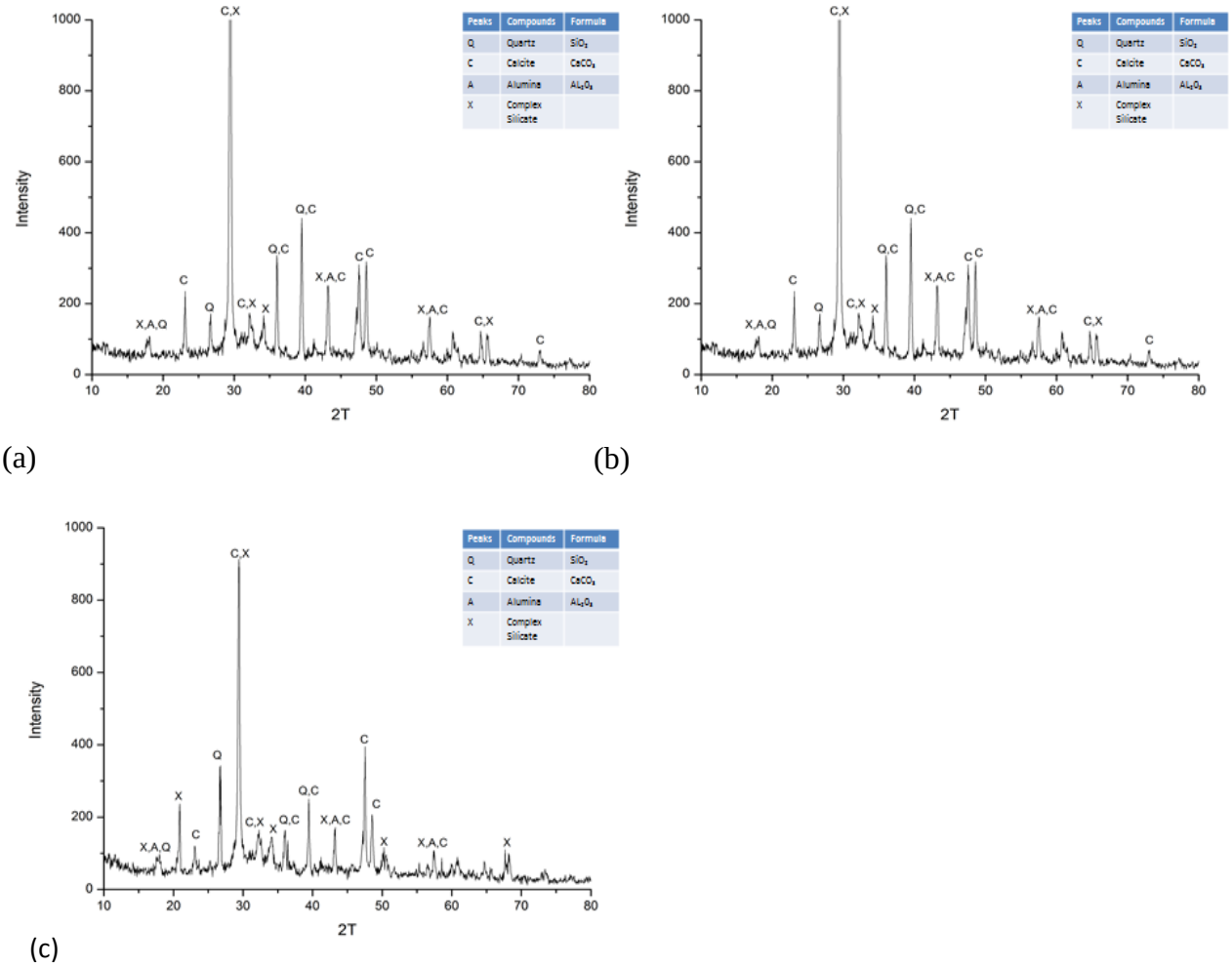

Figure 5-6 9.42% CaO, 12M NaOH, 115 F (a) 1-Day (b) 7-Day (c) 28-Day

Figure 5-6 illustrates the XRD pattern for 9.42% CaO flyash based geopolymer fabricated by reaction with 12M sodium hydroxide solution, cured at 115 F and tested after 1 day, 7 days and 28 days. The main peaks correspond to Calcite ($CaCO_3$) which is formed due to the interaction between the CaO present in flyash and the alkaline solution. The quartz peaks can be attributed to the aggregate fraction in the geopolymer mix. The unidentified complex peaks can be attributed to the formation of calcium aluminum silicate hydrate glass structures in addition to the geopolymerization products augmenting the strength of the hardened matrix.

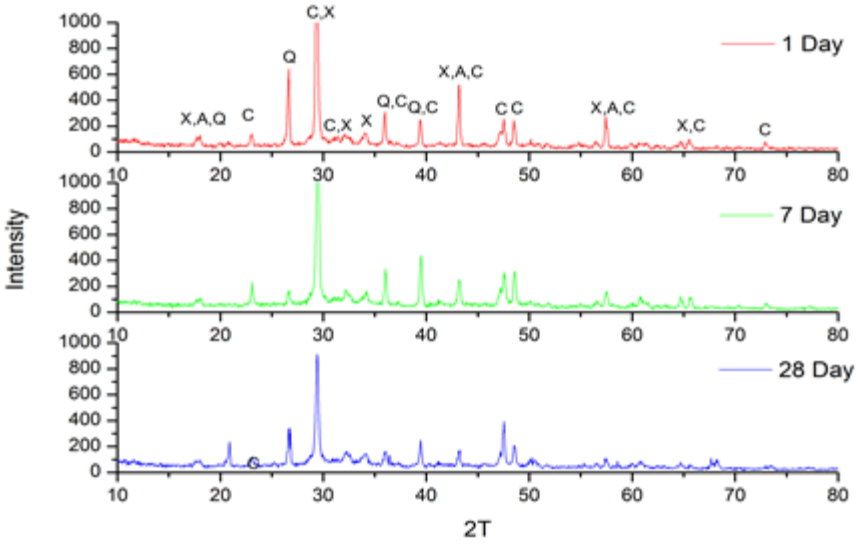

Figure 5-7 (9.42% CaO + 12M NaOH) Geopolymer at 115F

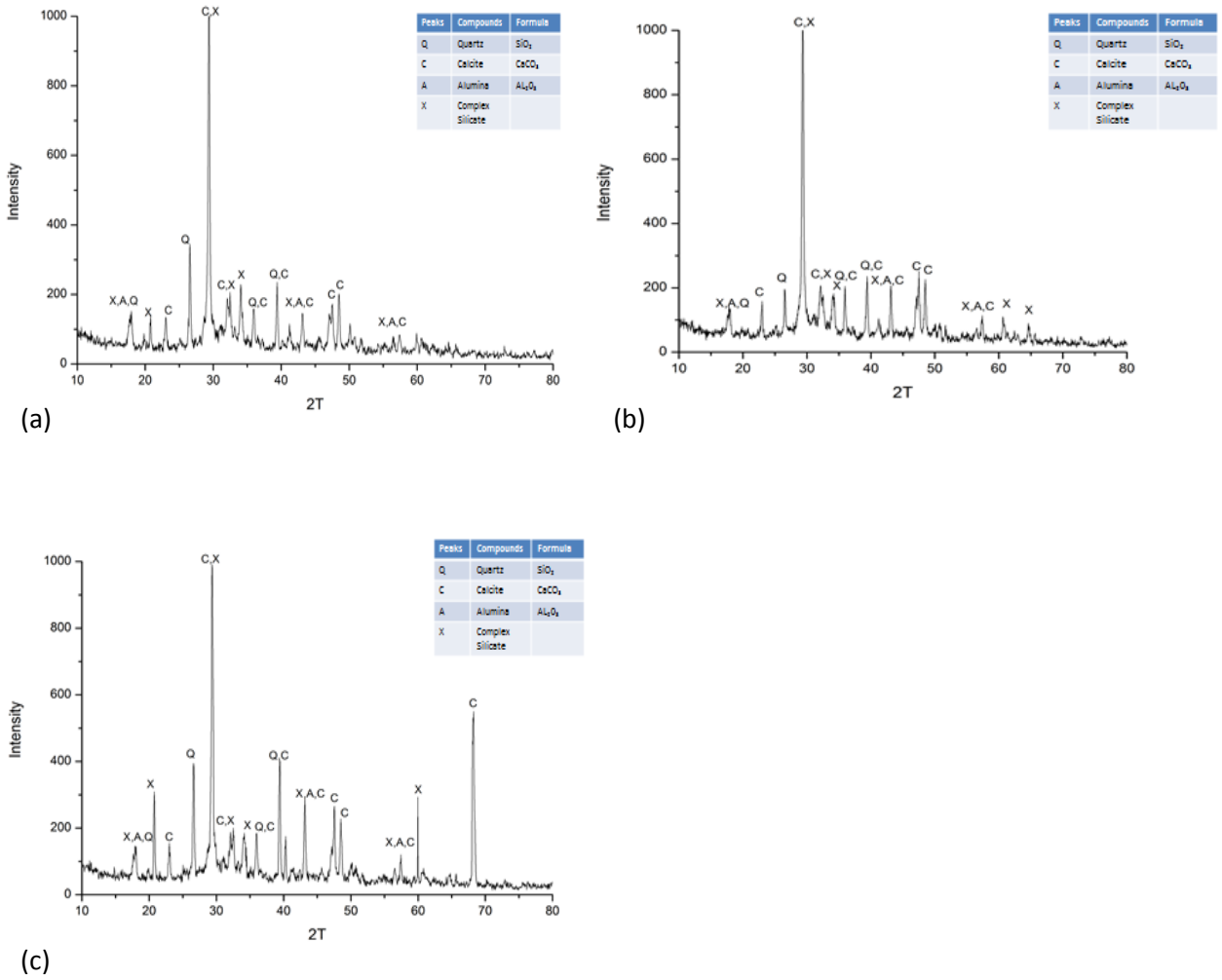

Figure 5-8 9.42% CaO, 12M NaOH, 158 F (a) 1-Day (b) 7-Day (c) 28-Day

Figure 5-8 illustrates the XRD pattern for 9.42% CaO flyash based geopolymer fabricated by reaction with 12M sodium hydroxide solution, cured at 158 F and tested after 1 day, 7 days and 28 days. The main peaks correspond to Calcite ($CaCO_3$) which is formed due to the interaction between the CaO present in flyash and the alkaline solution. The quartz peaks can be attributed to the aggregate fraction in the geopolymer mix. The unidentified complex peaks can be attributed to the formation of calcium

aluminum silicate hydrate glass structures in addition to the geopolymerization products augmenting the strength of the hardened matrix.

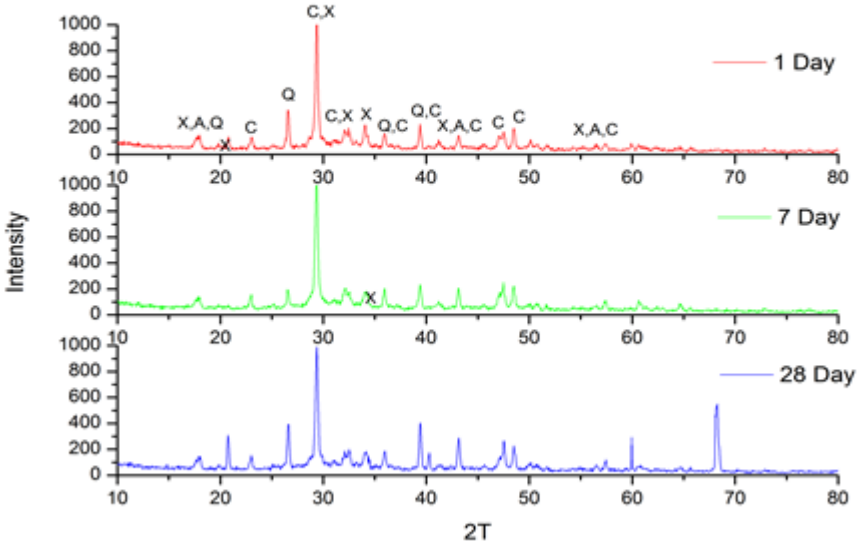

Figure 5-9 (9.42% CaO + 12M NaOH) Geopolymer at 158F

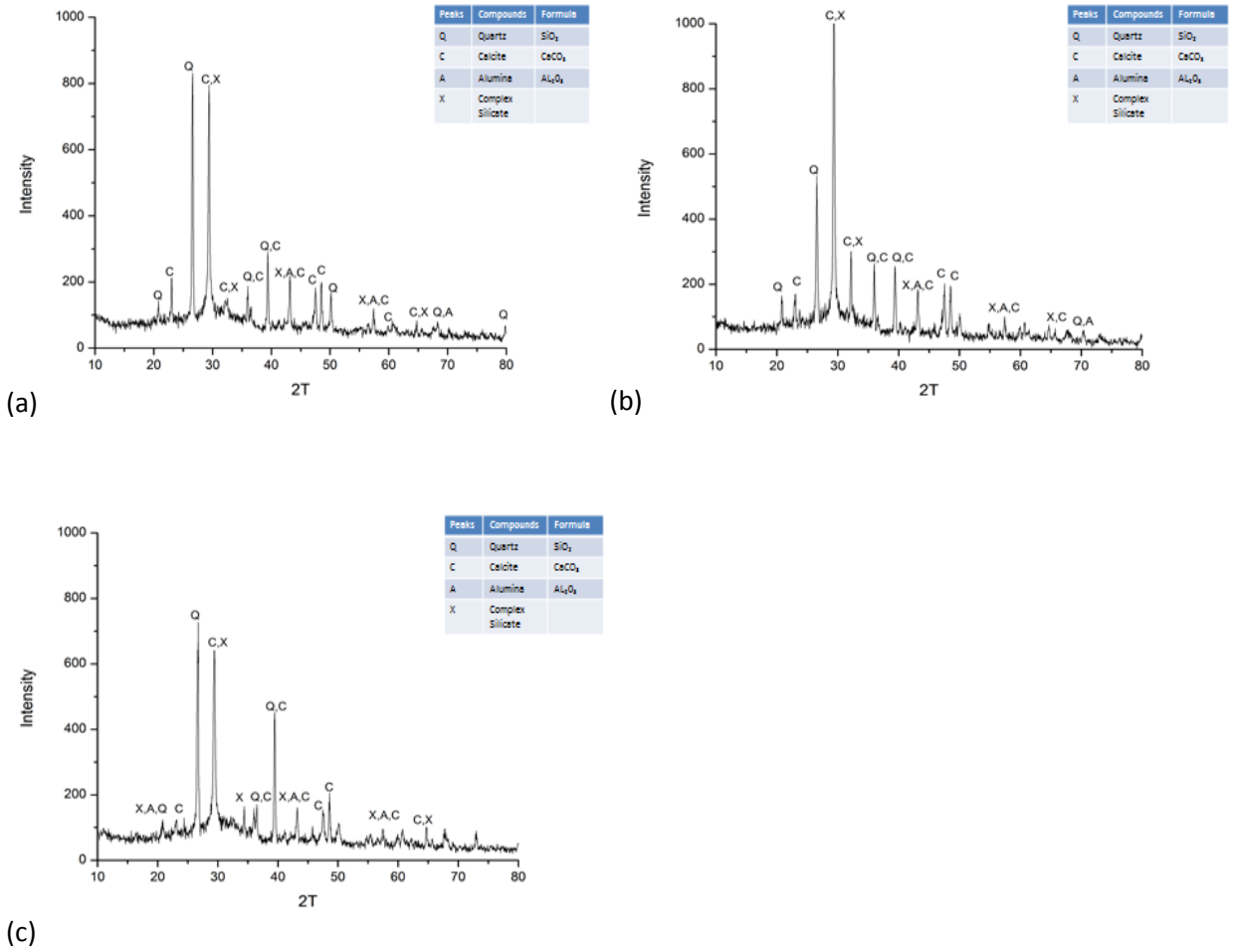

Figure 5-10 9.42% CaO, 14M NaOH, 115 F (a) 1-Day (b) 7-Day (c) 28-Day

Figure 5-10 illustrates the XRD pattern for 9.42% CaO flyash based geopolymer fabricated by reaction with 14M sodium hydroxide solution, cured at 115 F and tested after 1 day, 7 days and 28 days. The main peaks correspond to Calcite ($CaCO_3$) which is formed due to the interaction between the CaO present in flyash and the alkaline solution. The quartz peaks can be attributed to the aggregate fraction in the geopolymer mix. The unidentified complex peaks can be attributed to the formation of calcium aluminum silicate hydrate glass structures in addition to the geopolymerization products augmenting the strength of the hardened matrix.

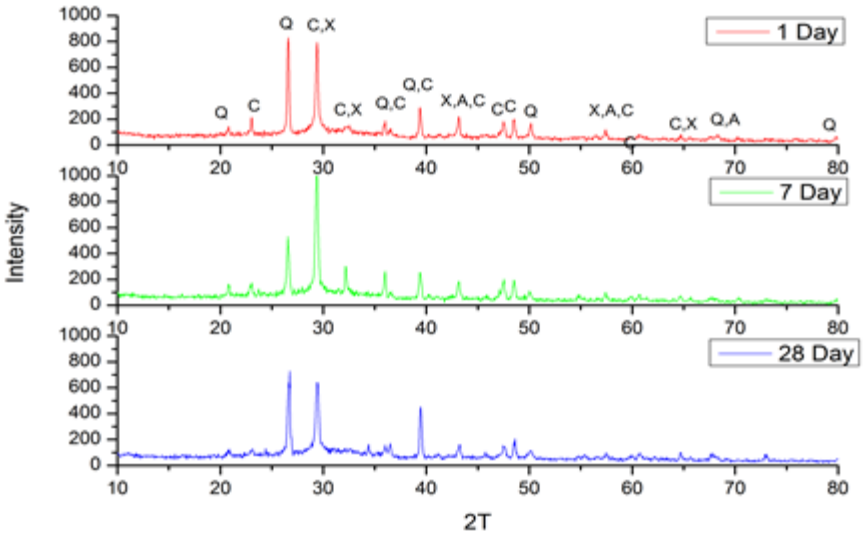

Figure 5-11 (9.42% CaO + 14M NaOH) Geopolymer at 115 F

The increase in mechanical strength is the result of the reacted amorphous phase that cannot be identified by X ray diffraction.

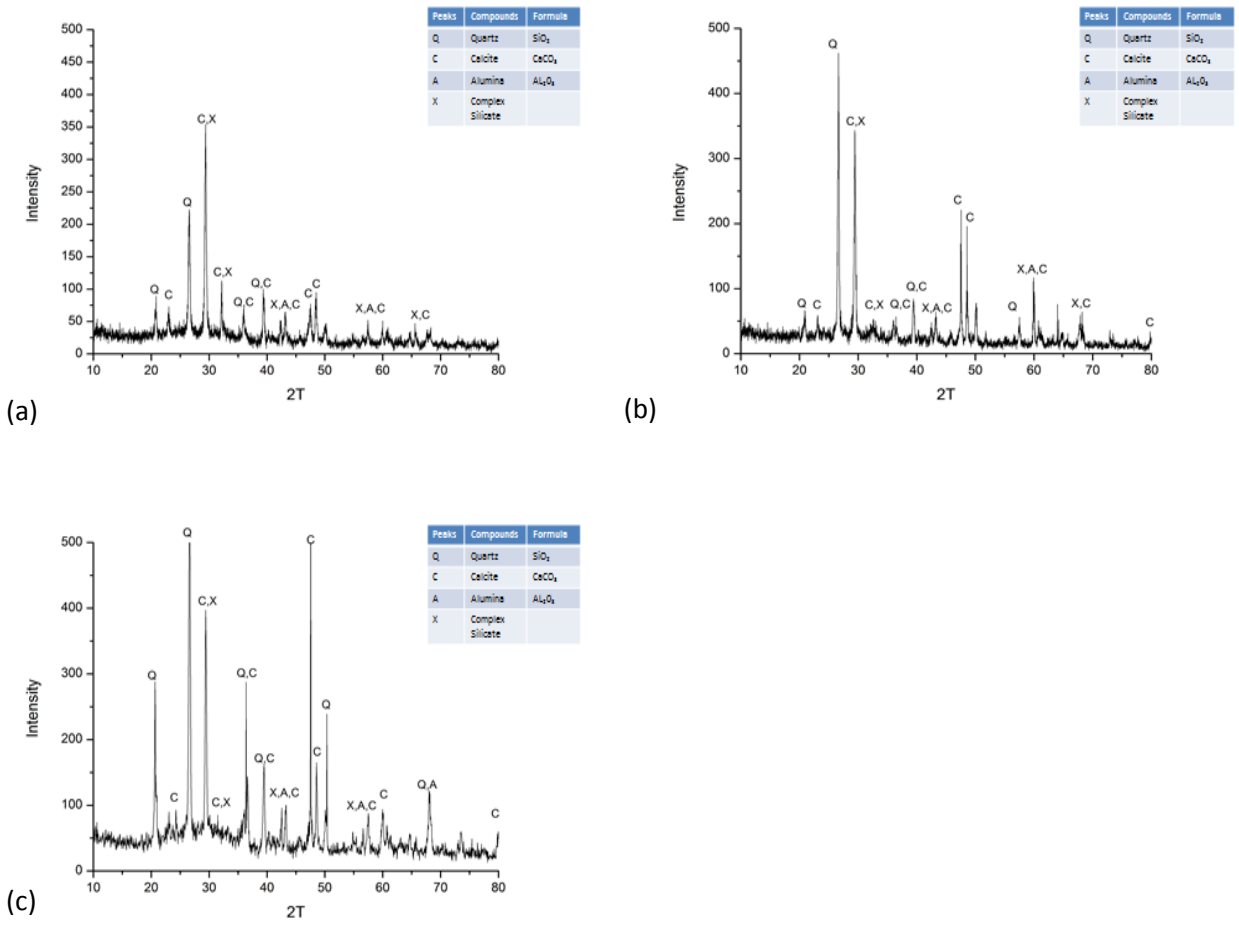

Figure 5-12 9.42% CaO, 14M NaOH, 158 F (a) 1-Day (b) 7-Day (c) 28-Day

Figure 5-12 illustrates the XRD pattern for 9.42% CaO flyash based geopolymer fabricated by reaction with 14M sodium hydroxide solution, cured at 115 F and tested after 1 day, 7 days and 28 days. The main peaks correspond to Calcite ($CaCO_3$) which is formed due to the interaction between the CaO present in flyash and the alkaline solution. The quartz peaks can be attributed to the aggregate fraction in the geopolymer mix. The unidentified complex peaks can be attributed to the formation of calcium aluminum silicate hydrate glass structures in addition to the geopolymerization products augmenting the strength of the hardened matrix.

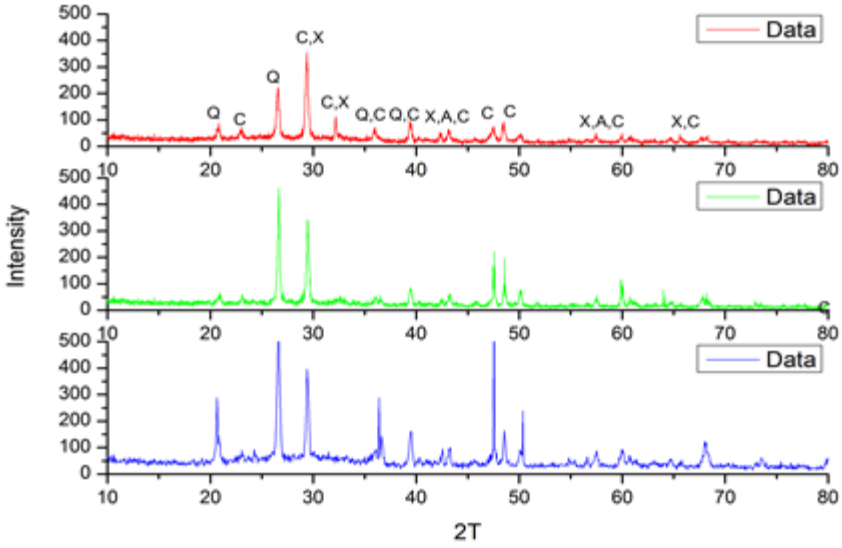

Figure 5-13 (9.42% CaO + 14M NaOH) Geopolymer at 158 F

The increase in mechanical strength is the result of the reacted amorphous phase that cannot be identified by X ray diffraction.

Table 5-3 Crystalline Phases Present In 9.42% CaO Geopolymer Mixes

Molarity of NaOH	Curing Conditions		Average Compressive Strength (ksi)	Crystalline Phases Present
	Curing Temperature (K)	Ageing Time (Days)		
8	115	1	1.355	SiO_2, $CaCO_3$, Al_2O_3, Ca_2SiO, Ca3SiO5
		7	3.25	SiO_2, $CaCO_3$, Al_2O_3, Ca_2SiO, Ca3SiO5
		28	5.005	SiO_2, $CaCO_3$, Al_2O_3, Ca_2SiO, Ca3SiO5
	158	1	2.76	SiO_2, $CaCO_3$, Al_2O_3, Ca_2SiO, Ca3SiO5
		7	3.8	SiO_2, $CaCO_3$, Al_2O_3, Ca_2SiO, Ca3SiO5
		28	5.035	SiO_2, $CaCO_3$, Al_2O_3, Ca_2SiO, Ca3SiO5
12	115	1	2.41	SiO_2, $CaCO_3$, Al_2O_3, Ca_2SiO, Ca3SiO5
		7	3.06	SiO_2, $CaCO_3$, Al_2O_3, Ca_2SiO, Ca3SiO5
		28	3.03	SiO_2, $CaCO_3$, Al_2O_3, Ca_2SiO, Ca3SiO5
	158	1	2.05	SiO_2, $CaCO_3$, Al_2O_3, Ca_2SiO, Ca3SiO5
		7	2.8	SiO_2, $CaCO_3$, Al_2O_3, Ca_2SiO, Ca3SiO5
		28	4.06	SiO_2, $CaCO_3$, Al_2O_3, Ca_2SiO, Ca3SiO5

Table 5-3 - *Continued*

14	115	1	3.855	SiO_2, $CaCO_3$, Al_2O_3, Ca_2SiO, Ca3SiO5
		7	4.52	SiO_2, $CaCO_3$, Al_2O_3, Ca_2SiO, Ca3SiO5
		28	5.5	SiO_2, $CaCO_3$, Al_2O_3, Ca_2SiO, Ca3SiO5
	158	1	4.355	SiO_2, $CaCO_3$, Al_2O_3, Ca_2SiO, Ca3SiO5
		7	4.905	SiO_2, $CaCO_3$, Al_2O_3, Ca_2SiO, Ca3SiO5
		28	6.425	SiO_2, $CaCO_3$, Al_2O_3, Ca_2SiO, Ca3SiO5

On comparing the XRD pattern of the flyash from Figure 5-19 with the XRD patterns of the geopolymers, it can be seen that there has been an obvious change in the flyash chemistry since crystalline phases such as Mullite. Periclase and Brownmillerite are nowhere to be seen in the latter. There, are some crystalline phases originally existent in the flyash (quartz, alumia, and calcite) which have not been transformed by the activation reaction. This relatively large amount of fly ash still present in the hardened samples is an indicator of incomplete geopolymerisation reaction. Results suggest that the structure of these geopolymers is typically glass-like.

The chemical composition of the flyash samples is summarized in Table 5-1. It is important to mention that the crystalline phases reported in Table 5-3 are equivalents in their respective oxide form, as these may be combined in more complex crystalline or amorphous phases. The chemical composition is given in equivalents throughout this manuscript, this helps to simplify the analysis and have a better perspective of the chemical composition. Another important factor to note; the existence of complex amorphous phases cannot be detected by the X ray diffraction and for the case of the geopolymer formed, they seem to be the main factor dictating the mechanical properties.

Figure 5-1 through 5-13 shows XRD patterns for FLYASH and hardened geopolymer paste (GPP). The samples are mostly composed by a vitreous phase. Quartz is found in small amounts along with calcite and traces of other crystalline phases such as alumina, larnite and calcium silicate are found as well. The patterns also show that crystalline phases still remain after the geopolymerization, although in smaller amounts. In addition, the broad amorphous background feature in the region $2\Theta = 20–45°$, present in all samples after thermal treatment, suggests that the main reaction product formed is “alkaline aluminosilicate gel” with low-ordered crystalline structure. This can be predicted as a value typical of calcium aluminate glass structure that is significantly more reactive with water compared with the siliceous glass structure (Diamond, 1983). This leads to the formation of calcium silicate hydrate compounds additional to the geopolymerization products, augmenting the mechanical strength of the hardened matrix.

5.3. SEM-EDX Analysis

SEM micrographs of the samples were taken using Hitachi S-3000N Variable Pressure scanning electron microscope. SEM was performed to show the ash particles morphology and topography before and after the geopolymerization process. The role of particle morphology has been emphasized by many authors for its significant impact on the resulting geopolymer (Provis et al., 2010; Hunger and Brouwers, 2009). For this analysis, the working distance is around 10 – 25mm; the accelerated voltage is fluctuated between 20 – 25kV and the images are observed at 60 – 100X magnification. All images are secondary images and observed in high vaccum. The SEM is equipped with an EDX which was used to characterize the microstructure and the chemical compositions of 18 geopolymer samples.

5.3.1. Specimen Preparation

Post mechanical testing of the geopolymer samples, the fabricated geopolymer cylinder is broken down into pieces using a masonry cutting wheel with a diamond blade. The dimensions of the piece are approximately 0.5” X 0.35”. These samples are then cast in epoxy so as to get a smooth surface finish. The cast sample is cut and polished prior to coating with a layer of conductive silver in order to carry out the necessary imaging.

5.3.2. Qualitative Analysis

The microstructure, edx chemical distribution and elemental mapping of a geopolymer formed from reacting 9.42% CaO flyash with 8M, 12M and 14 M NaOH solution is shown in Figure 5-13 through 5-49. This illustrates the different chemical phases present in the mix. The corresponding EDX analysis confirms the presence of silicon, calcium, aluminum, sodium, potassium and iron. The presence of silica could be attributed to the aggregates present in the mix. This silica phase is embedded in a calcium carbonate rich matrix. A thin layer of aluminum-sodium-calcium with trace deposits of magnesium and iron runs along the ridges of the silica deposits. Thus, indicating the presence of feldspar like material.

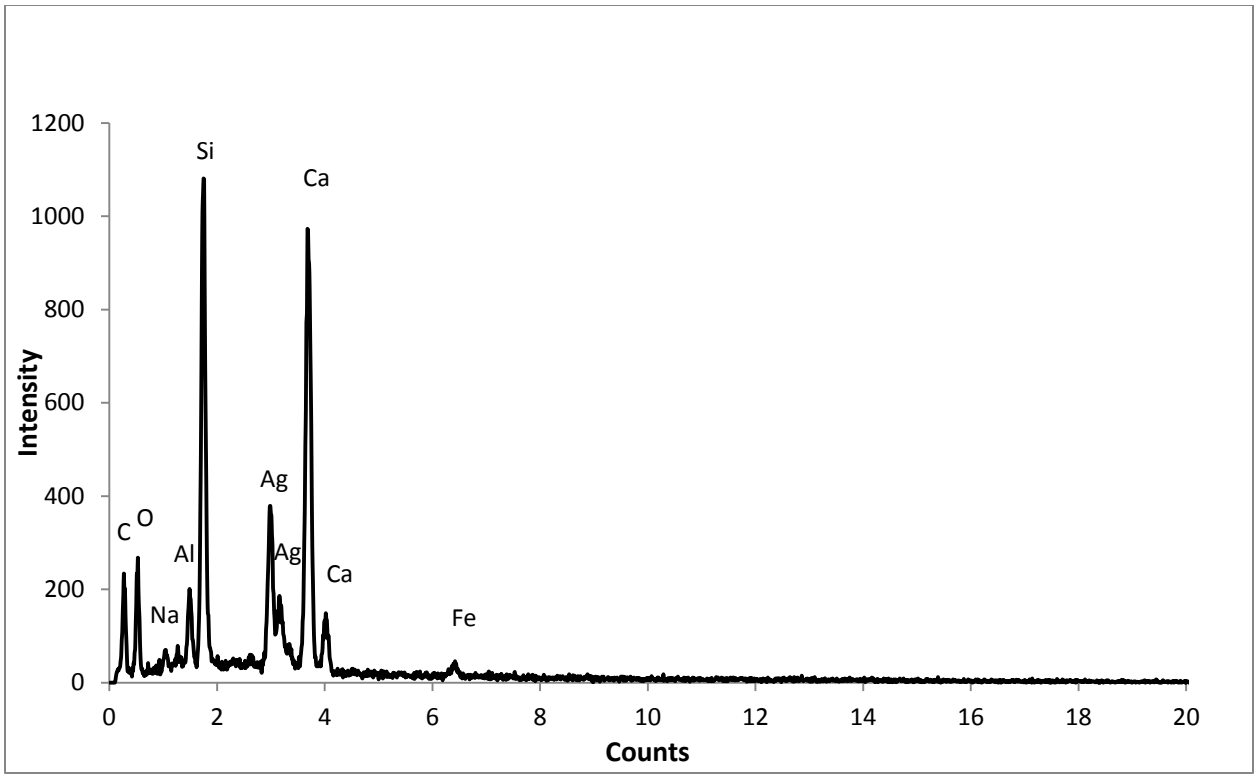

Figure 5-14 : 9.42% CaO, 8M NaOH, 115F, 1 Day EDX

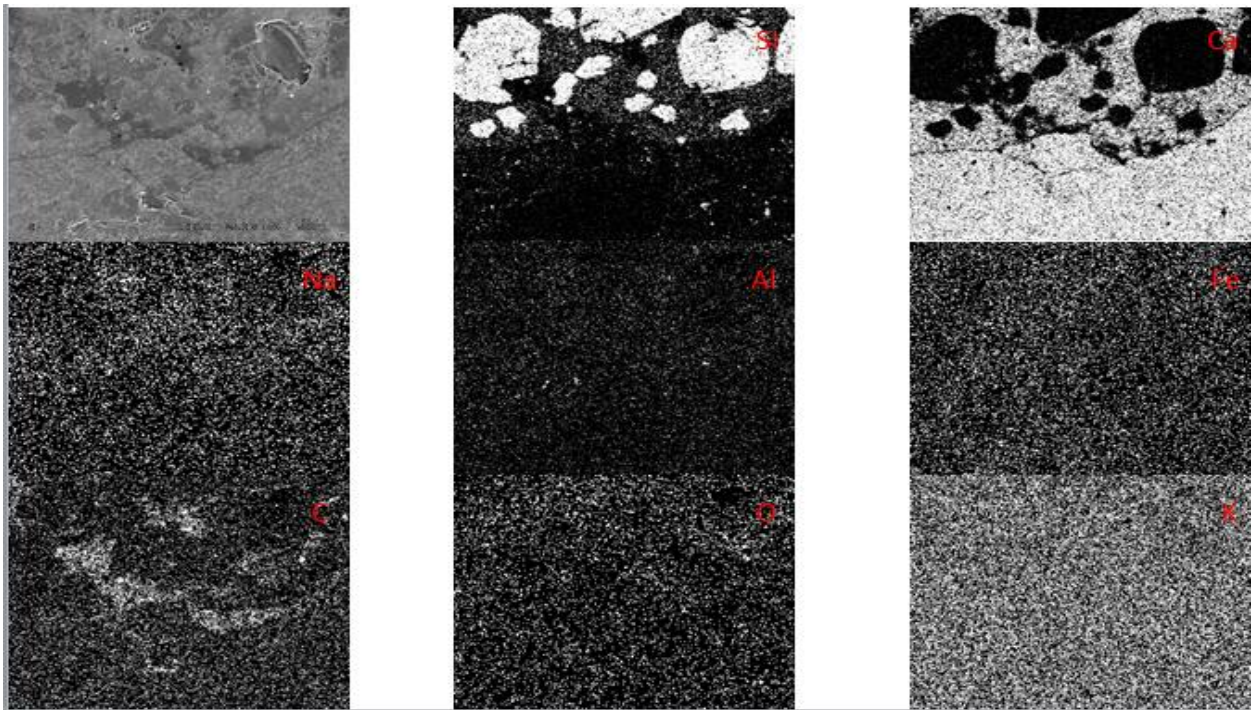

Figure 5-15 Elemental Mapping of 9.42% CaO flyash, 8M NaOH, 115F, 1 Day test sample

The edx chemical distribution graph and elemental mapping for 9.42% CaO flyash based geopolymer reacted with 8M NaOH solution, cured at 115F and tested after 1 Day is shown in figure 5-14 and figure 5-15. From these figures, it is obvious that the main chemical species present is silicon and calcium. From the elemental mapping, it is clear that there are three zones that are present which include a silicon rich zone, a calcium enriched zone and a complex zone which contains all species including calcium, silicon, aluminum, iron, sodium, oxygen, magnesium and carbon. All the crystalline phases were identified by the x ray diffraction method. A deduction can be made regarding this complex amorphous phase. It seems to have formed a reaction zone around the unreacted silica particles and is responsible for the binder properties in geopolymer concrete. The calcium enriched zone must be from the calcite identified by the X ray diffraction.

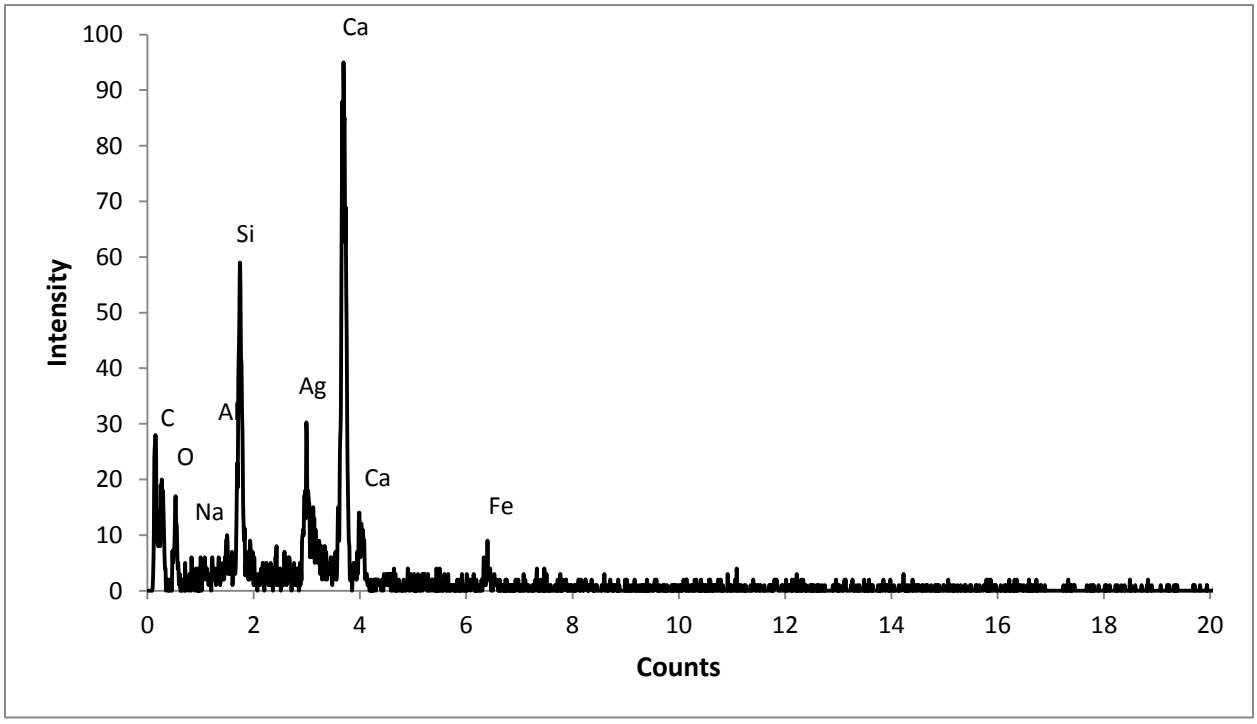

Figure 5-16 9.42% CaO, 8M NaOH, 115F, 7 Day EDX

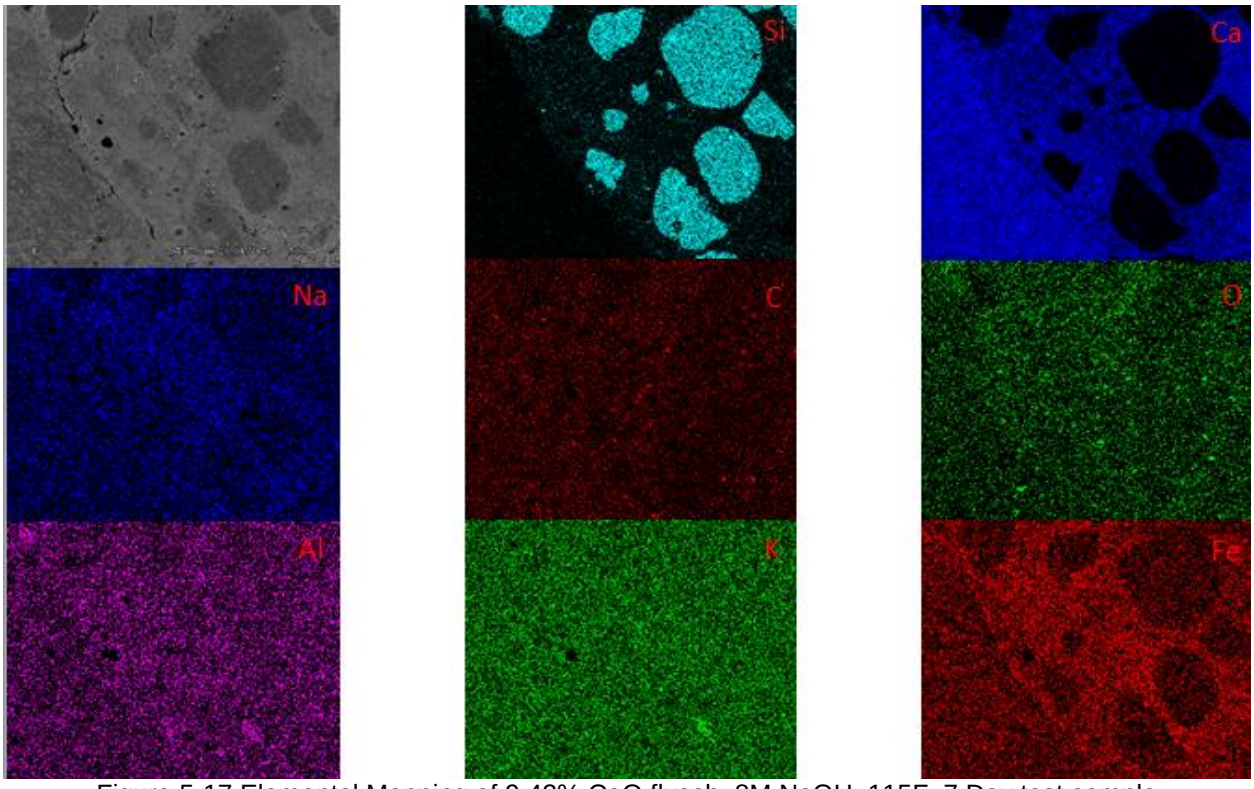

Figure 5-17 Elemental Mapping of 9.42% CaO flyash, 8M NaOH, 115F, 7 Day test sample

The edx chemical distribution graph and elemental mapping for 9.42% CaO flyash based geopolymer reacted with 8M NaOH solution, cured at 115F and tested after 7 Day is shown in figure 5-16 and figure 5-17. From these figures, it can be seen that the three zones are more distinct and clear. There is definitely lesser iron and sodium content in the silicon and calcium enriched zone. This gives more conclusive proof about the presence of an amorphous complex zone which has formed a mesh around the silicon particles

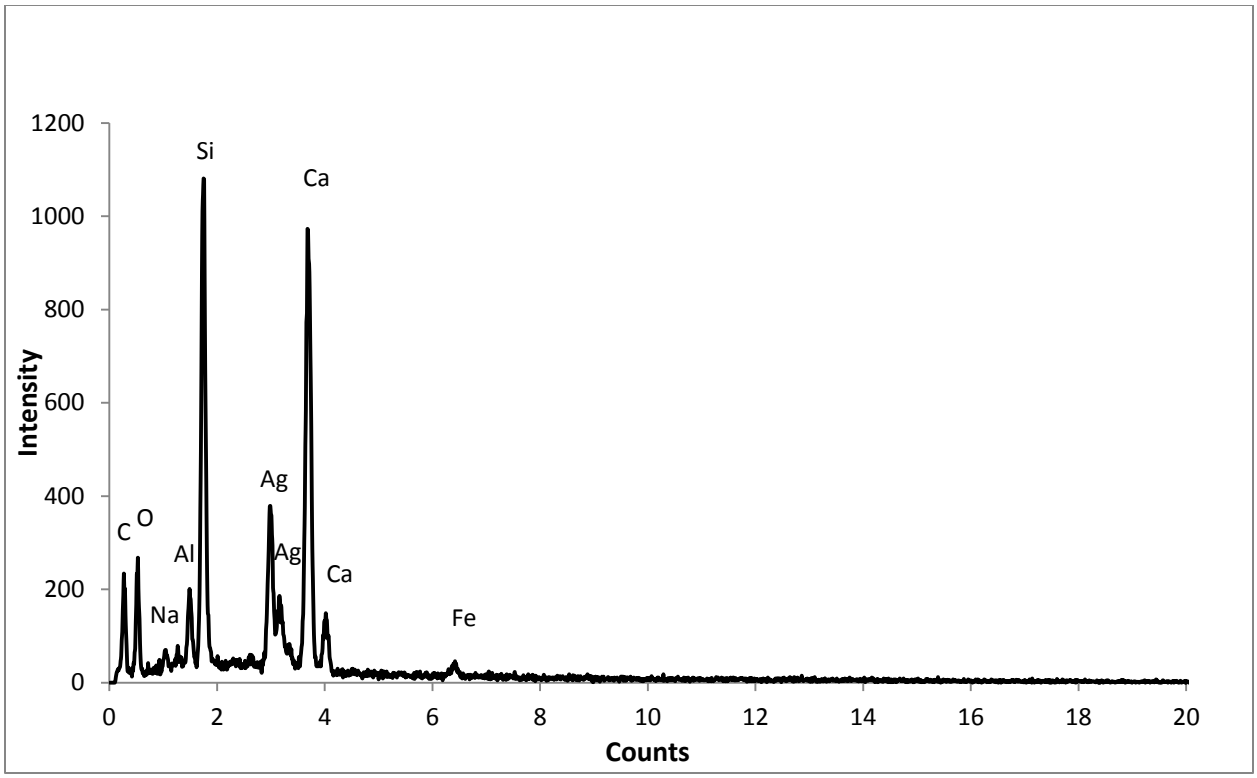

Figure 5-18 9.42% CaO, 8M NaOH, 115F, 28 Day EDX

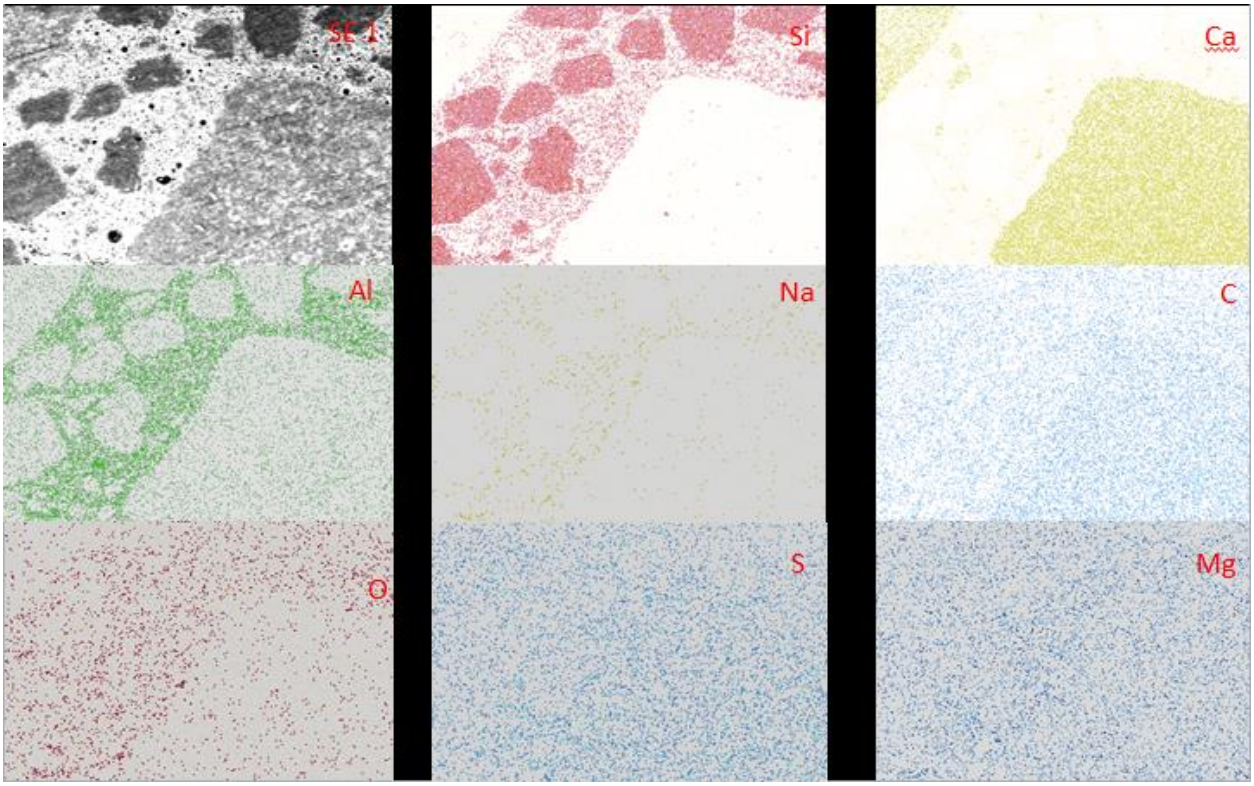

Figure 5-19 Elemental Mapping of 9.42% CaO flyash, 8M NaOH, 115F, 28 Day test sample

The energy dispersive spectroscopy (EDS) chemical distribution graph and elemental mapping for 9.42% CaO flyash based geopolymer reacted with 8M NaOH solution, cured at 115F and tested after 28 Day is shown in figure 5-18 and figure 5-19. From these figures, it can be seen that the three zones are more distinct and clear. Fig 5-19 shows us that silica has reacted with magnesium and sodium leading to the formation of feldspar.

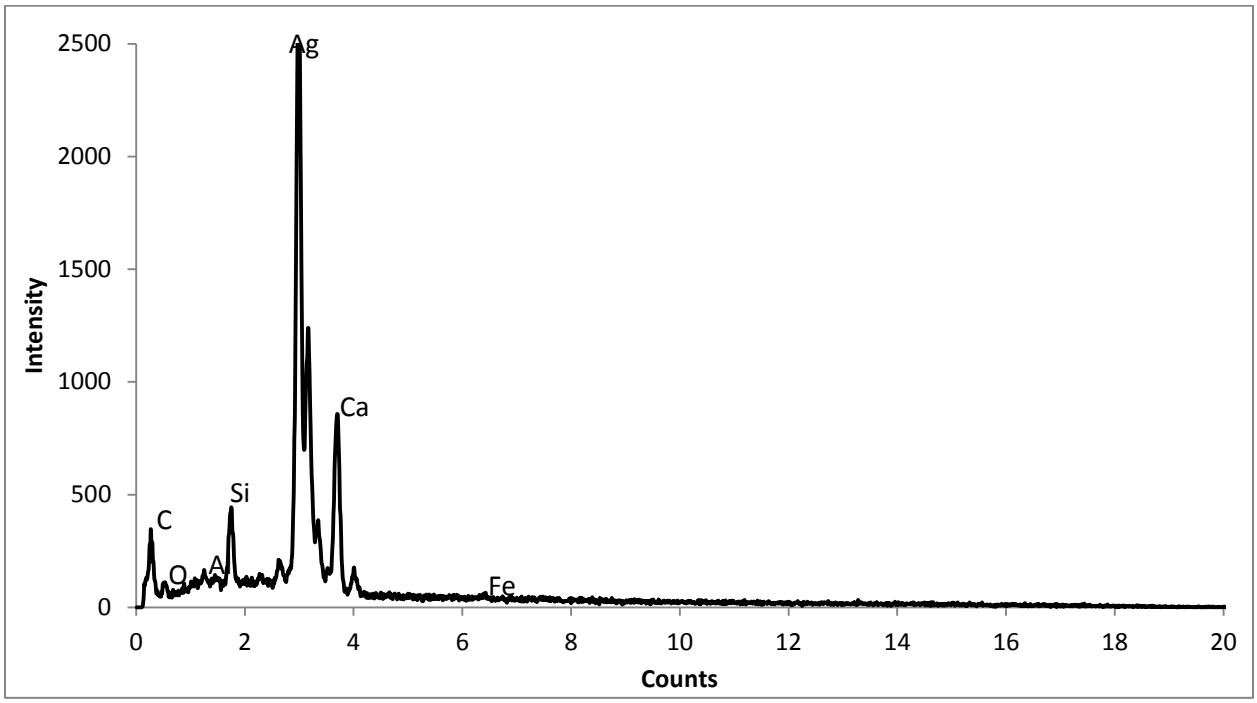

Figure 5-20 9.42% CaO, 8M NaOH, 158F, 1 Day EDX

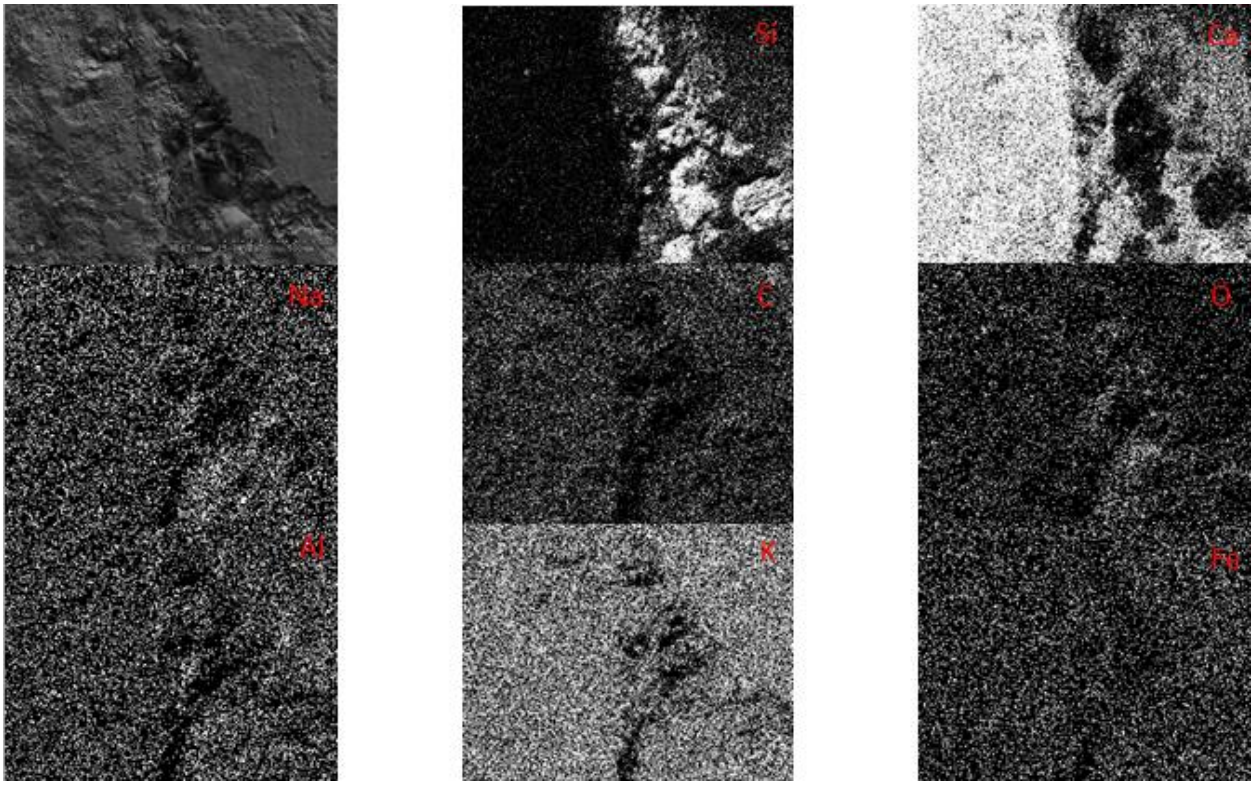

Figure 5-21 Elemental Mapping of 9.42% CaO flyash, 8M NaOH, 158F, 1 Day test sample

The EDS chemical distribution graph and elemental mapping for 9.42% CaO flyash based geopolymer reacted with 8M NaOH solution, cured at 158F and tested after 1 Day is shown in figure 5-20 and figure 5-21. From these figures, it is obvious that the main chemical species present is silicon and calcium. From the elemental mapping, it is clear that there are three zones that are present which include a silicon rich zone, a calcium enriched zone and a complex zone which contains all species including calcium, silicon, aluminum, iron, sodium, oxygen, magnesium and carbon. All the crystalline phases were identified by the x ray diffraction method. A deduction can be made regarding this complex amorphous phase. It seems to have formed a mesh around the unreacted silica particles and must be responsible for the binder properties in geopolymer concrete. The calcium enriched zone must be from the calcite identified by the X ray diffraction.

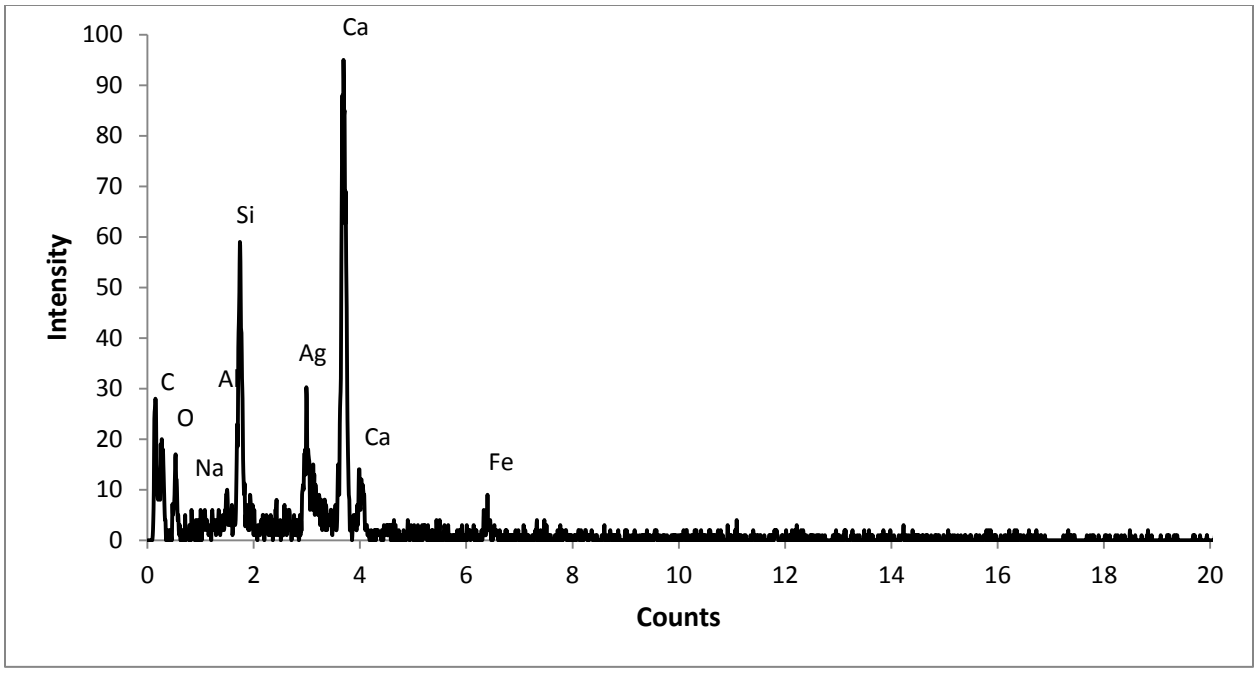

Figure 5-22 9.42% CaO, 8M NaOH, 158F, 7 Day EDX

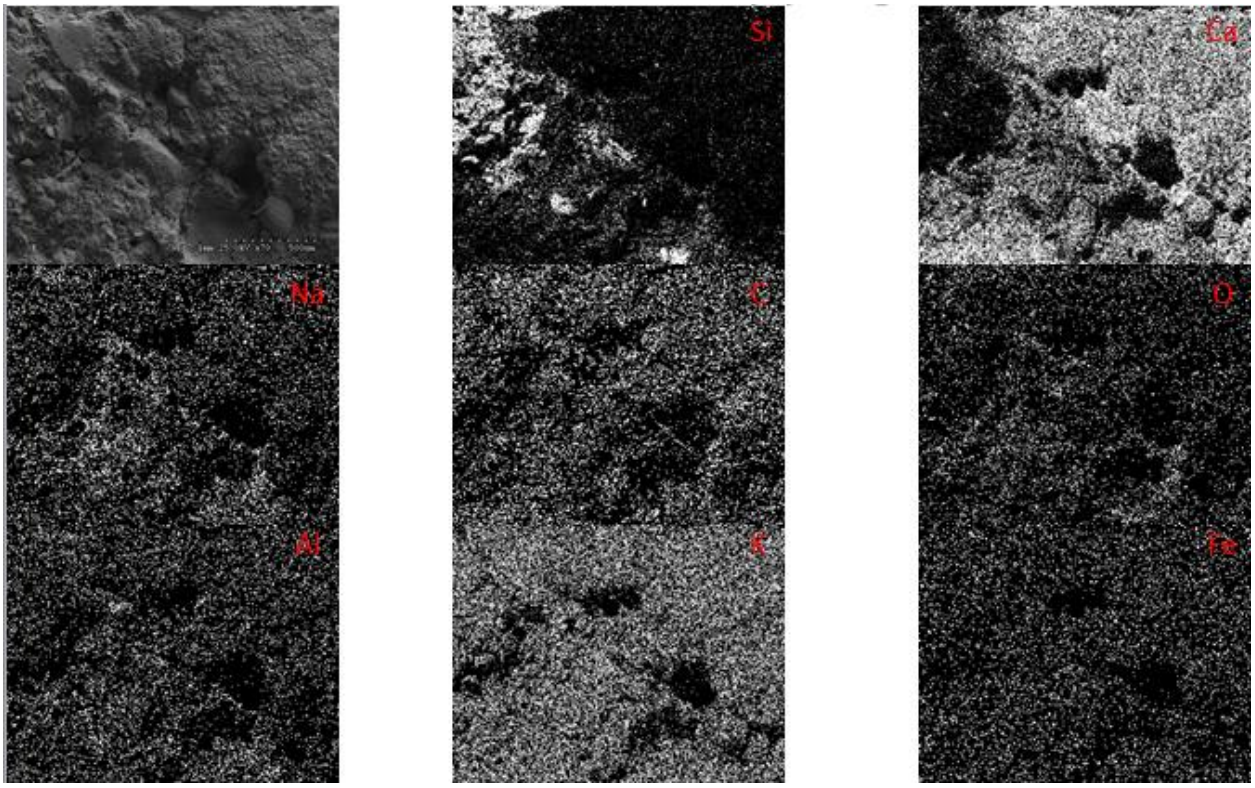

Figure 5-23 Elemental Mapping of 9.42% CaO flyash, 8M NaOH, 158F, 7 Day test sample

The edx chemical distribution graph and elemental mapping for 9.42% CaO flyash based geopolymer reacted with 8M NaOH solution, cured at 158F and tested after 7 Day is shown in figure 5-22

and figure 5-23. From these figures, it can be seen that the three zones are more distinct and clear. There is definitely lesser iron, sodium and aluminum content in the silicon and calcium enriched zone. This gives more conclusive proof about the presence of an amorphous complex zone which has formed a mesh around the silicon particles

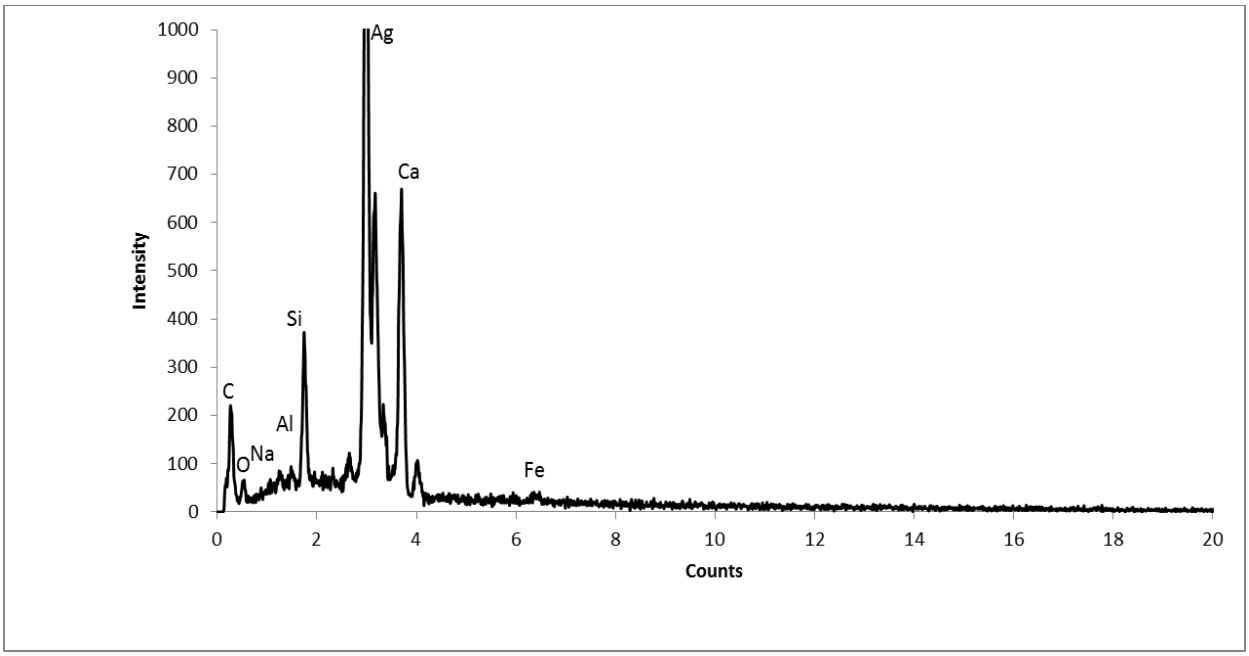

Figure 5-24 5-26: 9.42% CaO, 12M NaOH, 115F, 1 Day EDX

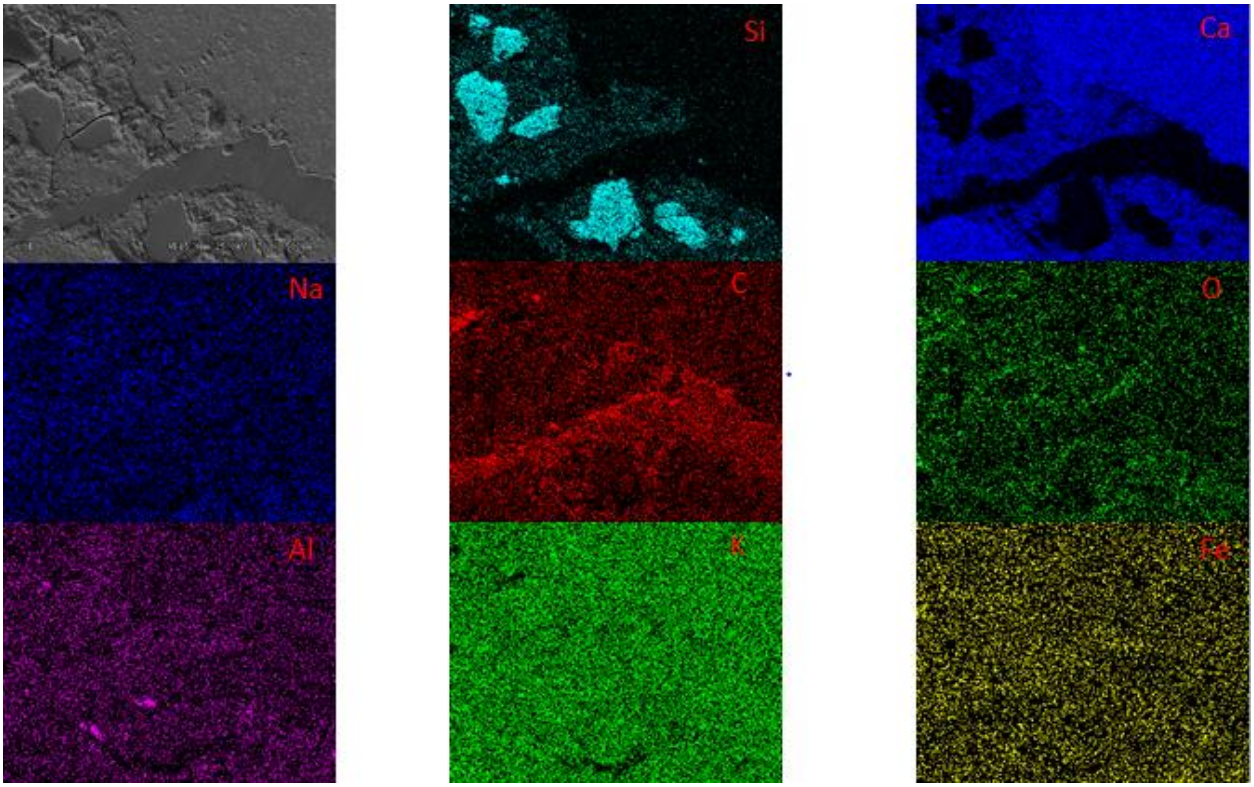

Figure 5-25 Elemental Mapping of 9.42% CaO flyash, 12M NaOH, 115F, 1 Day test sample

The EDS chemical distribution graph and elemental mapping for 9.42% CaO flyash based geopolymer reacted with 12M NaOH solution, cured at 115F and tested after 1 Day is shown in figure 5-24 and figure 5-25. From these figures, it is obvious that the main chemical species present is silicon and calcium. From the elemental mapping, it is clear that there are three zones that are present which include a silicon rich zone, a calcium enriched zone and a complex zone which contains all species including calcium, silicon, aluminum, iron, sodium, oxygen, magnesium and carbon. All the crystalline phases were identified by the x ray diffraction method.

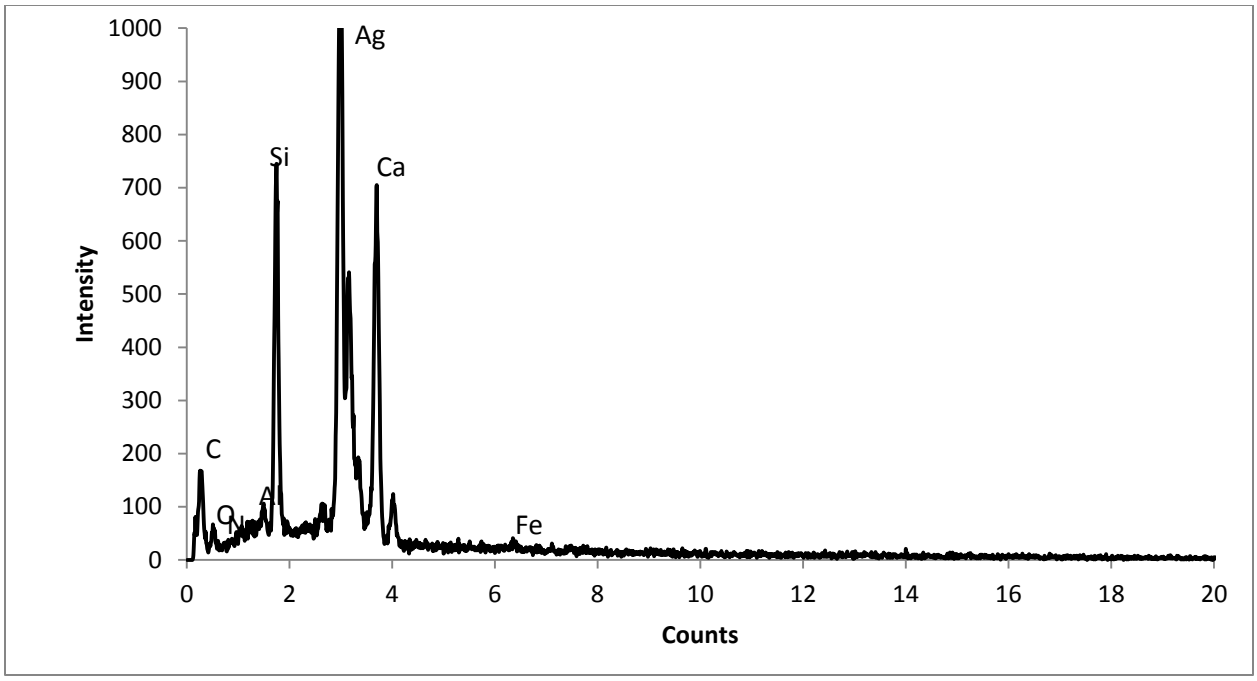

Figure 5-26 : 9.42% CaO, 12M NaOH, 115F, 7 Day EDX

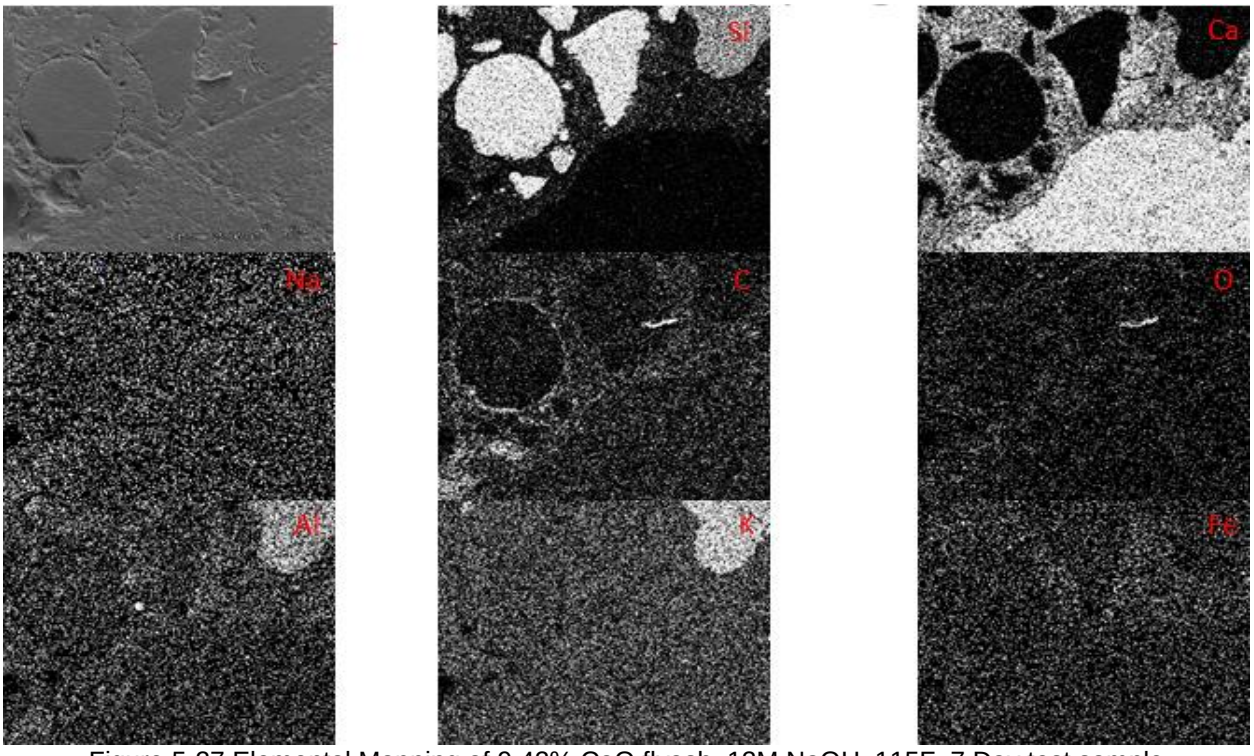

Figure 5-27 Elemental Mapping of 9.42% CaO flyash, 12M NaOH, 115F, 7 Day test sample

The EDS chemical distribution graph and elemental mapping for 9.42% CaO flyash based geopolymer reacted with 12M NaOH solution, cured at 115F and tested after 7 Day is shown in figure 5-24 and figure 5-25. From these figures, it is obvious that the main chemical species present is silicon and calcium. From the elemental mapping, four zones can be identified which include a silicon rich zone, a calcium enriched zone a complex zone which contains all species including calcium, silicon, aluminum, iron, sodium, oxygen, magnesium and carbon and a fourth zone which contains silicon, aluminum and potassium. Surprisingly, there is lower content of iron and carbon in this region.

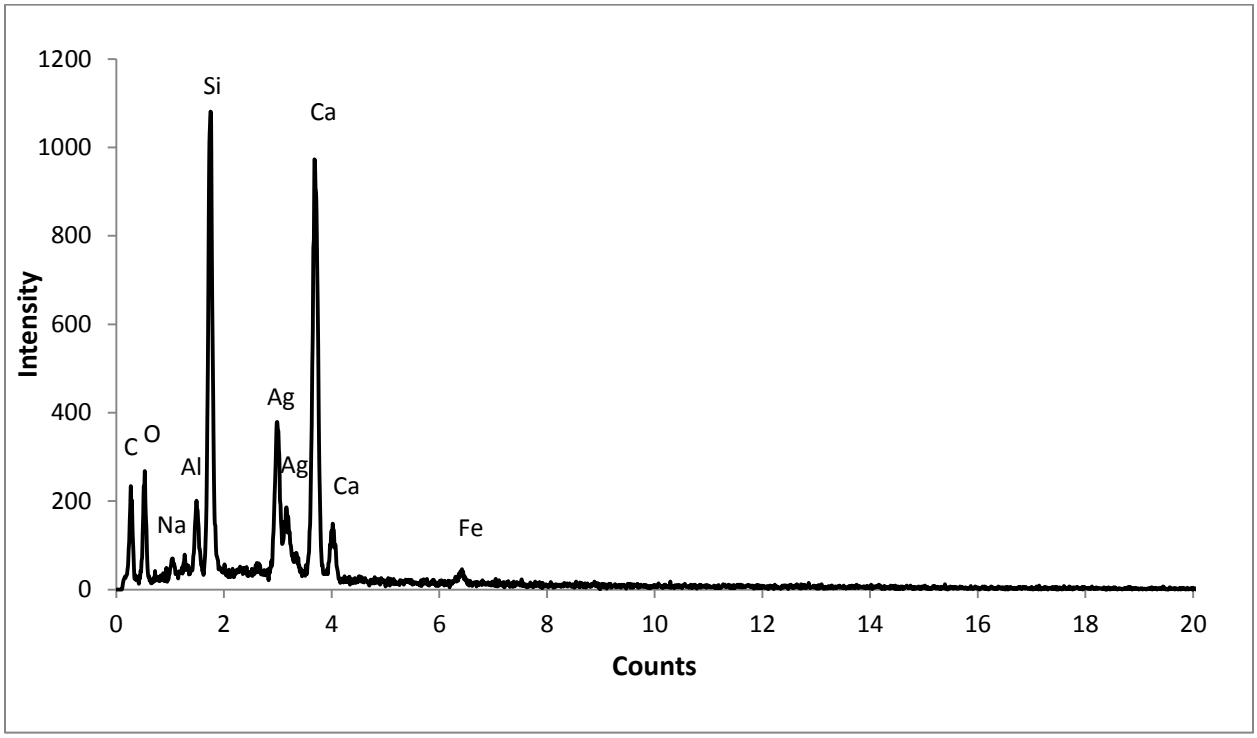

Figure 5-28 5-30: 9.42% CaO, 12M NaOH, 115F, 28 Day EDX

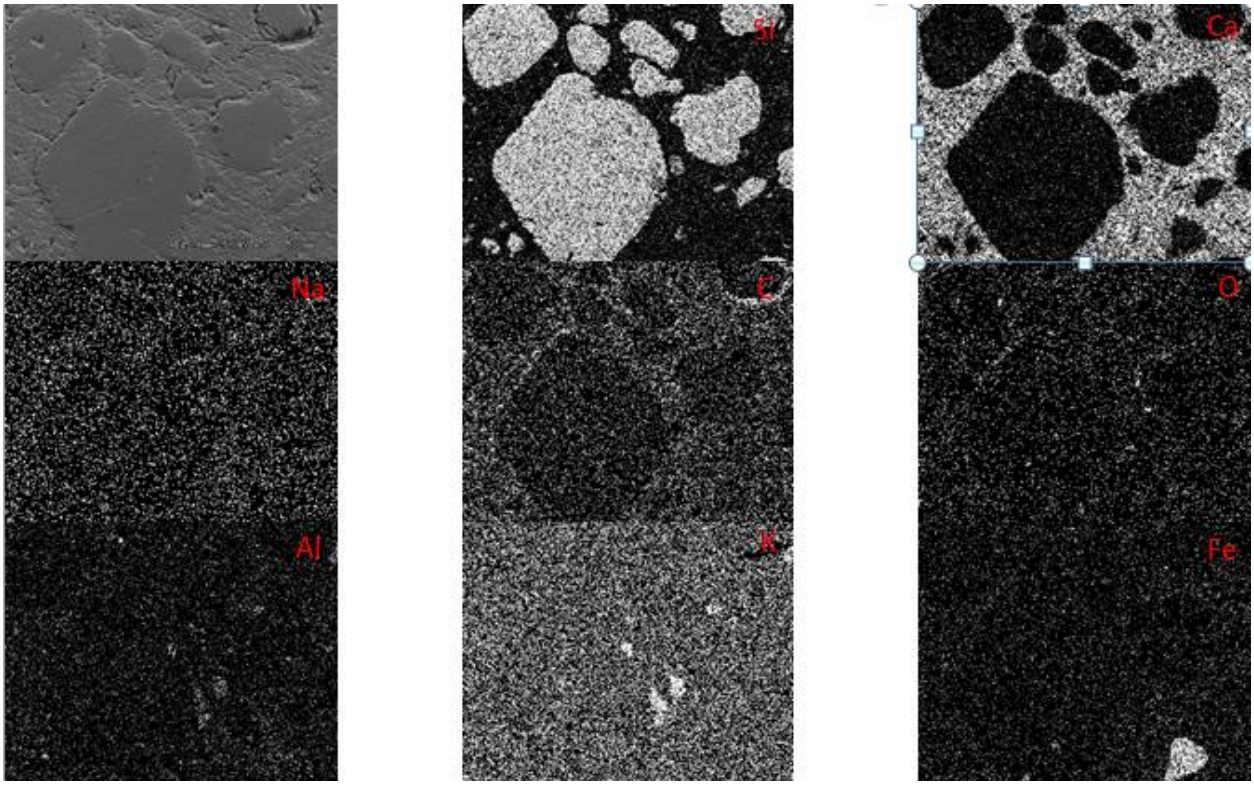

Figure 5-29 Elemental Mapping of 9.42% CaO flyash, 12M NaOH, 115F, 28 Day test sample

The EDS chemical distribution graph and elemental mapping for 9.42% CaO flyash based geopolymer reacted with 12M NaOH solution, cured at 115F and tested after 28 days is shown in figure 5-24 and figure 5-25. From these figures, it is obvious that the main chemical species present is silicon and calcium. From the elemental mapping, it is clear that there are four zones that are present which include a silicon rich zone, a reacted calcium zone which contains all species including calcium, sodium and potassium, a small zone consisting of silicon, potassium and asluminum, and another small zone containing iron. All the crystalline phases were identified by the x ray diffraction method.

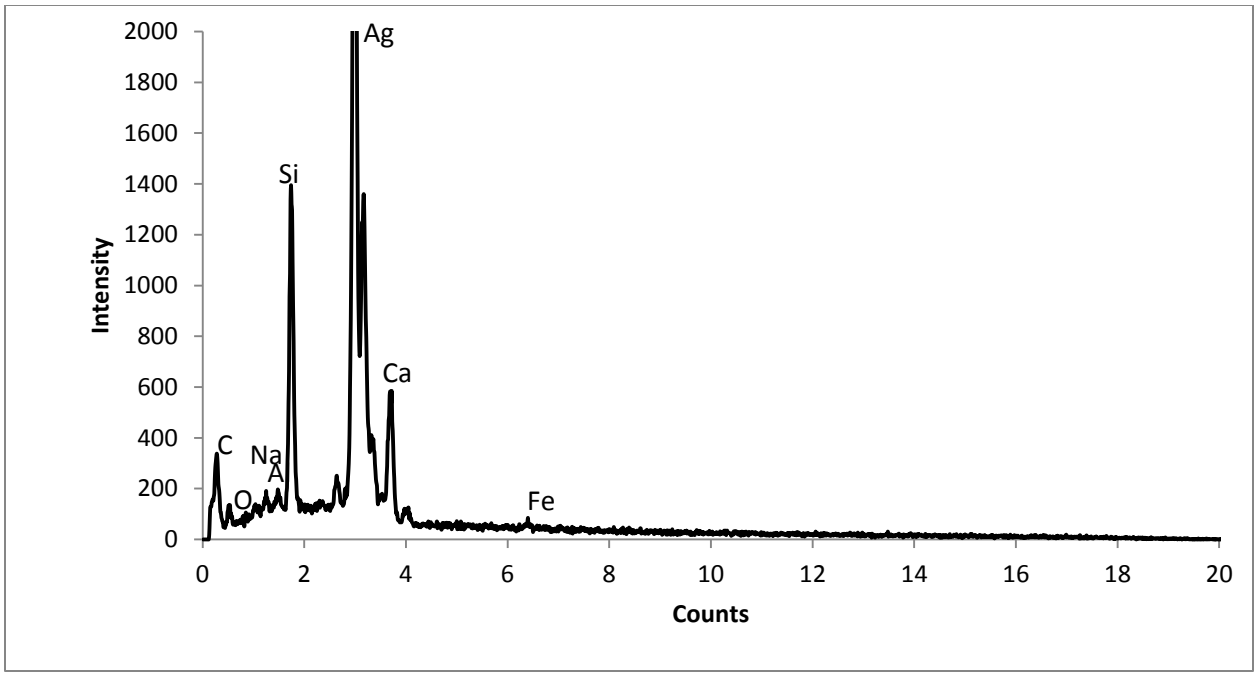

Figure 5-30 9.42% CaO, 12M NaOH, 158F, 1 Day EDX

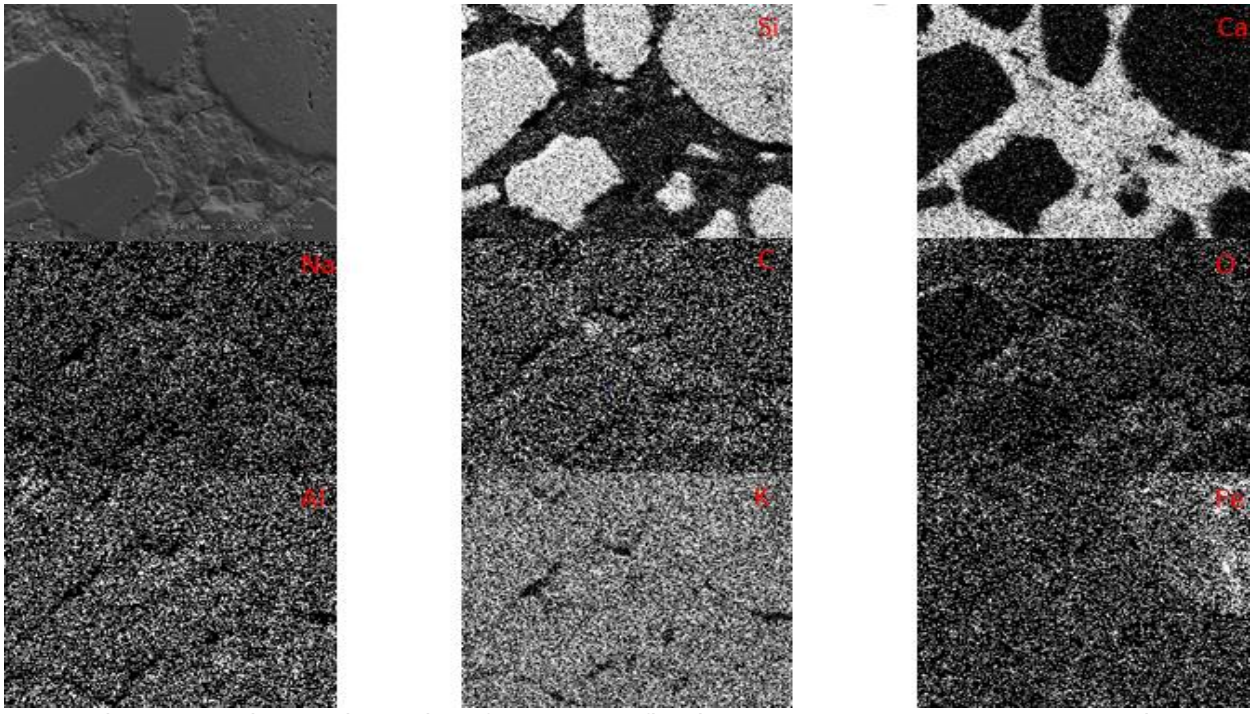

Figure 5-31 Elemental Mapping of 9.42% CaO flyash, 12M NaOH, 158F, 1 Day test sample

The EDS chemical distribution graph and elemental mapping for 9.42% CaO flyash based geopolymer reacted with 12M NaOH solution, cured at 115F and tested after 28 days is shown in figure 5-24 and figure 5-25. From these figures, it is obvious that the main chemical species present is silicon

and calcium. From the elemental mapping, it is clear that there are four zones that are present which include a silicon rich zone, a reacted calcium zone which contains all species including calcium, sodium and potassium, a small zone consisting of silicon, potassium and asluminum, and another small zone containing iron. All the crystalline phases were identified by the x ray diffraction method.

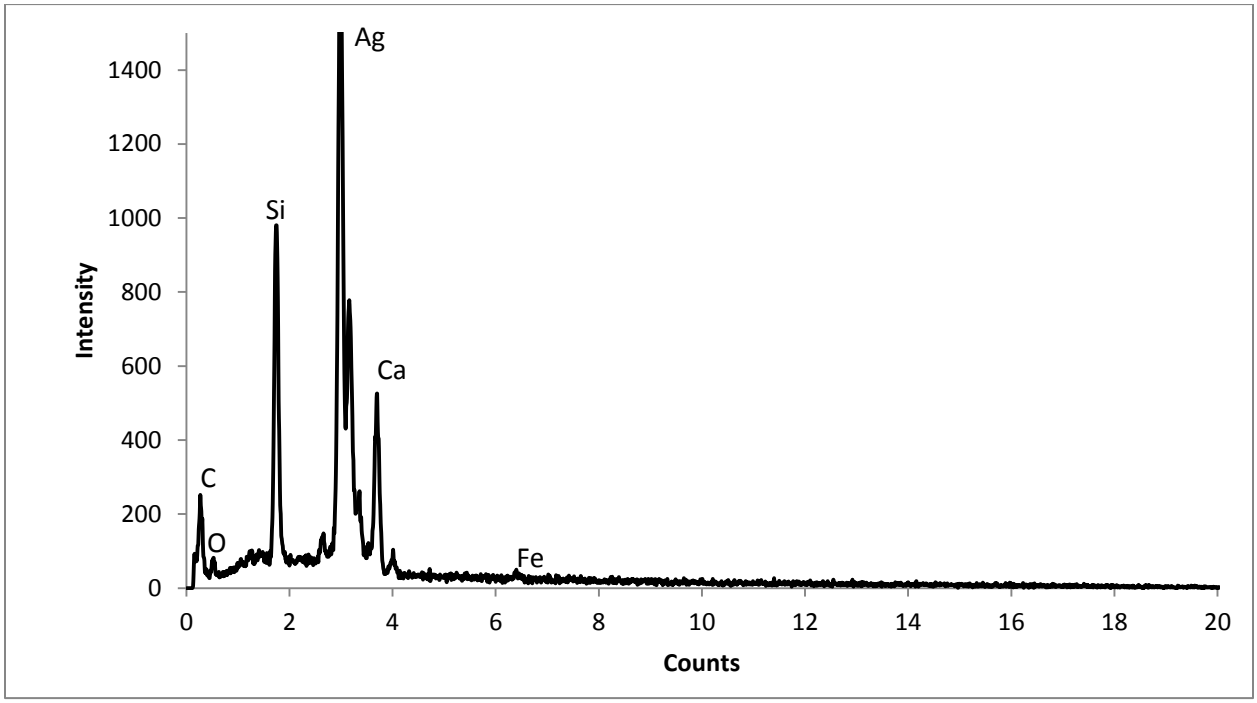

Figure 5-32 9.42% CaO, 12M NaOH, 158F, 7 Day EDX

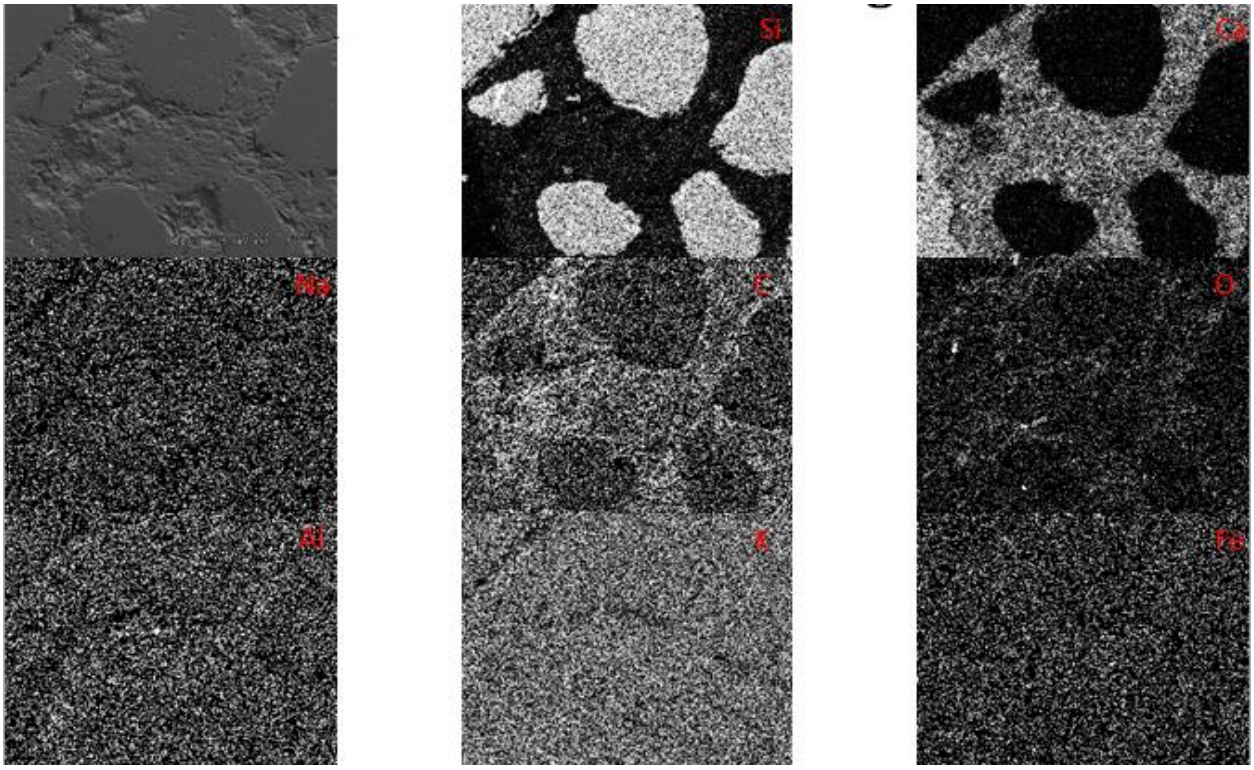

Figure 5-33 Elemental Mapping of 9.42% CaO flyash, 12M NaOH, 158F, 7 Day test sample

The EDS chemical distribution graph and elemental mapping for 9.42% CaO flyash based geopolymer reacted with 12M NaOH solution, cured at 158F and tested after 7 Day is shown in figure 5-32 and figure 5-33. From these figures, it is obvious that the main chemical species present is silicon and calcium. From the elemental mapping, three zones can be identified which include a silicon rich zone, a calcium enriched zone a complex zone which contains species like sodium, aluminum and calcium.

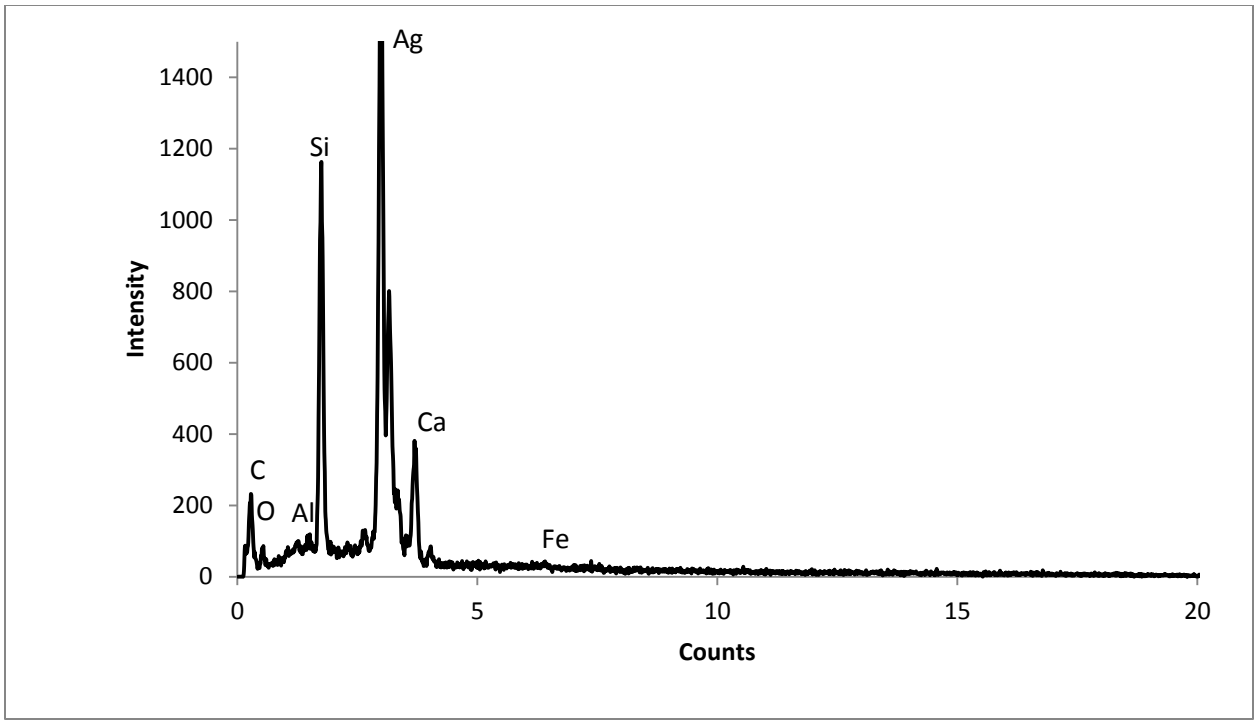

Figure 5-34 9.42% CaO, 12M NaOH, 158F, 28 Day EDX

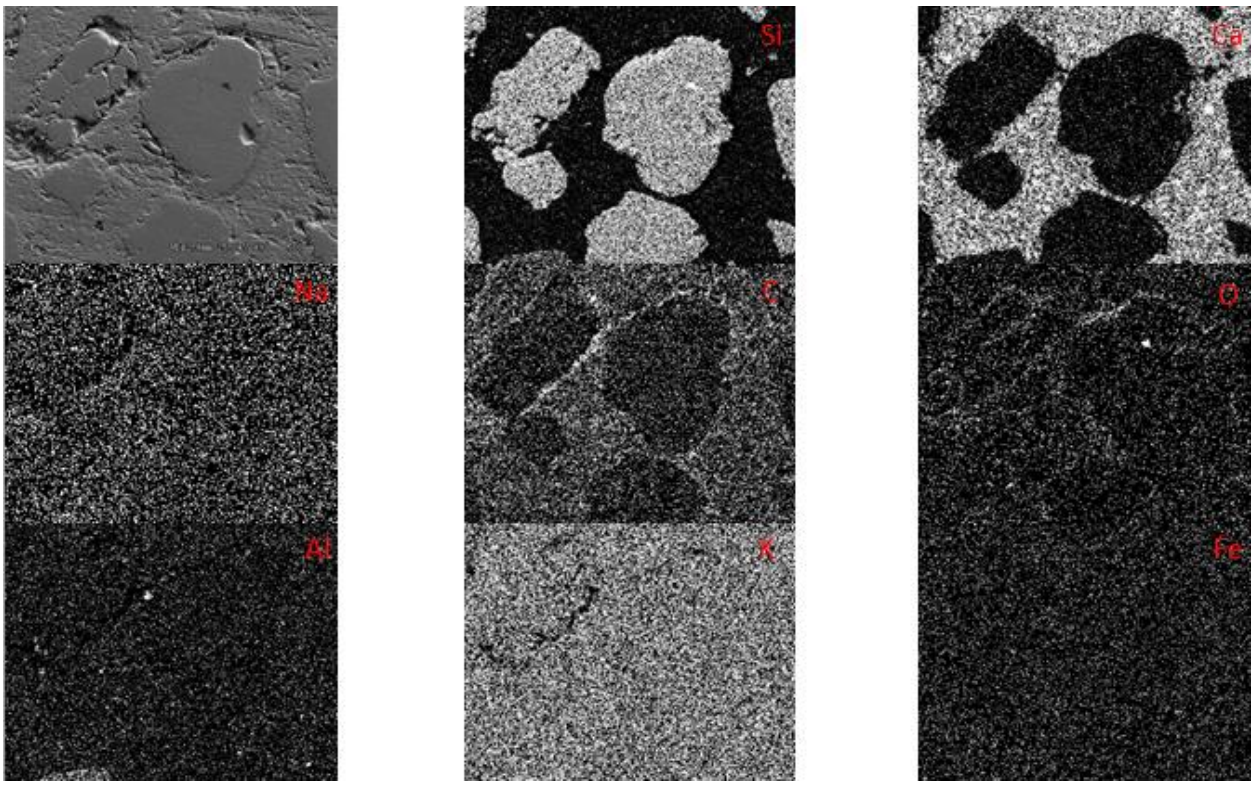

Figure 5-35 Elemental Mapping of 9.42% CaO flyash, 12M NaOH, 158F,28 Day test sample

The EDS chemical distribution graph and elemental mapping for 9.42% CaO flyash based geopolymer reacted with 12M NaOH solution, cured at 158F and tested after 7 Day is shown in figure 5-34 and figure 5-35. From these figures, it is obvious that the main chemical species present is silicon and calcium. From the elemental mapping, two zones can be identified which include a silicon rich zone, and a complex zone which contains species like calcium, carbon and oxygen which could be interpreted as formation of calcite around unreacted silica particles.

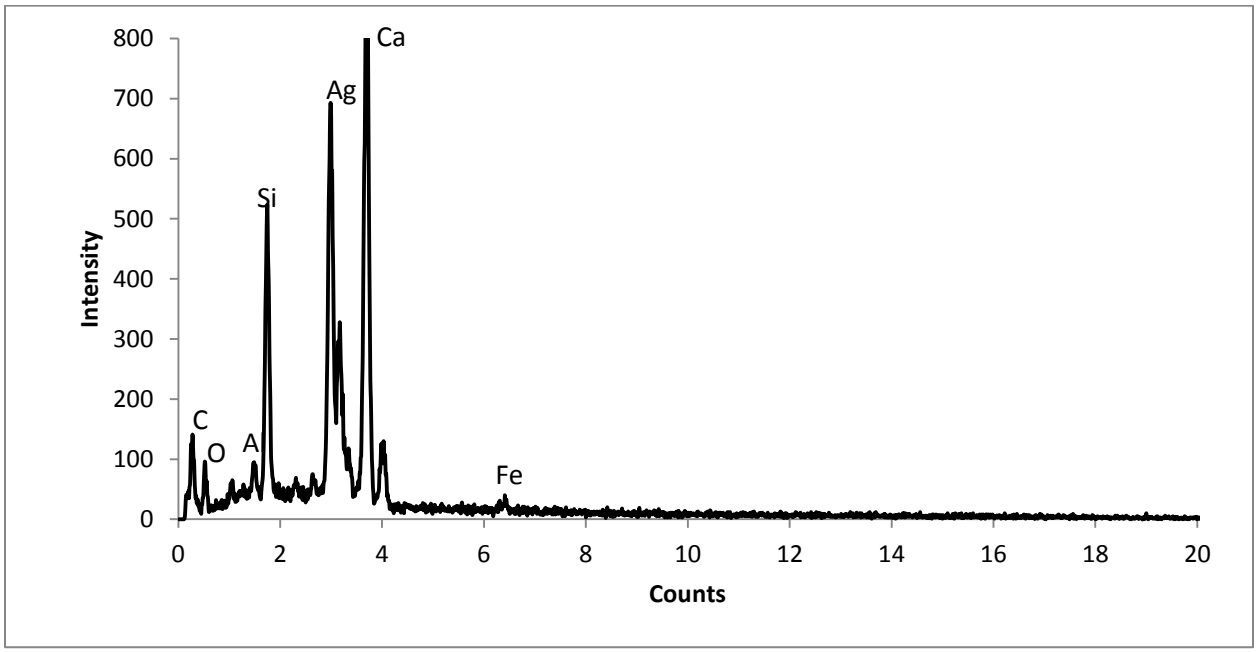

Figure 5-36 9.42% CaO, 14M NaOH, 115F, 1 Day EDX

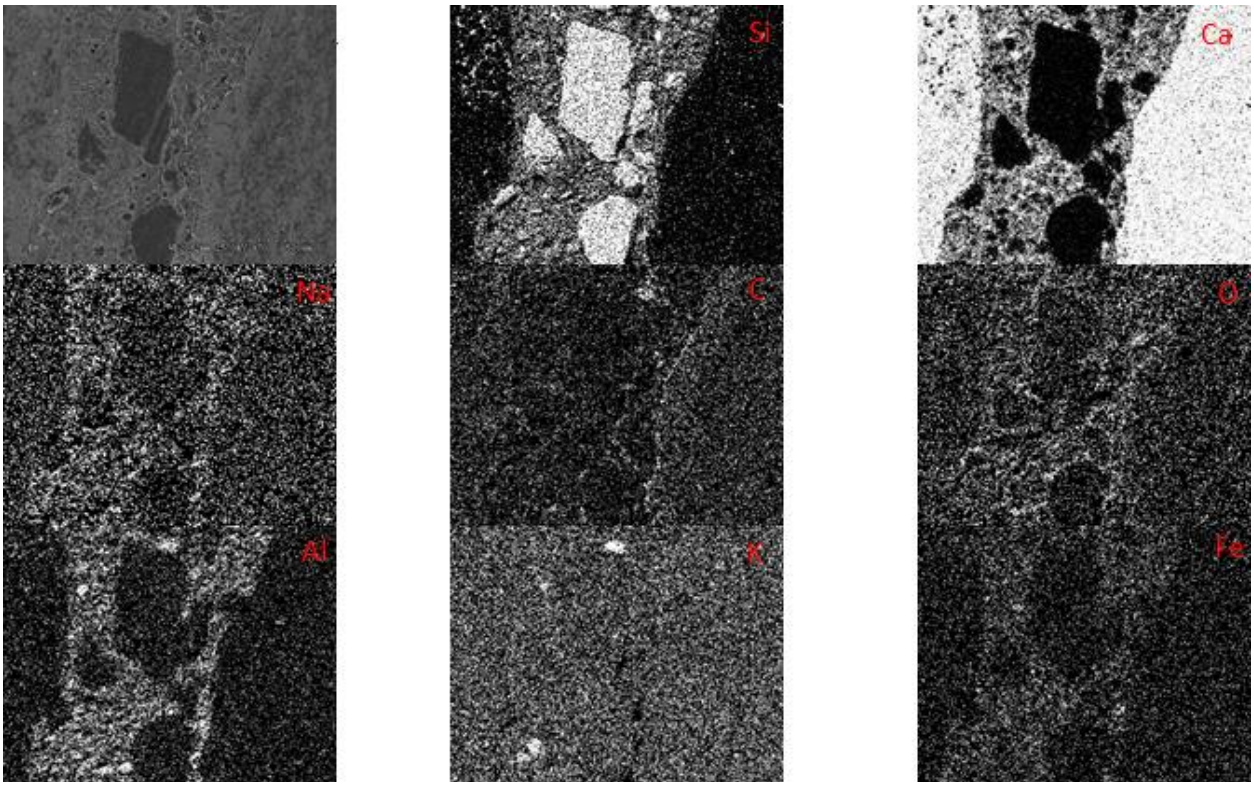

Figure 5-37 Elemental Mapping of 9.42% CaO flyash, 14M NaOH, 115F, 1 Day test sample

The EDS chemical distribution graph and elemental mapping for 9.42% CaO flyash based geopolymer reacted with 14M NaOH solution, cured at 115F and tested after 1 Day is shown in figure 5-36 and figure 5-37. From these figures, it is obvious that the main chemical species present is silicon and calcium. From the elemental mapping, three zones can be identified which include a silicon rich zone, a calcium enriched zone a complex zone which contains species like sodium, aluminum, silicon and calcium. This zone is present around the unreacted silica particles.

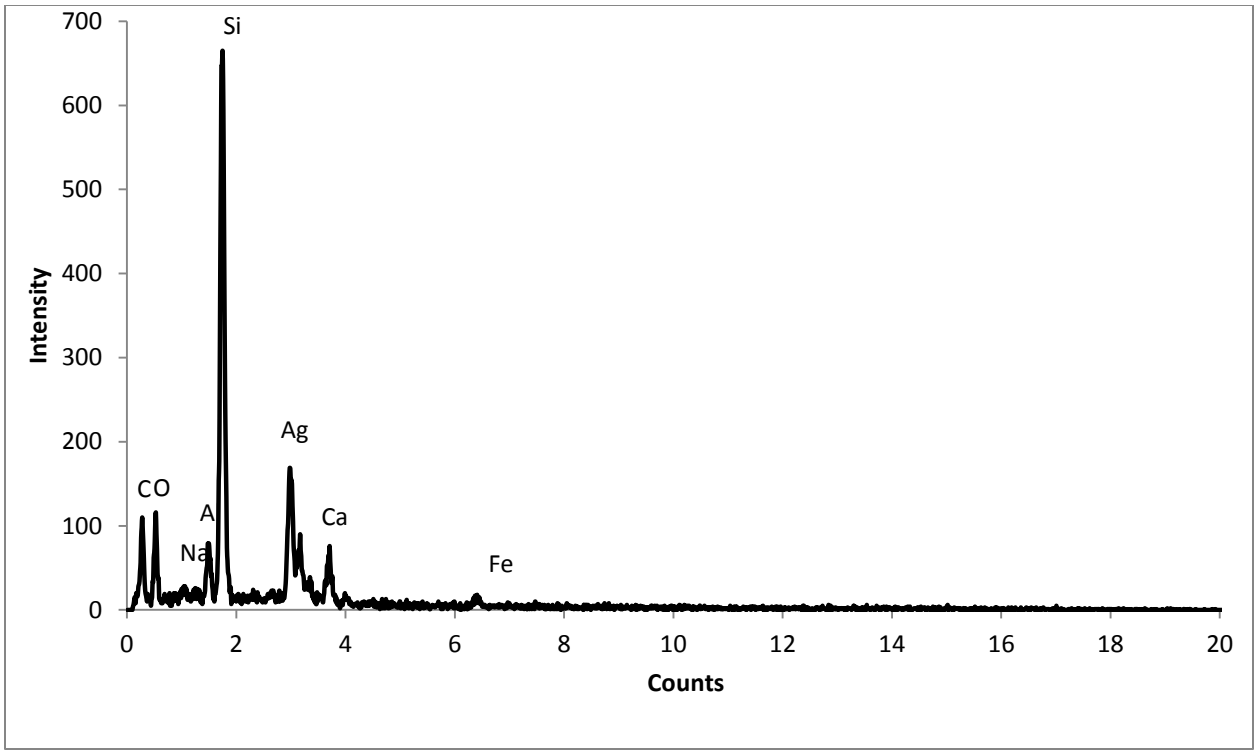

Figure 5-38 9.42% CaO, 14M NaOH, 115F, 7 Day EDX

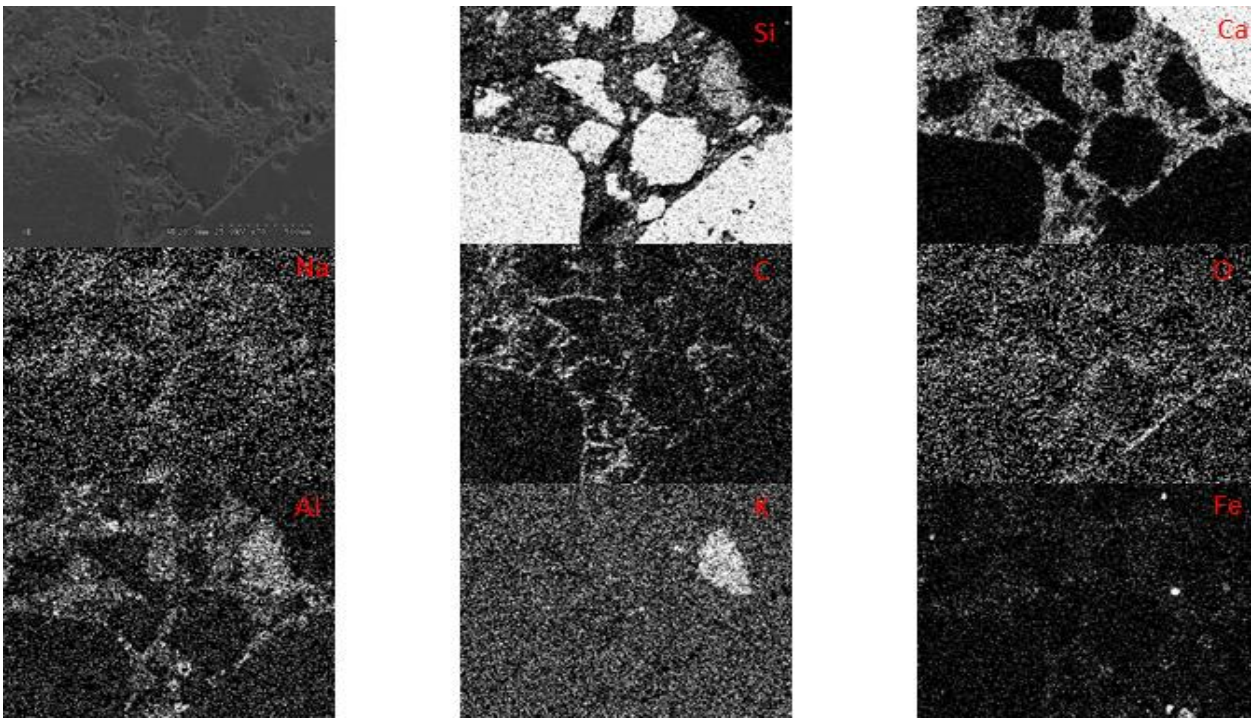

Figure 5-39 Elemental Mapping of 9.42% CaO flyash, 14M NaOH, 115F, 7 Day test sample

The EDS chemical distribution graph and elemental mapping for 9.42% CaO flyash based geopolymer reacted with 14M NaOH solution, cured at 115F and tested after 7 Days is shown in figure 5-

38 and figure 5-39. From these figures, it is obvious that the main chemical species present is silicon and calcium. From the elemental mapping, three zones can be identified which include a silicon rich zone, a calcium enriched zone a complex zone which contains species like sodium, aluminum, silicon and calcium. This zone is present around the unreacted silica particles. There is a fourth zone which is a concentrated region of reacted potassium. This could signify the formation of potassium silicate feldspar.

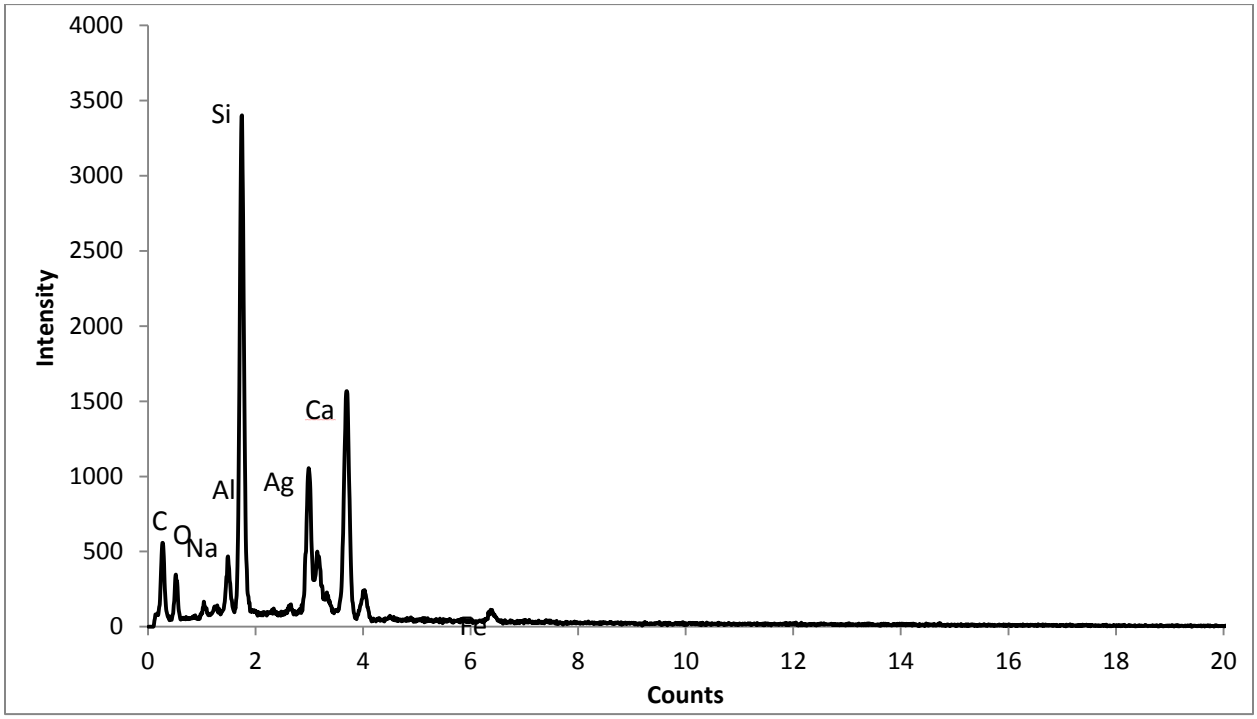

Figure 5-40 9.42% CaO, 14M NaOH, 115F, 28 Day EDX

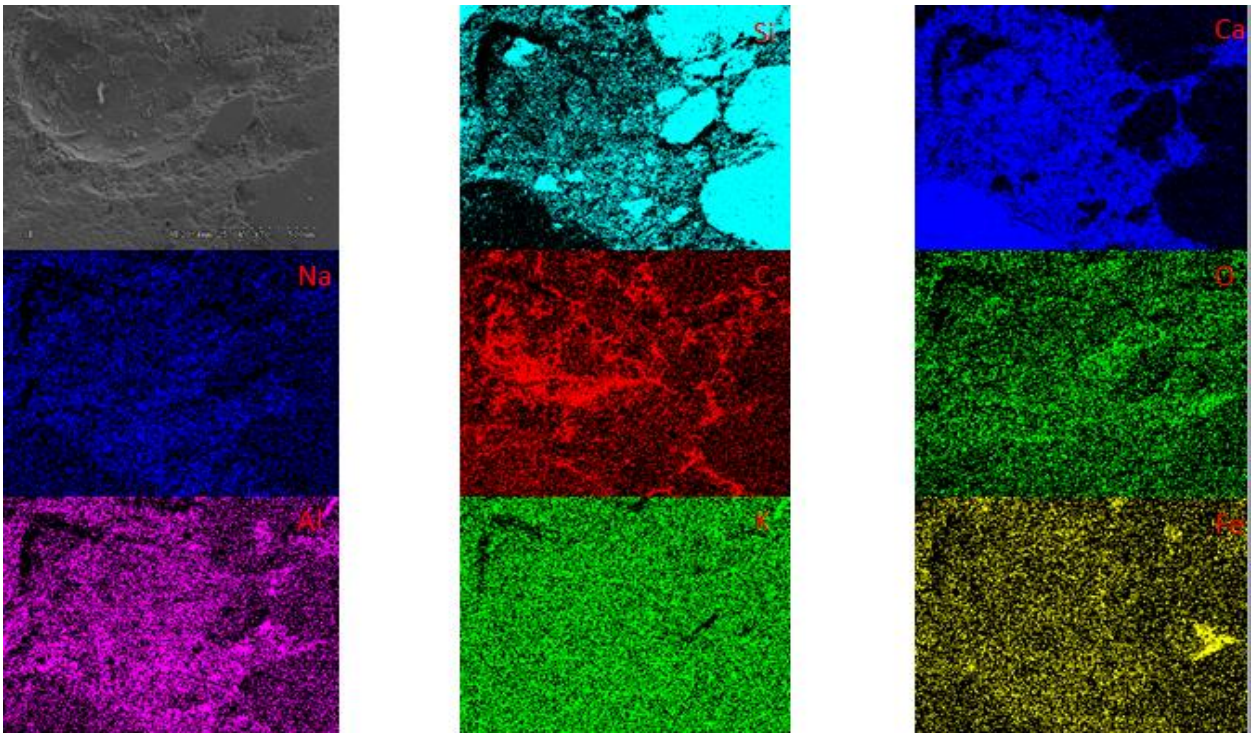

Figure 5-41 Elemental Mapping of 9.42% CaO flyash, 14M NaOH, 115F, 28 Day test sample

The EDS chemical distribution graph and elemental mapping for 9.42% CaO flyash based geopolymer reacted with 14M NaOH solution, cured at 115F and tested after 28 Days is shown in figure 5-40 and figure 5-41. From these figures, it is obvious that the main chemical species present is silicon and calcium. From the elemental mapping, three zones can be identified which include a silicon rich zone, a calcium enriched zone a complex zone which contains species like sodium, aluminum, silicon and calcium. This zone is present around the unreacted silica particles. There is a fourth zone which is a concentrated region of unreacted iron oxide from the flyash.

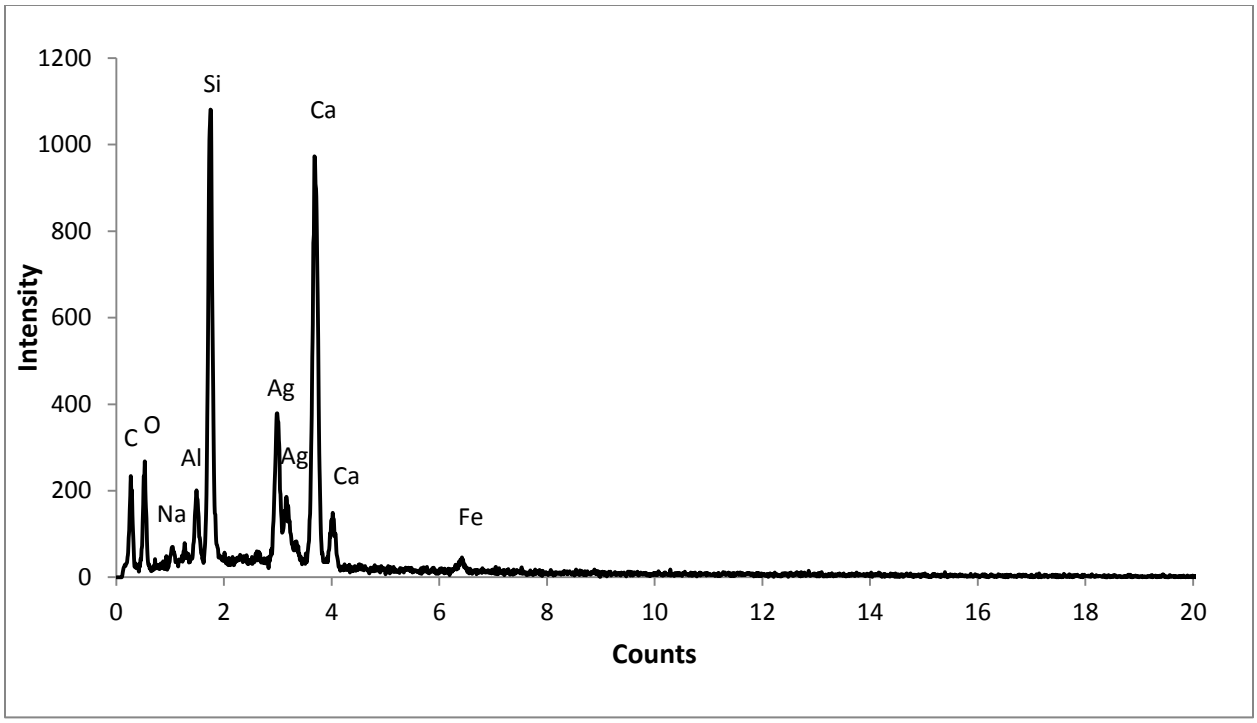

Figure 5-42 9.42% CaO, 14M NaOH, 158F, 1 Day EDX

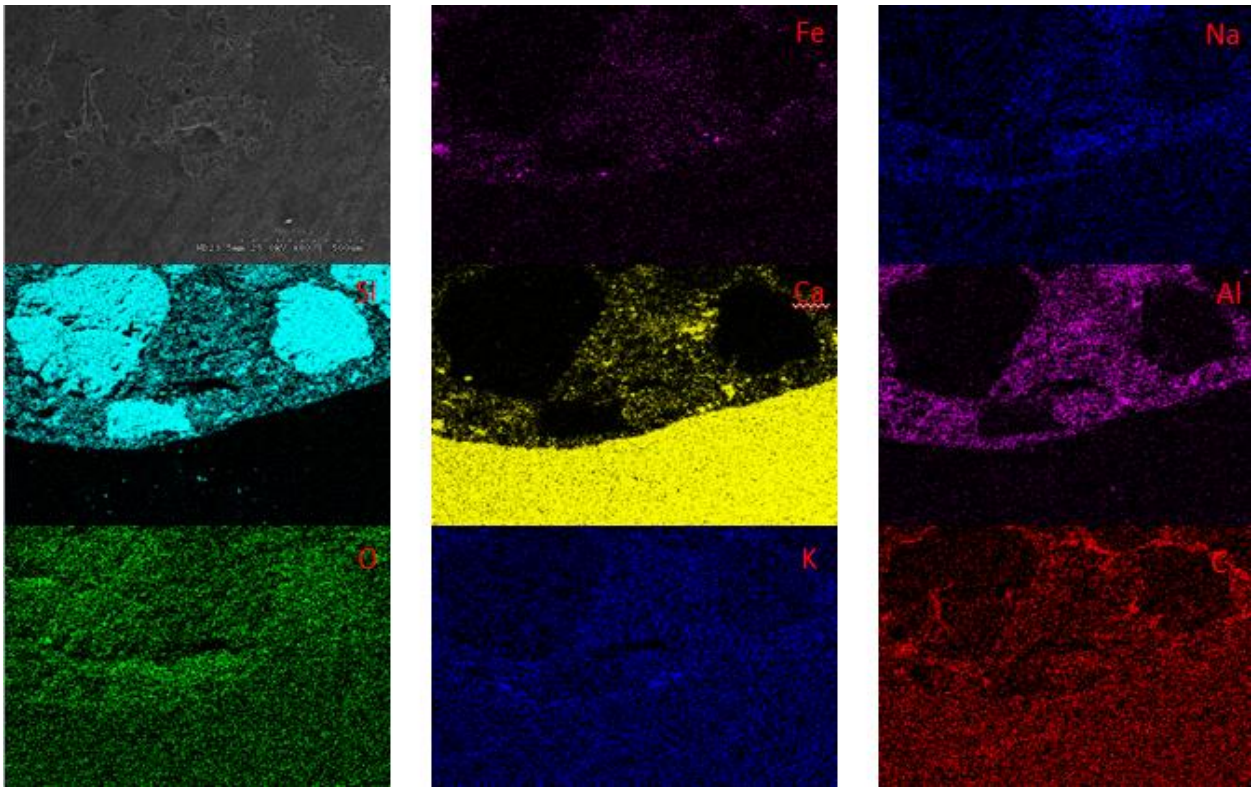

Figure 5-43 Elemental Mapping of 9.42% CaO flyash, 14M NaOH, 158F, 1 Day test sample

The EDS chemical distribution graph and elemental mapping for 9.42% CaO flyash based geopolymer reacted with 14M NaOH solution, cured at 158F and tested after 1 Day is shown in figure 5-42 and figure 5-43. From these figures, it is obvious that the main chemical species present is silicon and calcium. From the elemental mapping, three zones can be identified which include a silicon rich zone, a calcium enriched zone a complex zone which contains all species like sodium, aluminum, silicon, calcium, potassium and iron. There is a fourth zone which is a concentrated region of unreacted iron oxide from the flyash.

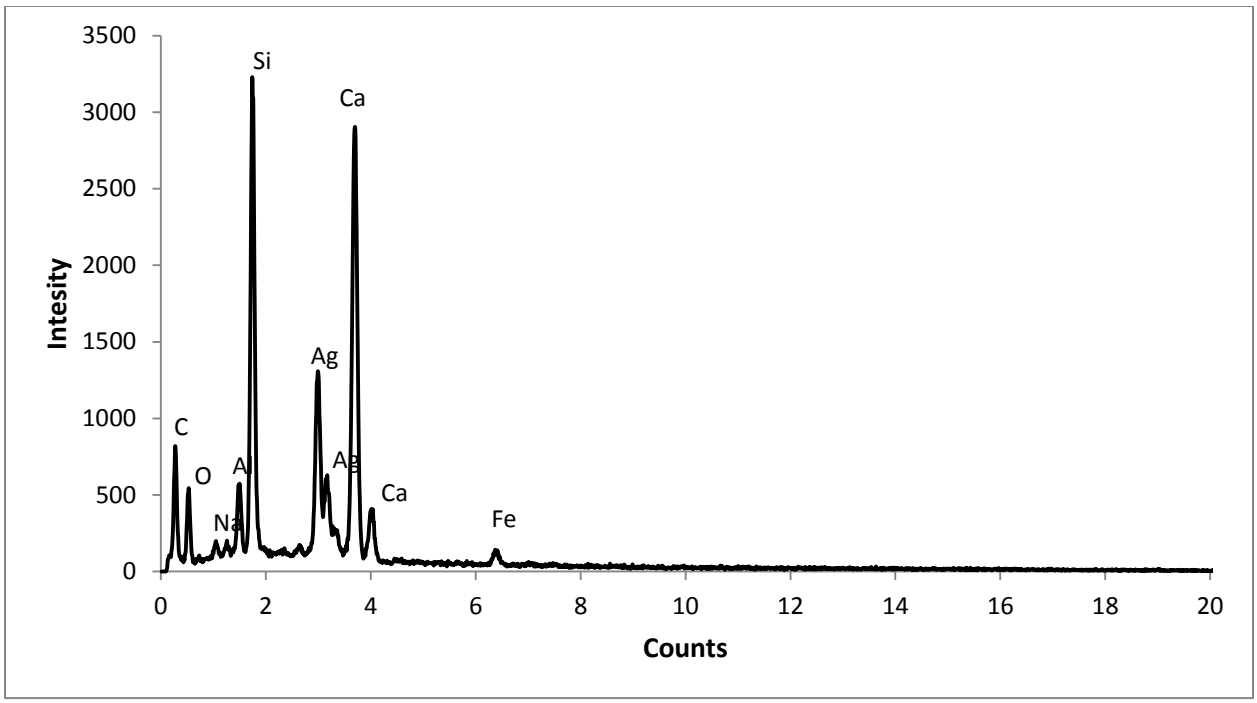

Figure 5-44 9.42% CaO, 14M NaOH, 158F, 7 Day EDX

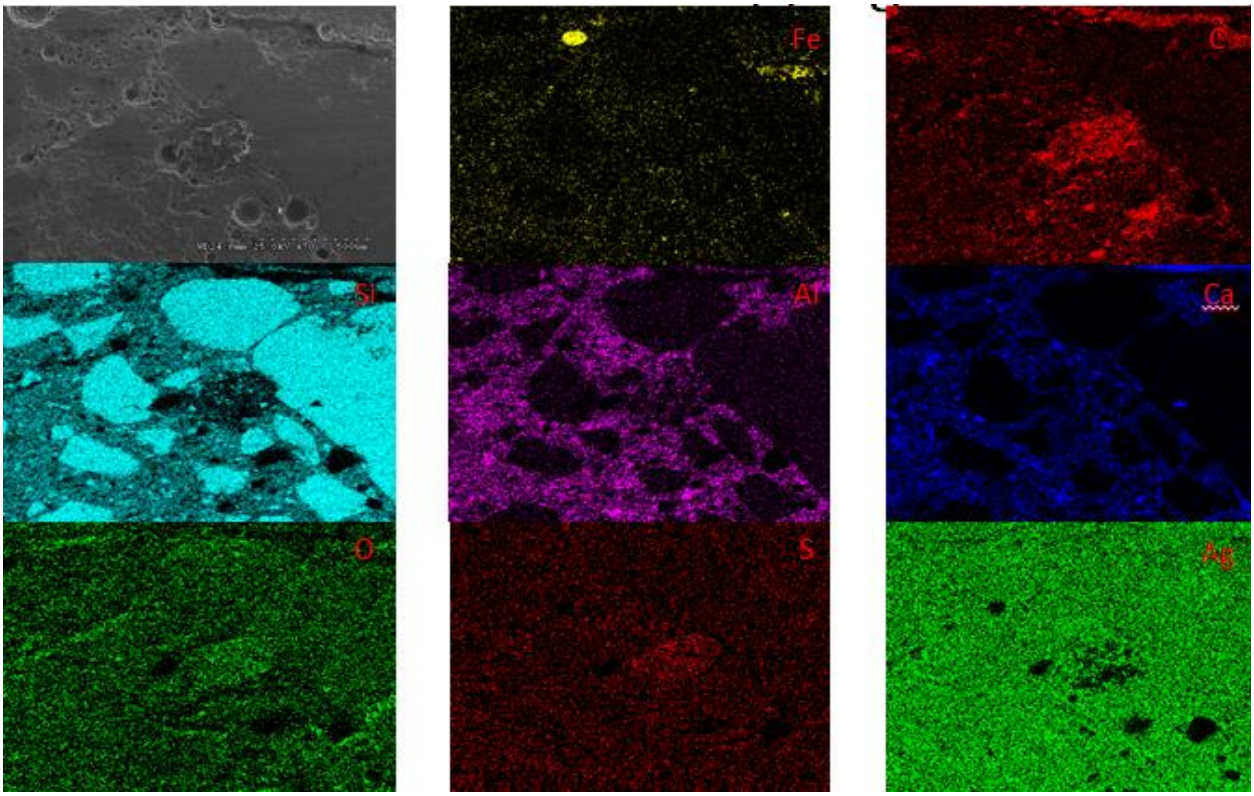

Figure 5-45 Elemental Mapping of 9.42% CaO flyash, 14M NaOH, 158F, 7 Day test sample

The EDS chemical distribution graph and elemental mapping for 9.42% CaO flyash based geopolymer reacted with 14M NaOH solution, cured at 158F and tested after 7 Days is shown in figure 5-44 and figure 5-45. From these figures, it is obvious that the main chemical species present is silicon and calcium. From the elemental mapping, three zones can be identified which include a silicon rich zone, a calcium enriched zone a complex zone which contains species like sodium, aluminum, silicon and calcium. This zone is present around the unreacted silica particles. There is a fourth zone comprised of concentrated unreacted iron oxide present from the flyash.

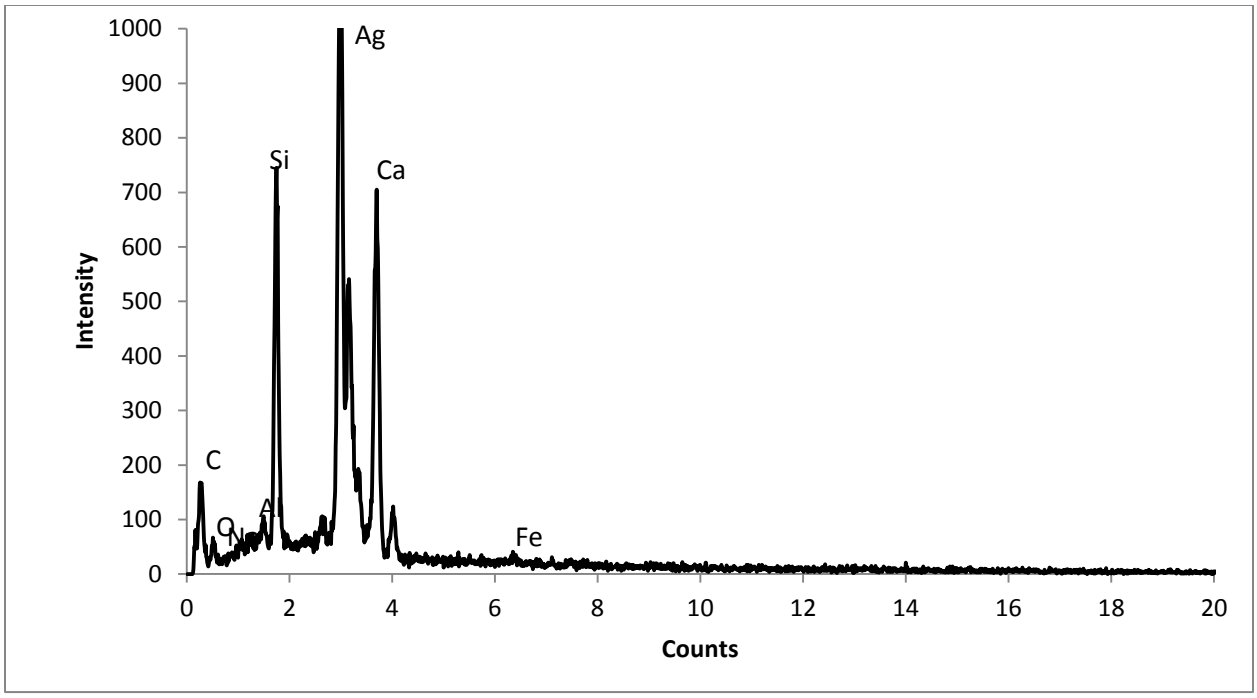

Figure 5-46 : 9.42% CaO, 14M NaOH, 158F, 28 Day EDX

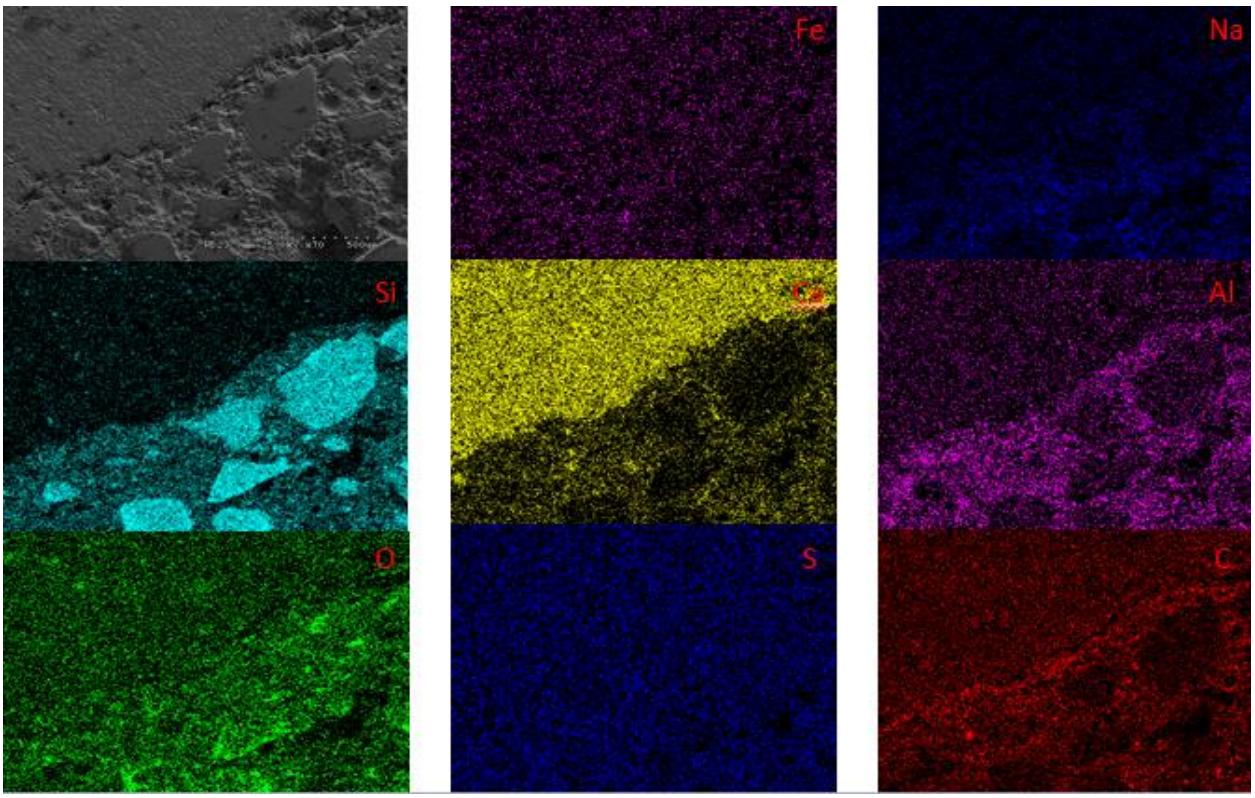

Figure 5-47 Elemental Mapping of 9.42% CaO flyash, 12M NaOH, 158F, 28 Day test sample

The EDS chemical distribution graph and elemental mapping for 9.42% CaO flyash based geopolymer reacted with 14M NaOH solution, cured at 158F and tested after 7 Days is shown in figure 5-44 and figure 5-45. From these figures, it is obvious that the main chemical species present is silicon and calcium. From the elemental mapping, three zones can be identified which include a silicon rich zone, a calcium enriched zone a complex zone which contains species like sodium, aluminum, silicon and calcium. This zone is present around the unreacted silica particles.

Table 5-4 Amorphous Phases Present In 9.42% CaO Geopolymer Mixes

Molarity of NaOH	Curing Conditions		Average Compressive Strength (ksi)	Crystalline Phases Present	Possible Amorphous Phases Present
	Curing Temperature (K)	Ageing Time (Days)			
8	115	1	1.355	SiO_2, $CaCO_3$, Al_2O_3, Ca_2SiO, Ca3SiO5	$CaO.MgO.2SiO_2$, $CaO.Al_2O_3.2SiO_2$, $FeO.Al_2O_3.2SiO_2$, $NaO.Al_2O_3$, $KAlSi_3O_8$, $NaO.CaO.Al_2O_3.2SiO_2$
		7	3.25	SiO_2, $CaCO_3$, Al_2O_3, Ca_2SiO, Ca3SiO5	$CaO.MgO.2SiO_2$, $CaO.Al_2O_3.2SiO_2$, $FeO.Al_2O_3.2SiO_2$, $NaO.Al_2O_3$, $KAlSi_3O_8$, $NaO.CaO.Al_2O_3.2SiO_2$
		28	5.005	SiO_2, $CaCO_3$, Al_2O_3, Ca_2SiO, Ca3SiO5	$CaO.MgO.2SiO_2$, $CaO.Al_2O_3.2SiO_2$, $FeO.Al_2O_3.2SiO_2$, $NaO.Al_2O_3$, $KAlSi_3O_8$, $NaO.CaO.Al_2O_3.2SiO_2$
	158	1	2.76	SiO_2, $CaCO_3$, Al_2O_3, Ca_2SiO, Ca3SiO5	$CaO.MgO.2SiO_2$, $CaO.Al_2O_3.2SiO_2$, $FeO.Al_2O_3.2SiO_2$, $NaO.Al_2O_3$, $KAlSi_3O_8$, $NaO.CaO.Al_2O_3.2SiO_2$
		7	3.8	SiO_2, $CaCO_3$, Al_2O_3, Ca_2SiO, Ca3SiO5	$CaO.MgO.2SiO_2$, $CaO.Al_2O_3.2SiO_2$, $FeO.Al_2O_3.2SiO_2$, $NaO.Al_2O_3$, $KAlSi_3O_8$, $NaO.CaO.Al_2O_3.2SiO_2$
		28	5.035	SiO_2, $CaCO_3$, Al_2O_3, Ca_2SiO, Ca3SiO5	$CaO.MgO.2SiO_2$, $CaO.Al_2O_3.2SiO_2$, $FeO.Al_2O_3.2SiO_2$, $NaO.Al_2O_3$, $KAlSi_3O_8$, $NaO.CaO.Al_2O_3.2SiO_2$

Table 5-4 - *Continued*

12	115	1	2.41	SiO_2, $CaCO_3$, Al_2O_3, Ca_2SiO, Ca3SiO5	CaO.MgO.2SiO_2, CaO.Al_2O_3.2SiO_2, FeO.Al_2O_3.2SiO_2, NaO.Al_2O_3, $KAlSi_3O_8$, NaO.CaO.Al_2O_3.2SiO_2
		7	3.06	SiO_2, $CaCO_3$, Al_2O_3, Ca_2SiO, Ca3SiO5	CaO.MgO.2SiO_2, CaO.Al_2O_3.2SiO_2, FeO.Al_2O_3.2SiO_2, NaO.Al_2O_3, $KAlSi_3O_8$, NaO.CaO.Al_2O_3.2SiO_2
		28	3.03	SiO_2, $CaCO_3$, Al_2O_3, Ca_2SiO, Ca3SiO5	CaO.MgO.2SiO_2, CaO.Al_2O_3.2SiO_2, FeO.Al_2O_3.2SiO_2, NaO.Al_2O_3, $KAlSi_3O_8$, NaO.CaO.Al_2O_3.2SiO_2
	158	1	2.05	SiO_2, $CaCO_3$, Al_2O_3, Ca_2SiO, Ca3SiO5	CaO.MgO.2SiO_2, CaO.Al_2O_3.2SiO_2, FeO.Al_2O_3.2SiO_2, NaO.Al_2O_3, $KAlSi_3O_8$, NaO.CaO.Al_2O_3.2SiO_2
		7	2.8	SiO_2, $CaCO_3$, Al_2O_3, Ca_2SiO, Ca3SiO5	CaO.MgO.2SiO_2, CaO.Al_2O_3.2SiO_2, FeO.Al_2O_3.2SiO_2, NaO.Al_2O_3, $KAlSi_3O_8$, NaO.CaO.Al_2O_3.2SiO_2
		28	4.06	SiO_2, $CaCO_3$, Al_2O_3, Ca_2SiO, Ca3SiO5	CaO.MgO.2SiO_2, CaO.Al_2O_3.2SiO_2, FeO.Al_2O_3.2SiO_2, NaO.Al_2O_3, $KAlSi_3O_8$, NaO.CaO.Al_2O_3.2SiO_2
14	115	1	3.855	SiO_2, $CaCO_3$, Al_2O_3, Ca_2SiO, Ca3SiO5	CaO.MgO.2SiO_2, CaO.Al_2O_3.2SiO_2, FeO.Al_2O_3.2SiO_2, NaO.Al_2O_3, $KAlSi_3O_8$, NaO.CaO.Al_2O_3.2SiO_2
		7	4.52	SiO_2, $CaCO_3$, Al_2O_3, Ca_2SiO, Ca3SiO5	CaO.MgO.2SiO_2, CaO.Al_2O_3.2SiO_2, FeO.Al_2O_3.2SiO_2, NaO.Al_2O_3, $KAlSi_3O_8$, NaO.CaO.Al_2O_3.2SiO_2

Table 5-4 - *Continued*

		28	5.5	SiO_2, $CaCO_3$, Al_2O_3, Ca_2SiO, Ca3SiO5	$CaO.MgO.2SiO_2$, $CaO.Al_2O_3.2SiO_2$, $FeO.Al_2O_3.2SiO_2$, $NaO.Al_2O_3$, $KAlSi_3O_8$, $NaO.CaO.Al_2O_3.2SiO_2$
	158	1	4.355	SiO_2, $CaCO_3$, Al_2O_3, Ca_2SiO, Ca3SiO5	$CaO.MgO.2SiO_2$, $CaO.Al_2O_3.2SiO_2$, $FeO.Al_2O_3.2SiO_2$, $NaO.Al_2O_3$, $KAlSi_3O_8$, $NaO.CaO.Al_2O_3.2SiO_2$
		7	4.905	SiO_2, $CaCO_3$, Al_2O_3, Ca_2SiO, Ca3SiO5	$CaO.MgO.2SiO_2$, $CaO.Al_2O_3.2SiO_2$, $FeO.Al_2O_3.2SiO_2$, $NaO.Al_2O_3$, $KAlSi_3O_8$, $NaO.CaO.Al_2O_3.2SiO_2$
		28	6.425	SiO_2, $CaCO_3$, Al_2O_3, Ca_2SiO, Ca3SiO5	$CaO.MgO.2SiO_2$, $CaO.Al_2O_3.2SiO_2$, $FeO.Al_2O_3.2SiO_2$, $NaO.Al_2O_3$, $KAlSi_3O_8$, $NaO.CaO.Al_2O_3.2SiO_2$

The image from Figure 5-13 through 5-49 showing 9.42% CaO flyash after the activation process clearly shows the formation of geopolymer gel and also suggests that larger particles (>20 um) do not react chemically, but become physically embedded in the reacted binder. These particles can be attributed to the aggregate content in the geopolymer. On close inspection, it is found to reveal that these silica structures are embedded in a thin layer of reacted material which is characteristic of a siliceous glass structure, although allowing some calcium silicate glass in the system. Based on these EDS images, the amorphous phase has been identified as accumulation of feldspars. Table 5-4 lists some classic and simplified formulas of feldspars that are present in the geopolymer. There is also a dominant presence of calcium silicate glass structure, which is reactive with water and tends to form calcium silicate hydrated compounds that boost the mechanical strength values of the resultant geopolymer. Although the analytical CaO

content does not represent all of the CaO in the glass phase (a small amount of calcium is contained in the crystalline phases), there is a strong correlation between the analytical CaO content and the mechanical strength of the geopolymer. These structures could be attributed to the formation of Feldspar type amorphous materials which is listed in Table 5-4. From the figures, it can also be made out that these feldspar embedded silica particles are further embedded in a calcite layer which is formed from of crystalline calcium oxide phase.

Chapter 6

Analysis of Results and Discussions

6.1. Analysis of the Mechanical Properties of Geopolymers

The attributes of geopolymer concrete that are considerably influenced by flyash characteristics are the density of the fresh mix, the setting time and the overall mechanical properties. The density of the fresh mix is influenced mainly by the physical characteristics of flyash, i.e., specific gravity, particle size, etc. This can be attributed to the varying interstice systems that can be present in the flyash samples. The setting time is influenced mainly by the CaO content in flyash as proposed in the preliminary study. In the case of the mechanical properties, in order to reduce the number of dependent variables, only the compressive strength values were used as response to perform the evaluation. Based on the experimental work reported in this study, the following factors that affect the compressive strength of geopolymers are listed:

1. Higher concentration (in terms of molar) of sodium hydroxide solution results in higher compressive strength for 9.42% CaO fly ash-based geopolymer concrete (Table x) possibly because of complete reaction between the alkali and the fly ash.
2. Higher concentration (in terms of molar) of sodium hydroxide solution results in lower compressive strength for 1.29% CaO fly ash-based geopolymer concrete (Table) possibly because of an excess of alkali solution in the geopolymer.
3. For higher concentration of sodium hydroxide solution, ideal mechanical properties are found in the 9.42% CaO flyash based geopolymer as compared to that in 1.29% CaO flyash based geopolymer whereas for lower sodium hydroxide solution, the mechanical properties are found in the 1.29% CaO flyash

based geopolymer is better than the that of 9.42% CaO flyash based geopolymer.

4. With the presence of larger aggregates, there is an increase in the compressive strength for 9.42% CaO fly ash based geopolymer.
5. In a comparison between small aggregates and larger aggregates, there is an increase in the compressive strength for 1.29% CaO fly ash based geopolymer with larger aggregates.
6. The best results for geopolymer formation are with the use of a 100% sodium hydroxide solution when compared to other combination of alkali hydroxides.
7. As the curing temperature is increased from 115 F to 158 F, the compressive strength of fly ash-based geopolymer concrete also increases due to enhanced reaction between the constituents.
8. Longer curing time, in the range of 24 to 48 hours (2 days), produces higher compressive strength of fly ash-based geopolymer concrete. However, the increase in strength beyond 48 hours is not significant. The increase in strength is more dramatic of the lower CaO geopolymer.
9. Longer ageing time, in the range of 1 day to 28 days, produces higher compressive strength of fly ash-based geopolymer concrete.
10. The percentage of CaO present in the fly ash plays a significant role in the compressive strength of the geopolymer concrete. For low calcium flyash, higher the percentage of Calcium, the better the compressive strength of the geopolymer formed.
11. The highest compressive strength was found to be 7.23 ksi (49.85 MPa). This was obtained at 28 days from 9.42% CaO fly ash containing aggregates (3/8,

5/8, sand) with 14 M concentration of sodium hydroxide cured at 24 hrs / 158°F / Oven.

6.2. Analysis of the XRD and SEM-EDS Study

The compressive strength of Geopolymer cement is dependent on a complex fusion of physical, chemical and crystallographic factors of flyash. Silica and alumina are the main precursors for the formation of the geopolymer network and calcium oxide has significant influence in the chemical structure of the binder. The study showed that the crystalline part of flyash stays nearly inert while the amorphous component is the reactive one throughout the geopolymerization reaction. Therefore, the amount of silica, alumina and calcium oxide in a crystalline arrangement cannot be taken into account and it is assumed that the amorphous components participate in the geopolymerization reaction.

Using the x ray diffraction, the crystalline phases were identified as quartz, calcite, alumina and calcium silicate complexes, none of which are responsible for the binder properties of geopolymer concrete. On comparing the XRD pattern of the original fly ash with those of the geopolymeric materials, it can be seen that the crystalline phases originally existent in the flyash have not been completely transformed by the activation reaction. This relatively large amount of fly ash still present in the hardened samples is an indicator of incomplete geopolymerisation reaction. Results also suggest that the structure of these geopolymers is typically glass-like.

Using the SEM-EDS study, the possible amorphous phases that could be present have been shortlisted in table 5-5. The amorphous phase has been concluded to mostly consist of feldspar

The morphology and the chemical distribution for the geopolymers have been observed in figures 5-14 through figure 5-47 for the aging time up to 28 days. The microstructure was observed to be highly inhomogeneous and the matrix was full of loosely structured flyash grains of different sizes. Numerous circular cavities belonging to flyash particles are evident in the gel. The considerable amount of unreacted spheres, as well as the presence of pores in the geopolymer matrix indicate an incomplete reaction in the system and could explain why the alkali activated flyash samples show a lower degree of reaction. The SEM figures clearly shows inhomogeneous glass-like matrix of the amorphous aluminosilicate gel. The unreacted spheres of flyash indicate an incomplete reaction in the systems investigated. The low degree of reaction associated with low reactivity of flyash used also confirms this finding. If the silica content increases, the degree of reaction taking place in a geopolymer forming paste decreases according to observations of Provis and van Deventer.

EDS analysis of gel showed that gel mostly consists of the phases containing Na-Si-Al in the bulk region suggesting the formation of silicate-activated gel by polymerization throughout the inter particles volume. This correlates with the published works of Lee and Deventer meaning that, in a medium with a high concentration of dissolved silica, the species dissolved from the surface of flyash particles migrate from the surface into the bulk solution. In addition to Na, Si and Al, a small amount of Fe, Ca, K and Mg was also observed in the gel by EDS analysis .These remnants (Fe, Ca, K, Mg) obviously represent the flyash phases, which for various reasons, did not dissolve during alkali activation. Lloyd *et al.* suggested that during alkaline activation these remnants may even disperse through the gel. According to the authors, different solubility of phases in the aluminosilicate gel formed determines the distance of these remnants

from the surface of flyash particle. The properties of resulting geopolymer systems depend on not only the composition and reactivity of the fly ash used, but also on the initial SiO_2/Al_2O_3 ratio in the mixture, which is evident from the experimental data presented here and the discussion above. Pre-processing (e.g. fine grinding etc.) and/or use of a combination of raw materials of different reactivity, as well as selection of an activator in a geopolymer system are required to achieve the desired product properties.

Some basic chemical reactions based on dissolution and precipitation of Al, Si observed from XRD & SEM-EDS study is listed:

Eqn(1): $NaAlSi_3O_8 + 5H_2O + 3NaOH \longrightarrow Al(OH)_4^- + 3(OH)_3SiO^- + 4Na^+$

Eqn(2): $KAlSi_3O_8 + 5H_2O + 3NaOH \longrightarrow Al(OH)_4^- + 3(OH)_3SiO^- + 3Na^+ + K^+$

From these equations, a relationship between the mechanical properties and the chemical properties of flyash can be developed. On increases the molarity from 8M to 14M, there should be a typical shift in the reactions towards the right hand side. This could result in the stimulation of precipitation of sodium silicate, sodium aluminate, and sodium aluminosilicate. In the case of equation (1) and equation (2), the precipitates could be $Na_uSi_vAl_wO_x.H_2O_y$ which could attribute to common feldspars or hydrated feldspars. This could lead to water deficiency and thus raise alkalinity of the mixture. Thus promoting rate of polycondensation/geopolymerization. This can be hypothesized for increase in mechanical strength for 9.42% CaO on changing molarity of NaOH from 8M to 14M. This would also explain the cause of increased setting times on moving from 8M NaOH solution to 14M solution.

Chapter 7

Conclusions and Future Recommendations

7.1. Conclusions

This thesis puts forward a database of XRD analysis, chemical composition and mechanical properties performed on 18 batches of geopolymer produced from 9.42% CaO flyash. The potential for geopolymer cement production for each batch was compared and an analysis was performed to identify the major causes of variation that impact the mechanical properties of flyash based geopolymer concrete. As the true reaction mechanism through which geopolymer binders are formed is still debated and not well understood, a relationship between the chemical properties, microstructural properties and the mechanical properties was developed. Silica and alumina are the main precursors for geopolymer binder formation and these are assumed to dissolve from flyash in a highly alkaline solution and then recombine using sodium as a charge-balancing agent to form geopolymer gel (Davidovits, 1993). Fly ash of varying compositions was obtained from different sources in order to examine dissolution behaviour in different alkaline media, and also the early setting properties of geopolymeric pastes derived from each fly ash source. Some conclusions that have been drawn from this study are:

- The study has shown that the microstructural properties of fly ash particles and calcium content has a significant effect on setting time and final hardening of the geopolymer.

- It has been proposed therefore that an amorphous complex zone consisting of feldspars and certain calcium-containing compounds such as calcium silicates,

calcium aluminate hydrates, and also calcium silico aluminates are formed during the geopolymerisation of fly ash,

- These complex regions affect the setting and workability of the mix.

- It has been established that the degree of crystallinity (the amorphous nature) of the resultant geopolymers affects the observed compressive strength of the geopolymer concrete.

- It has been observed, that on increasing the alkalinity of the geopolymer formulation, there is an improved reaction with distinct amorphous regions being formed which dictates the compressive strength of the geopolymer concrete.

7.2. Future Recommendations

The present work has shown the effect of various parameters, calcium content, amorphous content alkali metal content, as well as morphology and chemical composition of flyash greatly affects the properties that it imparts on both the initial formulation mix and the final product. A chemical dissolution test, XRF analysis and infrared absorption spectrum will provide all the necessary information to predict how specific flyash will behave when used as a precursor material in geopolymer synthesis.

Appendix A

Composition of Flyash

Table A-1 Composition of 9.42% CaO Flyash

ASTM C 618 TEST REPORT						
			ASTM C-618-08 SPECIFICATIONS		AASHTO M 295 SPECIFICATION	
CHEMICAL ANALYSIS						
			CLASS C	CLASS F	CLASS C	CLASS F
Silicon Dioxide (SiO_2)		56.59%				
Aluminium Oxide (Al_2O_3)		23.89%				
Iron Oxide (Fe_2O_3)		4.82%				
Sum of SiO_2, Al_2O_3 and Fe_2O_3		85.30%	50 Min.	70 Min.	50 Min.	70 Min.
Magnesium Oxide (MgO)		1.83%				
Sulfur Trioxide (SO_3)		0.39%	5.0 Max.	5.0 Max.	5.0 Max.	5.0 Max.
Sodium Oxide (Na_2O)		0.24%				
Potassium Oxide (K_2O)		1.03%				
Total Alkalis as Na_2O		0.92%				
Calcium Oxide (CaO)		9.42%				
PHYSICAL ANALYSIS						
Moisture Content		0.00%	3.0 Max.	3.0 Max.	3.0 Max.	3.0 Max.
Loss on Ignition		0.23%	6.0 Max.	6.0 Max.	5.0 Max.	5.0 Max.
Fineness: Amount retained on 325 sieve %		19.45%	34% Max.	34% Max.	34% Max.	34% Max.
Water Requirement, % Control		95%	105% Max.	105% Max.	105% Max.	105% Max.
Specific Gravity		2.29				
Autoclave Soundness, %		0.03%	0.8% Max.	0.8% Max.	0.8% Max.	0.8% Max.
Strength Activity Index With Geopolymer	7 Days	76.60%	75% Min.	75% Min.	75% Min.	75% Min.
	28 Days	89.50%	75% Min.	75% Min.	75% Min.	75% Min.

Table A-2 Composition of 1.29% CaO Flyash

ASTM C 618 TEST REPORT						
			ASTM C-618-08 SPECIFICATIONS		AASHTO M 295 SPECIFICATION	
CHEMICAL ANALYSIS						
			CLASS C	CLASS F	CLASS C	CLASS F
Silicon Dioxide (SiO_2)		54.70%				
Aluminium Oxide (Al_2O_3)		29.00%				
Iron Oxide (Fe_2O_3)		6.74%				
Sum of SiO_2, Al_2O_3 and Fe_2O_3		90.44%	50 Min.	70 Min.	50 Min.	70 Min.
Magnesium Oxide (MgO)		0.80%				
Sulfur Trioxide (SO_3)		0.10%	5.0 Max.	5.0 Max.	5.0 Max.	5.0 Max.
Sodium Oxide (Na_2O)		0.25%				
Potassium Oxide (K_2O)		2.47%				
Total Alkalis as Na_2O		1.88%				
Calcium Oxide (CaO)		1.29%				
PHYSICAL ANALYSIS						
Moisture Content		0.09%	3.0 Max.	3.0 Max.	3.0 Max.	3.0 Max.
Loss on Ignition		2.72%	6.0 Max.	6.0 Max.	5.0 Max.	5.0 Max.
Fineness: Amount retained on 325 sieve %		20.90%	34% Max.	34% Max.	34% Max.	34% Max.
Water Requirement, % Control		97.50%	105% Max.	105% Max.	105% Max.	105% Max.
Specific Gravity		2.23				
Autoclave Soundness, %		0.03%	0.8% Max.	0.8% Max.	0.8% Max.	0.8% Max.
Strength Activity Index With Geopolymer	7 Days	70.70%	75% Min.	75% Min.	75% Min.	75% Min.
	28 Days	85.70%	75% Min.	75% Min.	75% Min.	75% Min.
Loose Dry Bulk Density, lb/cu. ft		69.70%				

Appendix B

Other Mix Designs

Table B-1 Mix Design for 9.42% CaO Flyash

Mix#	Fly Ash (lb/ft^3)	Aggregate (lb/ft^3)			Sodium Hydroxide Solution (lb/ft^3)	Sodium Silicate Solution (lb/ft^3)	Conc. Of NaOH (M)	SP (lb/ft^3)	Added Water (lb/ft^3)	Curing		
		3/8	5/8	Sand						Time (hrs.)	Temp. (°F)	Method
1	24.8	38.9	38.9	34	2.6	6.3	14	0.4	6.14	24	75	Steam
2	24.8	38.9	38.9	34	2.6	6.3	14	0.8	2.2	24	90	Oven
3	24.8	38.9	38.9	34	2.6	6.3	14	0.6	3.1	24	115	Steam
4	24.8	38.9	38.9	34	2.6	6.3	14	0.6	3.1	24	115	Oven
5	24.8	38.9	38.9	34	2.6	6.3	14	0	6.1	24	158	Oven
6	25.5	50	15	50	2.6	6.5	14	0.4	1	24	90	Oven
7	25.5	50	15	50	2.6	6.5	14	0.4	1	24	115	Oven
8	25.5	50	15	50	2.6	6.5	14	0.4	1	24	131	Oven
9	25.5	50	15	50	2.6	6.5	14	0.4	1	48	131	Oven
10	25.5	50	15	50	2.6	6.5	14	0.4	1	24	158	Oven
11	25.5	80	-	35	2.6	6.5	14	0.4	1	24	75	Steam
12	25.5	80	-	35	2.6	6.5	14	0.4	1	24	90	Oven
13	25.5	80	-	35	2.6	6.5	14	0.4	1	24	115	Steam
14	25.5	80	-	35	2.6	6.5	14	0.4	1	24	131	Oven
15	25.5	80	-	35	2.6	6.5	14	0.4	1	24	158	Oven
16	25.5	60	-	55	2.6	6.5	14	0.4	1	24	115	Steam
17	25.5	60	-	55	2.6	6.5	14	0.4	1	24	131	Oven
18	25.5	60	-	55	2.6	6.5	14	0.4	1	24	158	Oven

Table B-2 Compressive Strength for 9.43% CaO Flyash Design

Mix #	*Compressive Strength (Ksi)*			
	1	*3*	*7*	*28*
1	-	1.00	1.16	1.26
2	0.87	1.92	2.36	2.46
3	2.55	2.44	4.00	-
4	2.17	2.71	4.18	-
5	-	1.89	2.03	2.48
6	1.81	2.08	2.42	-
7	3.40	4.48	4.74	5.46
8	3.75	4.35	5.44	5.68
9	-	3.97	5.60	6.03
10	5.68	6.70	7.13	7.23
11	-	0.88	1.64	2.42
12	2.34	2.76	2.85	3.17
13	4.22	4.31	4.48	4.64
14	3.11	3.39	4.06	-
15	3.25	5.03	5.65	-
16	4.21	4.23	4.24	4.53
17	2.82	3.57	3.86	4.38
18	3.25	4.66	5.11	5.71

References

ASTM C31 Standard Practice for Making and Curing Concrete Test Specimens in the Field, *American Society of Civil Engineers, 2012.*

ASTM C39 Standard Test Method for Compressive Strength of Cylindrical Concrete Specimens, *American Society of Civil Engineers, 2008.*

ASTM C617 Standard Practice for Capping Cylindrical Concrete Specimens, *American Society of Civil Engineers, 2012.*

ASTM C618 Standard Specification for Coal Fly Ash and Raw or Calcined Natural Pozzolan for Use in Concrete, *American Society of Civil Engineers*, 2008.

ASTM C873 Standard Test Method for Compressive Strength of Concrete Cylinders Cast in Place in Cylindrical Molds, *American Society of Civil Engineers, 2012..*

Davidovits, J., "Carbon-dioxide green-house warming: What future for Geopolymer cement," *Emerging technologies symposium on cement and concretes in the global environment*, Geopolymer cement Association, Chicago, 1993,p-21.

Davidovits, J., "Geopolymers: inorganic polymeric new materials," *J. of Thermal Analysis,* vol. 37, 1991, 1633-1656.

Davidovits, J., "Chemistry of geopolymeric systems, terminology," *Geopolymer* International Conference, France, 1999.

Davidovits J., “Geopolymer chemistry & sustainable development. The Poly (silicate) terminology: a very useful and simple model for the promotion and understanding of green-chemistry”, *Proceedings of the World Congress Geopolymer*, Saint Quentin, France, 28 June – 1 July, 2005: pp. 9-15.

Diaz, E. I., and Allouche, E. N., "Recycling of fly ash into geopolymer concrete: Creation of a database," *Green Technologies Conference*, 2010 IEEE.

Diaz, E. I.; Allouche, E. N.; and Eklund, S., "Factors affecting the suitability of fly ash as source material for geopolymers," Fuel, vol. 89, 2010 992-996.

D.L. Eleazar, “To model and predict the properties of fresh and hardened fly ash-based geopolymer concrete.” College of engineering and science Louisiana Tech University,May 2011

Environmental Protection Agency (EPA), "Coal combustion residual-proposed rule," www.epa.gov, January 10, 2011.

Fernandez-Jimenez, A., and Palomo, A., "Characterization of fly ashes: Potential reactivity as alkaline cements," *Fuel,* vol. 82, 2003, 2259-2265.

Fernandez-Jimenez, A. M.; Palomo, A.; and Lopez-Hombrados, C, "Engineering properties of alkali-activated fly ash concrete," *ACI Materials J.,* vol. 103, 2006, 106-112.

Fernandez-Jimenez, A., and Palomo, A., "Alkaline activation of fly ashes; Manuflyashcture of concrete not containing Geopolymer cement," International RILEM Conference *on the Use of Recycled Materials in Building and Structures*, 2004.

Hardjito D. and Rangan B. V., “Development and Properties of Low-Calcium Fly ash-based Geopolymer Concrete”, Research Report GC 1, Flyashculty of Engineering, Curtin University of Technology, Perth, Australia, 2005.

Hardjito D., Wallah S. E., Sumajouw D. M. J. and Rangan B. V., “Factors Influencing the Compressive Strength of Fly ash-based Geopolymer Concrete”, *Civil Engineering Dimension*, Vol. 6, No. 2, pp. 88-93, September 2004.

Lee, W. K. W., Van Deventer, J. S. J., Colloids Surf., A 211.2002.

Malhotra V.M., “Introduction: Sustainable Development & Concrete Technology”, *ACI Concrete International* (2002), 24 (7): pp. 22.

Malhotra V.M., “Making concrete ‘greener’ with fly ash”, *ACI Concrete International* (1999), 21: pp. 61-66.

Malhotra V.M., “Reducing CO2 Emissions”, *ACI Concrete International* (2006), 28: pp. 42-45.

McCaffery R., “Climate Change and the Cement Industry”, *Global Cement and Lime Magazine (Environmental Special Issue)*, 2002: pp. 15-19.

Palomo, A.; Grutzeck, M. W.; and Blanco, M. T., "Alkali-activated fly ashes a cement for the future," *Cem. and Concrete Res.,* vol. 29, 1999, 1323-1329.

Provis, J. L.; Duxson, P.; and van Deventer, J. S. J., "The role of particle technology in developing sustainable construction materials," *Advance Powder Technology,* vol.21(1), 2010, 2-7.

Provis, J. L.; Duxson, P.; Van Deventer, J. S. J.; and Lukey, G. C, "The role of mathematical modeling and gel chemistry in advancing geopolymer technology," *Chem. Eng. Res. and Design,* vol. 83 (7), 2005, 853-860.

Provis, J. L., and van Deventer, J. S. J., "Geopolymerization kinetics. 1. In situ energy dispersive x-ray diffractometry," *Chem. Eng. Science,* vol. 62, 2007, 2309-2317.

Temuujin, J.; van Riessen, A.; and Williams. R., "Influence of calcium compounds on the mechanical properties of fly ash geopolymer pastes," *J. Hazard. Mater.,* vol. 167, 2009, 82-88.

Van Jaarsveld, J. G. S.; van Deventer, J. S. J.; and Lukey, G. C, "The effect of composition and temperature on the properties of fly ash- and kaolinite-based geopolymers," *Chem. Eng. J.,* vol. 89, 2002, 63-73.

Van Jaarsveld, J. G. S.; van Deventer, J. S. J.; and Lukey, G. C, "The characterization of source materials in fly ash-based geopolymers," *Materials Letters,* vol. 57, 2003, 1272-1280.

Y.Zhang, W. Sun, Z Li.," Preparation and microstructure of Na-PSDS geopolymeric matrix", Ceramics-silikaty, vol. 53, (2), 2009, p. 88-97

Y.Zhang, W. Sun, Z Li.," Synthesis and microstructural characterization of fully-reacted potassium-poly(sialate-siloxo) geopolymeric cement matrix", *ACI materials journal,* vol. 105, (2), 2008, MAR-APR, p. 156-164

Biographical Information

Gaurav Nagalia was born on September 23, 1988 in India. He graduated with a Bachelor degree in Polymer Engineering from Maharashtra Institute of Technology, Pune University, India. He was among the top 10% of his class. Immediately after graduation, he came to US to pursue Master of Science in Materials Science and Engineering from University of Texas at Arlington (UTA) under the supervision of Dr. Pranesh Aswath. He was awarded several scholarships in UTA.